Supporting Information

Humans simplified trophic structures in island lake ecosystems

Authors

Miguel G. Matias[1,2*], Vítor Gonçalves[3,4], Sergi Pla-Rabés[5,6,7], Armand Hernández[8], Manuel Mendoza[1], Miguel B. Araújo[1,2,9], Jacqueline van Leeuwen[10,11], Sandra Nogué[5,7], Nora Richter[12], Martin Souto[3,4], Ricardo Trigo[13], Roberto Bao[7], Alberto Sáez[14], Santiago Giralt[15] and Pedro M. Raposeiro[3,4]

Affiliations

[1] Departamento de Biogeografía y Cambio Global, Museo Nacional de Ciencias Naturales, CSIC, Madrid, Spain

[2] Rui Nabeiro Biodiversity Chair, MED– Mediterranean Institute for Agriculture, Environment and Development & CHANGE Global Change and Sustainability Institute, Institute for Advanced Studies and Research, University of Évora, Évora, Portugal

[3] CIBIO, Centro de Investigação em Biodiversidade e Recursos Genéticos, InBIOLaboratório Associado, Pólo dos Açores, Rua da Mãe de Deus, 9500-321 Ponta Delgada, Portugal

[4] Faculdade de Ciências e Tecnologia, Universidade dos Açores, Rua da Mãe de Deus, 9500-321 Ponta Delgada, Portugal

[5] Universitat Autònoma de Barcelona, Edifici C, 08193 Cerdanyola del Vallès, Spain

[6] Department of Geography, Environmental Management and Energy Studies, University of Johannesburg, Corner Ditton and University Avenue, Auckland Park, Johannesburg, South Africa

[7] CREAF, Cerdanyola del Vallès (Bellaterra), Spain

[8] Universidade da Coruña, GRICA-BIOpast Group, Centro Interdisciplinar de Química e Bioloxía (CICA), Rúa das Carballeiras, 15071 A Coruña, Spain

[9] German Centre for Integrative Biodiversity Research (iDiv), Halle-Jena-Leipzig, Puschstrasse 4, Leipzig 04103, Germany

[10] Institute of Plant Sciences, University of Bern, Altenbergrain 21, Bern 3013, Switzerland

[11] Oeschger Centre for Climate Change Research, University of Bern, Hochschulstrasse 4, Bern 3012, Switzerland
[12] Department of Surface Waters - Research and Management, Swiss Federal Institute of Aquatic Science and Technology (EAWAG), Dübendorf, Switzerland
[13] Instituto Dom Luiz, Faculdade de Ciências, Universidade de Lisboa, 1749-016 Lisboa, Portugal
[14] UB-Geomodels Research Institute. Departament de Dinàmica de la Terra i de l'Oceà, Facultat de Ciències de la Terra, Universitat de Barcelona, Martí i Franquès s/n, 08028 Barcelona, Spain
[15] Geosciences Barcelona (GEO3BCN), CSIC, Lluís Solé i Sabarís s/n, 08028 Barcelona, Spain

* Corresponding Author: Miguel G. Matias: miguel.matias@mncn.csic.es

Appendix S1 - Supplementary Methods

Coring

Sediment cores were collected from seven lakes across the Azores between 2011 and 2021 using UWITEC® and Russian coring systems. In September 2011, a 2.7 m core was retrieved from Lake Empadadas, and a 2.0 m core from Lake Azul, both using a UWITEC® piston corer mounted on a floating platform (UWITEC Ltd., Mondsee, Austria). During the same campaign, a 1.40 m core was collected using a UWITEC® gravity corer. In June 2015, a 253 cm core was extracted from the deepest part of Lake Peixinho with a UWITEC® piston corer and platform system. In June 2017, two long sediment cores were obtained using the same UWITEC® piston platform setup: a 994 cm core from the deepest area of Lake Funda and a 460 cm core from Lake Caldeirão. In July 2018, a 350 cm core was collected from Lake Ginjal using a Russian corer equipped with a 50 cm long, 7 cm diameter sampler. Finally, in January 2021, a 450 cm core was recovered from Lake Prata using the same Russian corer system.

Dating

Radiocarbon AMS dating samples were prepared using acid digestion following Rull et al. (2010). Seven plant macrofossil samples (from Lakes Azul and Prata) and 37 pollen-concentrated samples were analysed at Beta Analytic Inc. (USA), the Keck-CCAMS Group at the University of California, Irvine (USA) and the Laboratoire de Radiochronologie at Université Laval (Québec, Canada). AMS radiocarbon dates were calibrated using Calib 7.1 and the IntCal20 calibration curve (Reimer et al., 2020). ^{210}Pb concentration profiles were determined at 1 cm resolution for the uppermost sediments of Lakes Azul, Santiago, Empadadas Norte, Peixinho, Caveiro, Funda and Caldeirão by quantifying ^{210}Po via alpha-particle spectrometry. Analyses were conducted at the Autonomous University of Barcelona following the protocol described in Sanchez-Cabeza et al. (1998), and at the Laboratorio de Geoquímica Isotópica y Geocronología (Instituto de Ciencias del Mar y Limnología, UNAM, Mazatlán, México) following Ruiz-Fernández and Hillaire-Marcel (2009), based on the method of Flynn (1968). Briefly, aliquots of dried, ground sediment (0.08–0.40 g) were spiked with a known amount of ^{209}Po yield tracer and digested in a concentrated acid mixture (HF + HNO_3 + HCl) at temperatures exceeding 120 °C. Polonium isotopes were then spontaneously deposited onto silver discs. Activities of ^{209}Po and ^{210}Po were measured by alpha-particle spectrometry using high-resolution, low-background silicon detectors, with counting uncertainties maintained below 5%.

^{226}Ra (via ^{214}Pb) and ^{137}Cs activities were determined by gamma spectrometry in selected samples from the sediment cores of Lakes Azul, Santiago, Caveiro, Peixinho and Funda. Approximately 1 g of dried, ground sample was packed into polyethylene calibration tubes (length: 40 mm; diameter: 10 mm), sealed with rubber caps and Teflon tape, and stored for 21 days to allow secular equilibrium between ^{226}Ra and ^{214}Pb. Samples were analysed for at least 48 hours using a high-resolution, low-background HPGe well-type detector (Ortec-Ametek). Excess ^{210}Pb was calculated by subtracting ^{226}Ra from total ^{210}Pb activity. Activities are reported in Bq kg^{-1} with uncertainties expressed as ±1σ. Analytical quality was verified using replicate analyses of the IAEA-300 reference material, with results falling within certified ranges for ^{210}Pb, ^{226}Ra and ^{137}Cs. $^{210}Pb_{ex}$-derived sedimentation rates were calculated using the Constant Flux (CF) model for Lake Azul and the Constant Flux–Constant Sedimentation (CF:CS) model for the remaining cores (Appleby & Oldfield, 1978; Robbins, 1978; Sanchez-Cabeza & Ruiz-Fernández, 2012). Age uncertainties were estimated via Monte Carlo simulation with 10,000 iterations (Sanchez-Cabeza et al., 2014). Final age–depth models were constructed using the R package *clam* (v2.3.9), which calibrated all radiocarbon dates at 2σ using the IntCal20 calibration curve (Blaauw et al., 2020).

Lake Azul

The chronological model for Lake Azul was constructed using two ^{14}C dates and ^{210}Pb and ^{137}Cs profiles that span the uppermost 74 cm of the sediment record. The age-depth model was previously published (Raposeiro et al., 2021) and spans the last ca. 700 years with a confidence interval for the age-depth model that ranges between 1.4 (top) and 223 (bottom) years.

Lake Santiago

The age–depth model for Lake Santiago was established using a combination of chronostratigraphic constraints, including 210Pb and 137Cs profiles, two AMS 14C dates on terrestrial plant macroremains, and stratigraphic tie-points derived from lithological correlations among sediment cores. The chronology was previously published (6) and integrates additional validation using historically documented events, such as the P17 volcanic eruption (~1290 CE) and the first appearance of pollen from introduced *Cryptomeria japonica* and *Pinus* spp. The resulting age–depth model spans approximately the last 600 years, with confidence intervals ranging from 1 years at the core top to 60 years at the base.

Lake Empadadas Norte

The chronological model for Lake Empadadas Norte was constructed using four ^{14}C dates and ^{210}Pb and 137Cs profiles. The age-depth model was previously published (Hernández et al., 2017) and spans the last ca. 700 years with a confidence interval for the age-depth model that ranges between 0.65 (top) and 61 (bottom) years.

Lake Prata

The chronological framework for Lake Prata was constructed using five new radiocarbon dates spanning the past ~1,200 years, supplemented by a previously published age for the P17 volcanic eruption from Lake Azul (Raposeiro et al., 2017), which occurred within the Sete Cidades caldera. The P17 tephra, identified as a pumice-rich layer at 373–363 cm depth in the Prata core, was used as a stratigraphic tie point in the age model (Raposeiro et al., 2024).

Lake Ginjal

The age–depth model for Lake Ginjal was constructed using three radiocarbon dates and a smooth spline fit (Raposeiro et al., 2021), yielding a chronology spanning ~600 years (1400–1950 CE). Modelled age uncertainty ranges from 10 years near the core top to 110 years at depth.

Lake Peixinho

The age–depth model for Lake Peixinho was developed using four radiocarbon dates (Raposeiro et al., 2021), together with ^{210}Pb and ^{137}Cs profiles spanning the uppermost 18 cm of the core. The resulting chronology spans the past ~690 years, with modelled age uncertainty ranging from 1 to 112 years.

Lake Caveiro

The age–depth model for Lake Caveiro was constructed using nine radiocarbon dates (Benavente Marín, 2024), together with ^{210}Pb and ^{137}Cs profiles, spanning the past ~5200 years. Modelled age uncertainty ranging from 1 to 50 years.

Lake Funda

The age–depth model for Lake Funda was developed using six AMS 14C dates together with 210Pb and 137Cs activity profiles for the uppermost 74 cm of the core. The chronology spans approximately the last 720 years and the associated confidence intervals range from approximately 1 to 50 years.

Lake Caldeirão

The age–depth model for Lake Caldeirão was developed using nine radiocarbon dates and a ^{210}Pb profile covering the uppermost 20 cm of sediment (Raposeiro et al., 2021). The resulting chronology spans the past ~4,000 years. Modelled age uncertainty ranges from 1.5 to 124 years.

Community data and Taxonomic references

Diatoms

Diatom assemblages were analysed from all lake sediment cores collected for this study (see SI Appendix, Table S5). Sediment subsamples were prepared for diatom analysis following standard protocols for siliceous microfossils (Renberg, 1990). Briefly, approximately 0.5 g of wet sediment was treated with 30% hydrogen peroxide (H_2O_2) to oxidize organic matter, and with dilute hydrochloric acid (HCl) to remove carbonates. The cleaned suspensions were repeatedly rinsed with distilled water through settling and decanting, then allowed to air-dry on cover slips. Permanent microscope slides were prepared using Naphrax® mountant with a high refractive index (1.7). At least 400 diatom valves were identified and counted per sample along randomly selected transects to ensure statistical robustness. Counting was conducted at 1,000× magnification under oil immersion using a Zeiss Axio Imager A1 microscope equipped with a 100× Zeiss Plan-Apochromat objective (NA 1.4) and differential interference contrast (DIC) optics. Taxonomic identification was based on standard diatom floras (Krammer & Lange-Bertalot, 1986, 1988, 1991b, 1991a, 2000) and cross-referenced with existing floristic surveys from the Azores archipelago to ensure regional consistency (Gonçalves et al., 2010). Identifications were made to the lowest possible taxonomic level, typically species or variety. Raw diatom valve counts were converted to relative abundance data and expressed as percentages of the total diatom assemblage for each sample.

Chironomids

Chironomid larval head capsules (HCs) were analysed from all lake sediment cores (see SI Appendix, Table S5 for core metadata). Subsamples of 2 cm^3 were taken at 1–5 cm intervals along each core and processed following established protocol (Brooks et al., 2007). Each subsample was first deflocculated in a 10% potassium hydroxide (KOH) solution by heating to 70 °C for approximately 5 minutes to disaggregate organic material. The resulting material was rinsed with deionized water and sieved into two size fractions: 90–212 µm and >212 µm, to ensure capture of a broad size range of head capsules. Residues were examined under a Zeiss Stemi stereomicroscope at 40× magnification. Chironomid head capsules were manually sorted and mounted in Euparal mounting medium on microscope slides for taxonomic identification. Identification was carried out under a Zeiss Axio Imager A1 compound microscope at 100× to 400× magnification. Taxonomic identification was based primarily on mentum morphology and other diagnostic features, using published keys and descriptions (Brooks et al., 2007; Moller Pillot, 2009, 2014; Rieradevall & Brooks, 2001; Vallenduuk & Moller Pillot, 2007). Identifications were made to the lowest feasible taxonomic level, typically species morphotype, and harmonized with existing chironomid reference datasets from the Azores. For each sample, the relative abundance of each taxon was calculated as a percentage of the total number of head capsules identified.

Pollen

Palynological analyses were conducted on sediment cores from all study lakes (see SI Appendix, Table S4). Subsamples were subsequently subjected to standard palynological digestion procedures, which included sequential treatment with 10% potassium hydroxide (KOH) to remove humic acids, hydrochloric acid (HCl) to dissolve carbonates, hydrofluoric acid (HF) to remove siliceous components, and acetolysis (acetic anhydride and sulfuric acid) to remove cellulose and concentrate resistant palynomorphs. The cleaned residues were suspended and mounted in glycerine, and permanent slides were prepared using the same medium. Processing followed established protocol (Rull et al., 2010). Pollen, pteridophyte spores and non-pollen palynomorphs (NPPs) were identified under 400× magnification using a Zeiss compound microscope. Identifications were made using standard pollen floras (Cugny et al., 2010; Demske et al., 2013; Reille, 1999; van Geel et al., 2003; van Geel & Aptroot, 2006) and by comparison with the Azorean modern reference collection, curated by the Freshwater Ecology Research Group of the University of the Azores, Ponta Delgada.

To assess vegetation dynamics across the Azores archipelago, we conducted a multivariate analysis of terrestrial pollen and fern spore assemblages from nine sedimentary pollen records distributed across multiple islands. The pollen datasets were taxonomically harmonised to ensure consistency in the identification and grouping of taxa, allowing for robust comparisons across sites and through time. We standardised pollen identification according to the methods outlined in Strandsberg et al. (2024). The steps taken include: 1) Removing categories of indeterminable pollen and spores; 2) Excluding taxa with a taxonomic resolution higher than the family level; 3) Preserving the lowest level of resolution, for instance, updating *Alnus* cf. *glutinosa* to *Alnus glutinosa*; and 4) Aggregating taxa with multiple names to the highest possible taxonomic level, such as upgrading an unclear genus identification *Picconia*/*Olea*-type to Oleaceae. Finally, we matched the pollen and spore taxa in the dataset with the accepted names in "Plants of the World" (https://powo.science.kew.org/) to resolve any potential synonyms (e.g., *Morella faya* was updated to *Myrica faya*). The pollen records included in this analysis were compiled from previously published data including from Lake Caldeirão, Corvo Island (Connor et al., 2024; Raposeiro et al., 2021); Lake Funda, Flores Island (Ritter et al., 2022), Lake Peixinho, Pico Island (Raposeiro et al., 2021), Lake Caveiro and Pico Bog, Pico Island (Connor et al., 2012), Lake do Ginjal, Terceira Island (Raposeiro et al., 2021) and Lake Azul, São Miguel Island (Raposeiro et al., 2021; Rull et al., 2017). In addition, we incorporated new data from Lake Pico da Esperança, São Jorge Island.

Historical Context

Land-use

Before human arrival, the Azorean landscape was dominated by extensive laurisilva forests composed primarily of native evergreen tree species, forming a dense and biodiverse canopy across the archipelago (Connor et al., 2012; Raposeiro et al., 2021; Rull et al., 2017). However, the arrival of Portuguese settlers marked the beginning of widespread and sustained anthropogenic change (Frutuoso, 1978, 1981). Over subsequent centuries, large-scale deforestation was carried out to clear land for agriculture, produce charcoal for domestic energy needs, and extract timber and other plant materials for construction (Moreira, 1987). This intense and continuous exploitation of natural resources, both for local subsistence and for economic export, resulted in the progressive degradation and fragmentation of native forest ecosystems. By the 20th century, more than 95% of the original native vegetation had been lost across the archipelago (Triantis et al., 2010), leading to a drastic reduction in habitat availability for endemic species and a significant decline in ecological complexity (Lhoumeau & Borges, 2023; Oyarzabal

et al., 2025). Besides, a notable landscape transformation on São Miguel Island occurred in the mid-20th century when there was a shift in forest dominance from *Pinus pinaster* to *Cryptomeria japonica*, a fast-growing conifer native to Japan, favoured for timber production and commercial forestry (Moreira, 1987). Concurrently, the expansion of intensive agriculture and livestock farming reshaped the lowland and mid-elevation landscapes, driving the proliferation of monoculture systems, particularly for pasture and forage crops (Connor et al., 2012; Raposeiro et al., 2021; Rull et al., 2017). This transformation not only led to the homogenisation of the terrestrial landscape but also had cascading effects on freshwater ecosystems (Raposeiro et al., 2017, 2021; Richter et al., 2022; Ritter et al., 2022). Changes in land use and vegetation cover altered catchment runoff patterns, increased sedimentation in lakes, and modified their nutrient dynamics, ultimately reshaping the extent and composition of littoral vegetation and aquatic communities across many of the island's lakes and wetlands (Connor et al., 2012; Raposeiro et al., 2021; Rull et al., 2017).

Fish introductions

Before human colonisation, the majority of Azorean lakes were naturally devoid of fish, reflecting the islands' volcanic origin and geographic isolation. The intentional introduction of freshwater fish species, primarily for recreational purposes such as angling and ornamental stocking, became increasingly widespread from the late 18th century onwards (Raposeiro et al., 2017; Skov et al., 2010), particularly on São Miguel Island (Costa et al., 2021b). Although historical records suggest that goldfish (*Carassius auratus* Linnaeus, 1758) were introduced to mainland Portugal as early as 1611 CE (Kottelat & Freyhof, 2007) the earliest known record of their presence in the Azores dates to 1792 CE, in Furnas Lake (Valois & Silva, 1886). This marked the beginning of a broader trend of species introductions into island freshwater systems. By 1879 CE, systematic stocking efforts had commenced, targeting several lakes including Lakes Azul, Verde and Furnas, with the deliberate release of both native and non-native species (Vicente, 1956). These introductions were often driven by aesthetic, cultural and utilitarian motivations, with fish perceived as enhancing the value and appeal of these aquatic environments. During the mid-20th century, fish stocking was institutionalised by the regional forestry services (Junta Geral Distrital de Ponta Delgada), which oversaw further introductions to promote local fisheries and support recreational angling. These interventions significantly altered the ecological character of the lakes, contributing to long-term changes in trophic dynamics, biodiversity and biogeochemical cycling (Buchaca et al., 2011; Raposeiro et al., 2017; Skov et al., 2010).

Sensitivity analysis

To assess the robustness of the inferred contributions of vegetation change and climate variability to long-term trophic reorganisation, we conducted four complementary sensitivity analyses. Together, these analyses test whether our conclusions depend on (i) the influence of individual lakes, (ii) the temporal structure imposed by moving-window analyses, (iii) the precise placement of historical phase boundaries, or (iv) the regional temporal alignment of lake records independent of their internal variability of lake sediment records within the regional compilation. Importantly, these analyses were designed to evaluate the robustness of inference rather than to redefine model structure or temporal segmentation. Sensitivity analyses consistently supported the robustness of our main conclusions.

Sensitivity to historical phase boundaries (grid test)

We evaluated whether unequal sample sizes among historical phases—particularly the smaller number of temporal bins in the most recent phase—could influence phase-based variance partitioning results. Starting from the baseline phase boundaries (<750, 750–1050, 1050–1450, 1450–1750, >1750 CE), we systematically perturbed each boundary by ±30–60 years (corresponding to ±1–2 bins), generating a grid of alternative phase definitions while preserving

chronological order and enforcing a minimum number of bins per phase. For each admissible boundary configuration, we recomputed phase-specific variance partitioning using partial redundancy analysis (RDA), quantifying the adjusted R^2 associated with the pure vegetation component, the pure climate (NAO) component, and their shared fraction. Results from each perturbed configuration were compared to the baseline solution to quantify absolute and relative deviations (SI Appendix, Table S6). This analysis was explicitly designed to test robustness to discretization and sample-size imbalance, rather than to optimize or redefine phase limits. Variance partitioning results were robust to reasonable perturbations of historical phase boundaries. Importantly, the most recent phase did not exhibit elevated sensitivity relative to earlier phases. Instead, the largest deviations from baseline estimates were consistently associated with Phase 4, indicating higher sensitivity during this transitional interval rather than an artefact of unequal bin numbers. Across all tested boundary configurations, dominance patterns and qualitative conclusions remained unchanged.

Leave-one-out sensitivity across historical phases

We assessed whether variance partitioning results within predefined historical phases were driven disproportionately by any single lake. Starting from the lake-level 30-yr binned guild data, we iteratively removed one lake at a time and recomputed the regional mean community time series for each leave-one-out (LOO) iteration. For each reduced dataset, we rebuilt the aligned environmental table (vegetation change and NAO), applied the same scaling procedure used in the main analysis (z-scaling after alignment), and recalculated phase-specific variance partitioning using partial RDA. For each historical phase, we quantified the adjusted R^2 associated with the pure vegetation component, the pure climate component, and their shared fraction. LOO effects were summarized by computing the mean and median contribution of each component across phases, as well as the difference between vegetation and climate effects (vegetation minus climate), allowing us to evaluate whether the relative dominance of vegetation over climate was stable across lake exclusions.

Leave-one-out analyses across historical phases revealed strong robustness of variance partitioning results to the exclusion of individual lakes (SI Appendix, Table S7). In all LOO iterations, vegetation change consistently explained more unique variance than climate, with vegetation dominating in every phase regardless of which lake was removed. Mean and median differences between vegetation and climate effects remained positive across all LOO runs, indicating that no single lake disproportionately drove the observed dominance of vegetation in the phase-based analysis. Although absolute effect sizes varied slightly depending on the excluded lake, the direction and relative strength of effects were stable, demonstrating that phase-level conclusions reflect a coherent regional signal rather than a small subset of influential records.

Leave-one-out sensitivity in the moving-window analysis

We extended the LOO approach to the continuous moving-window framework to test the robustness of temporal patterns in variance partitioning. Using a 300-yr sliding window stepped every 30 years, we recalculated pure and shared variance components after sequentially removing each lake from the regional dataset. For each LOO iteration, we rebuilt the regional time series, realigned environmental predictors, applied scaling, and recomputed window-based variance partitioning. Results were summarized in two complementary ways: (i) average effect sizes (mean and median adjusted R^2) of pure vegetation and pure climate across all windows, and (ii) the proportion of windows in which vegetation explained more variance than climate. These metrics test whether the dominance of vegetation observed in the moving-window analysis reflects a few influential records or a consistent regional signal.

The moving-window leave-one-out analysis showed that the temporal dominance of vegetation over climate was highly consistent across lake exclusions (SI Appendix, Table S8). In all LOO iterations, vegetation explained more variance than climate in the majority of windows, typically exceeding climate in approximately 75–90% of windows. Mean and median effect sizes changed only modestly relative to the baseline analysis using all lakes. Importantly, the timing of major peaks in vegetation-associated variance remained coherent across LOO iterations, indicating that the observed temporal structure of trophic reorganisation is not driven by any single lake. Climate effects were smaller and more intermittent, but their relative contribution was also stable across LOO runs, supporting the interpretation of a genuine, albeit secondary, climatic signal.

Null model for lake record position and length (circular shift)

Finally, we tested whether moving-window results could arise solely from differences in record position and length among lakes. We constructed a null model by circularly shifting age bins within each lake independently, thereby randomizing the temporal alignment of community composition while preserving (i) within-lake variance structure, (ii) record length, and (iii) the overall distribution of ages in the regional dataset. For each null iteration (n = 50), we rebuilt the regional community time series, rejoined it with aligned environmental predictors, applied scaling, and recalculated moving-window variance partitioning. For each window midpoint and variance component, we derived the 5th, 50th, and 95th percentiles of adjusted R^2 across null iterations. Observed values from the original (non-shuffled) data were compared against median null value across all iterations to assess whether inferred vegetation and climate effects exceeded expectations based solely on record structure.

Comparison of observed moving-window results against the circular-shift null model confirmed that both vegetation and climate signals depend on the real temporal alignment of lake records (SI Appendix, Fig. S11). Observed vegetation-associated adjusted R^2 values frequently exceeded the median, particularly during periods of pronounced ecological reorganisation, indicating that the strong vegetation signal cannot be explained by uneven record coverage or record length alone. Climate effects exhibited lower average explained variance, but showed discrete intervals where observed values exceeded null expectations. These departures demonstrate that the climate signal is not a trivial consequence of record structure, but reflects temporally coherent forcing across lakes.

Appendix S2

Appendix S2. Lake-level stratigraphic diagrams and community turnover (diatoms and chironomids). Each subsequent page shows one study lake. Panels are: (a) diatom relative abundances for the top 10 taxa (remaining taxa pooled as Other); (b) diatom DCA1 generalised additive model (GAM) smooth with 95% confidence band; (c) chironomid relative abundances for the top 10 taxa (plus Other); (d) chironomid DCA1 GAM smooth with 95% confidence band. Age (Common Era) is shared on the vertical axis, with the present at the top. Lake titles use the same island abbreviations as Fig. 2b (CR = Corvo, FL = Flores, PI = Pico, SM = S<c3><a3>o Miguel, TE = Terceira).

1.1. Azul [SM]

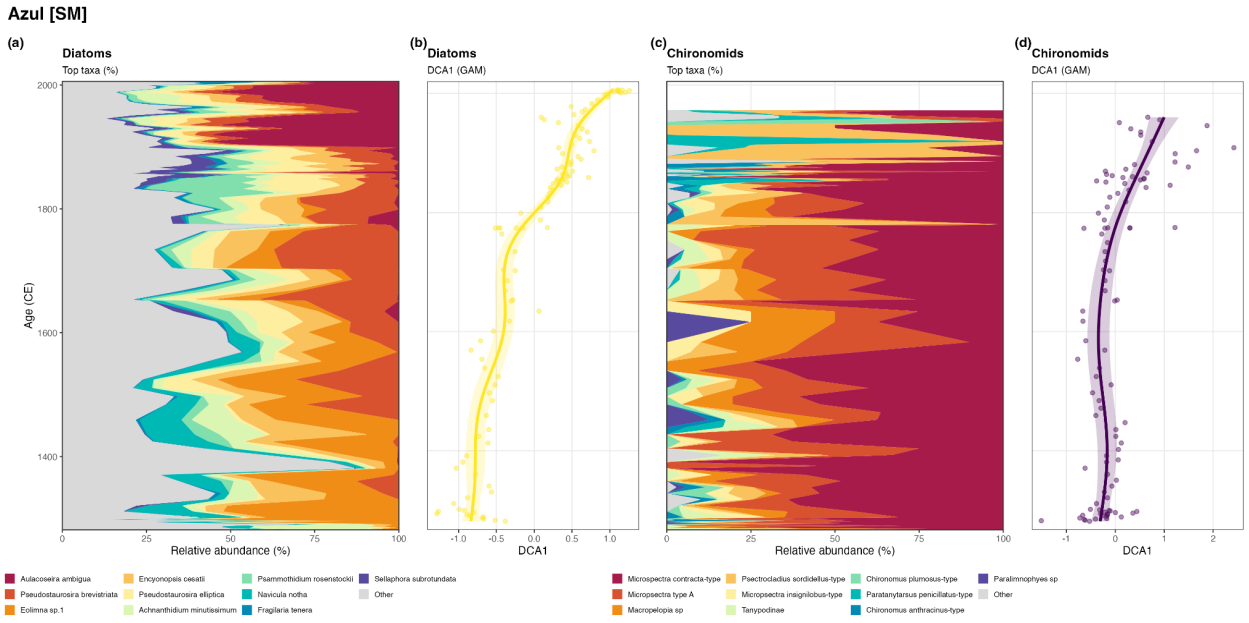

1.2. Caldeirão [CR]

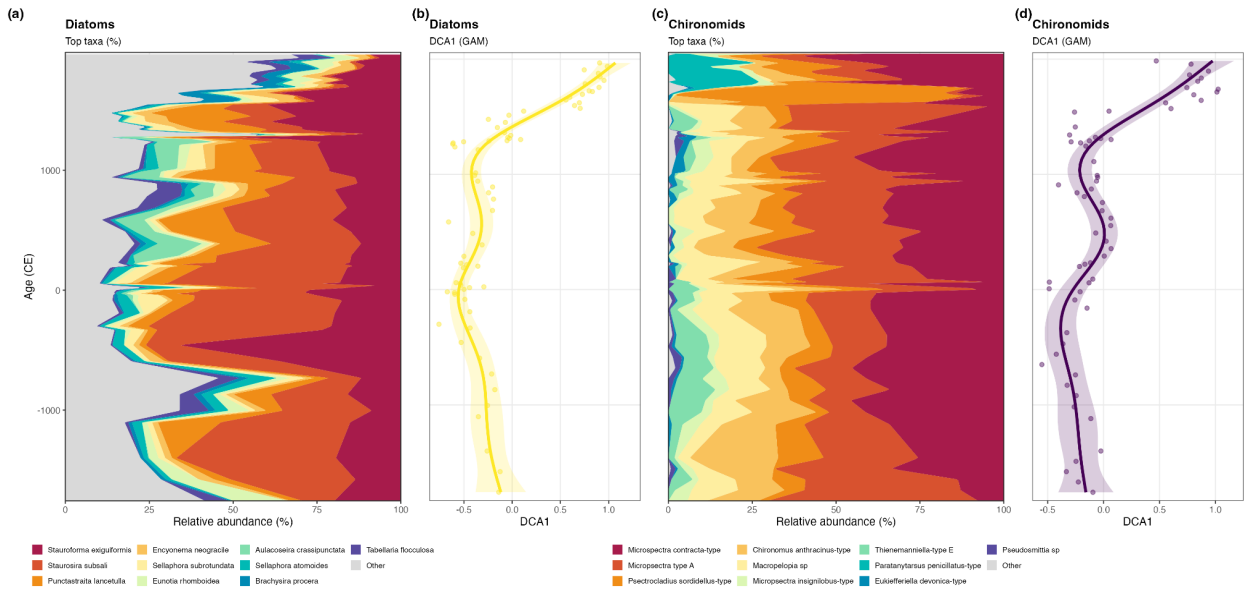

1.3. Caveiro [PI]

Caveiro [PI]

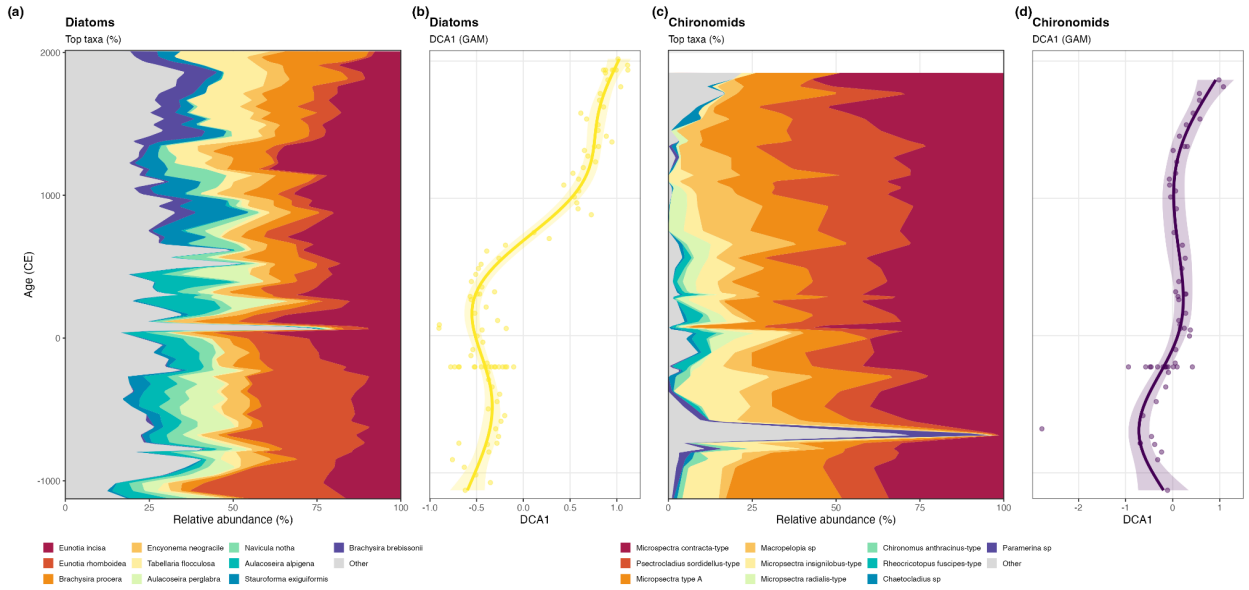

1.4. Empada. Norte [SM]

Empada. Norte [SM]

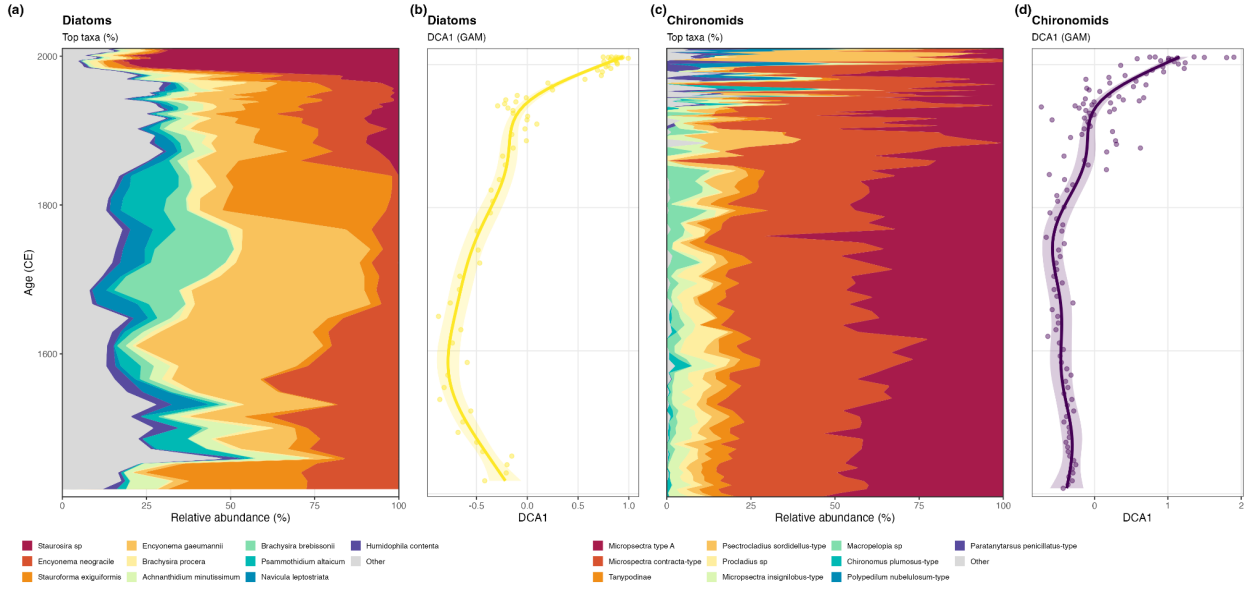

1.5. Funda [FL]

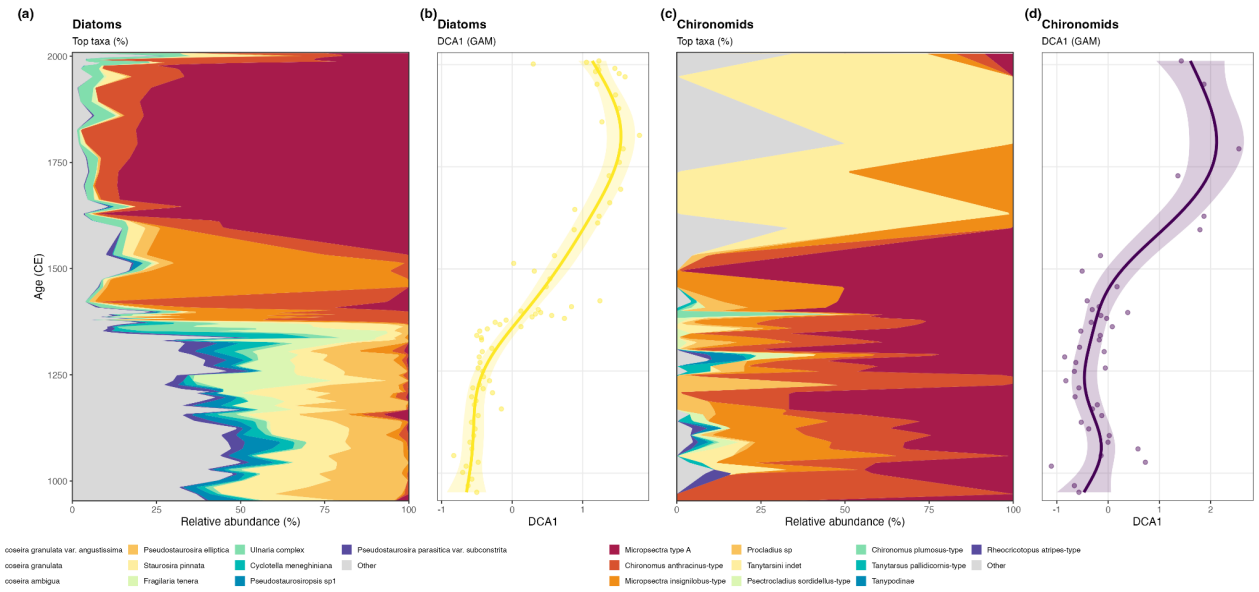

1.6. Ginjal [TE]

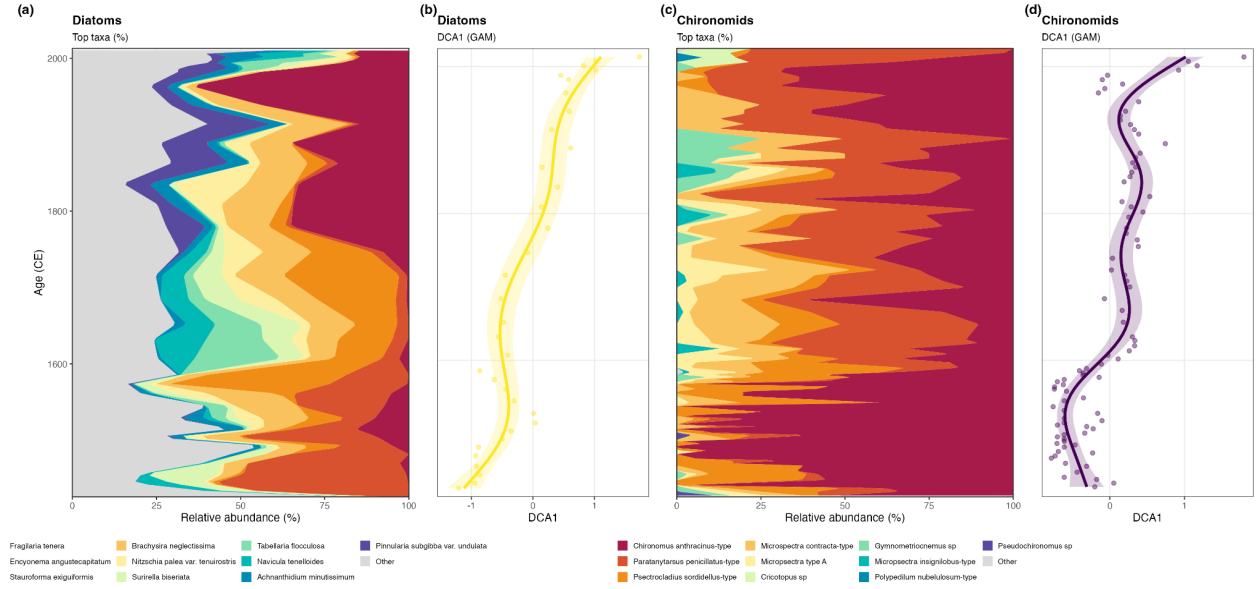

1.7. Peixinho [PI]

Peixinho [PI]

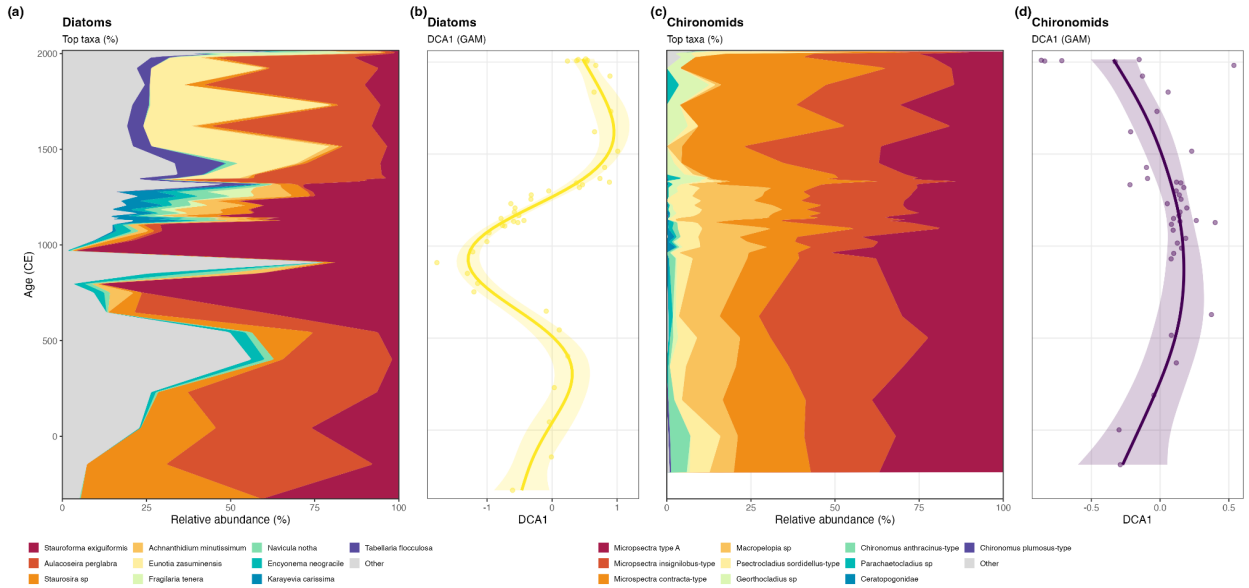

1.8. Prata [SM]

Prata [SM]

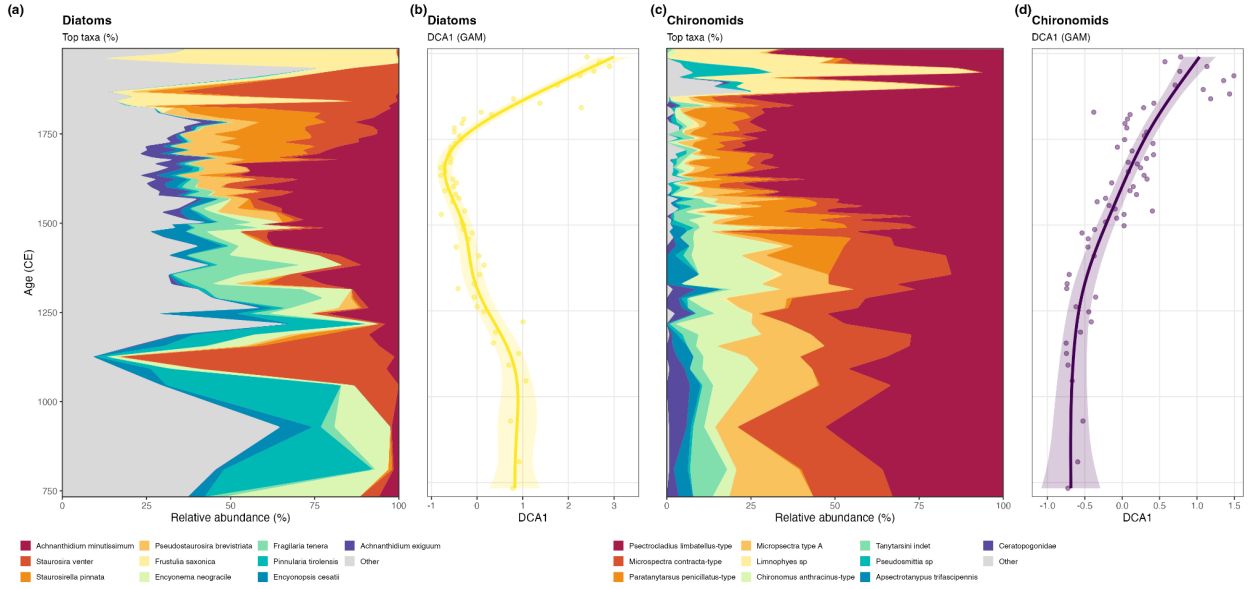

1.9. Santiago [SM]

Santiago [SM]

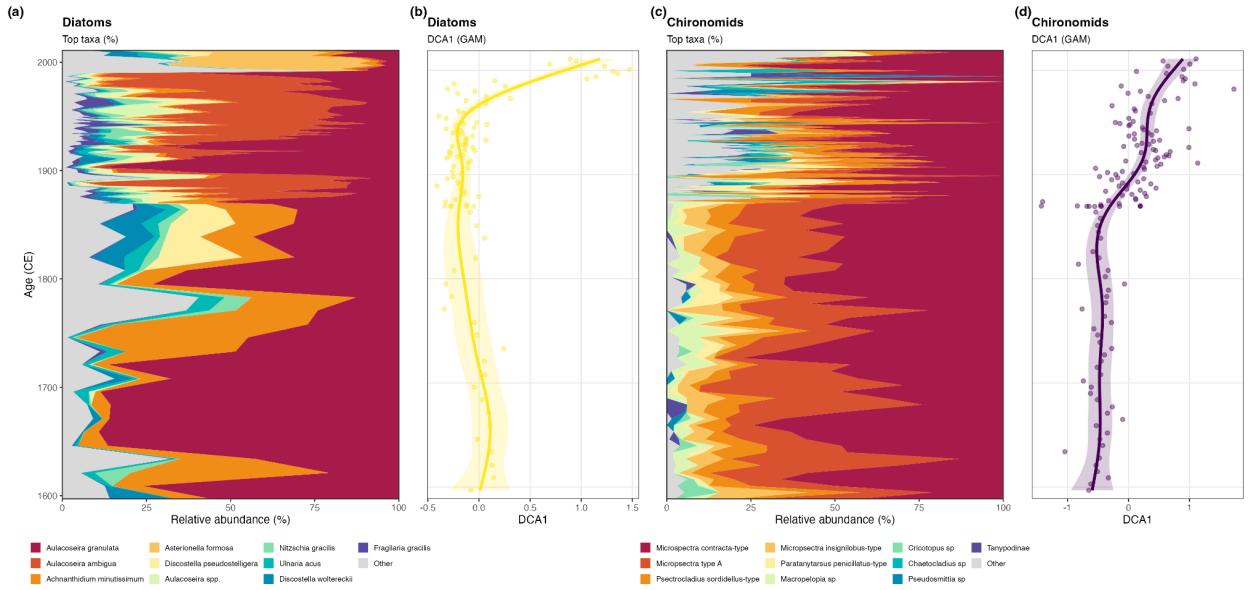

Figures

Fig. S1.

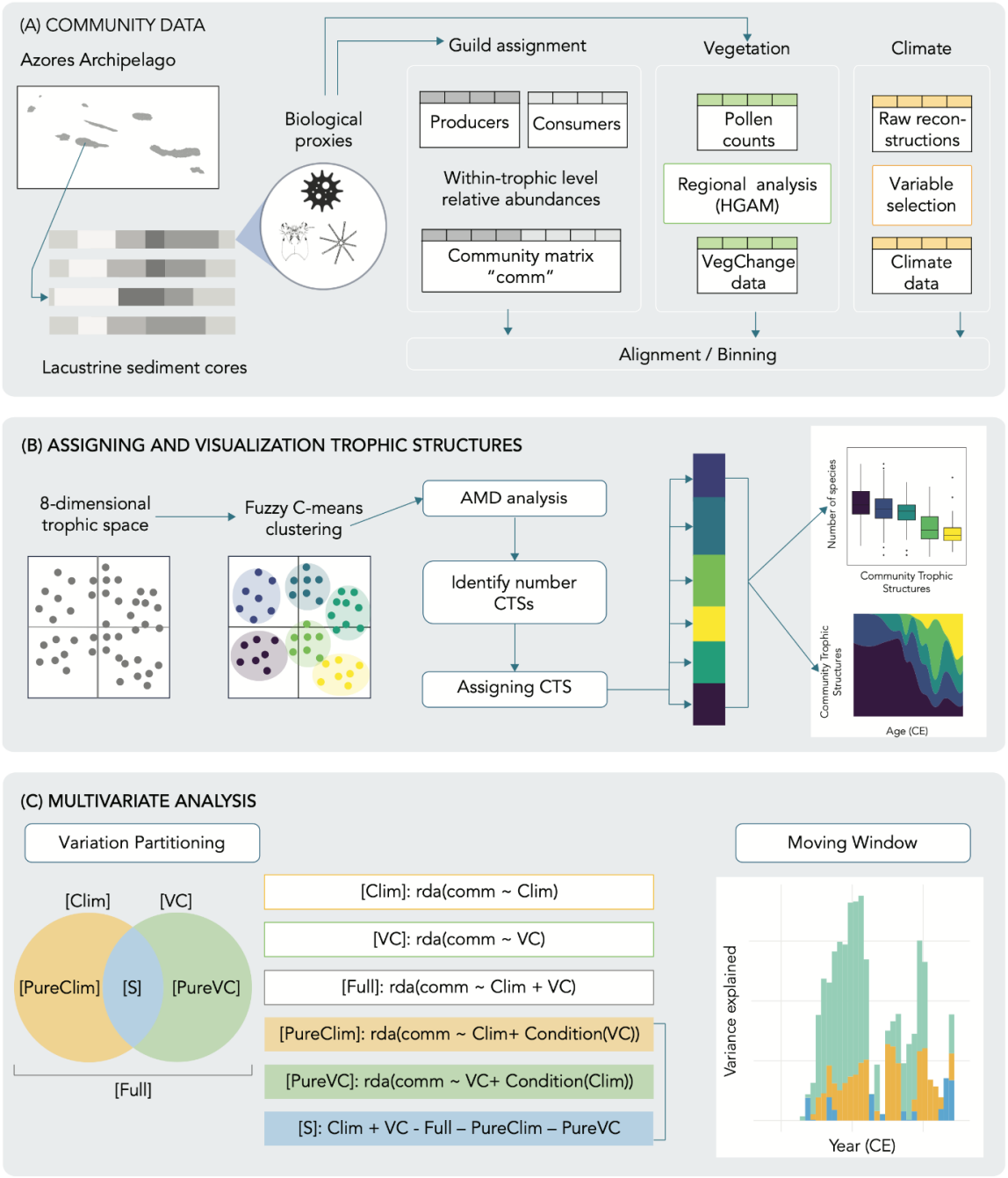

Figure S1. Conceptual workflow for reconstructing lake community trophic structure and quantifying the relative contributions of vegetation change and climate variability. (A) Fossil assemblage data (diatoms and chironomids) are extracted from lacustrine sediment cores across the Azores archipelago and taxonomically identified. Taxa are assigned to producer or consumer trophic levels and classified into eight functional guilds. Relative abundances are calculated within each trophic level and combined into a community composition matrix ("comm"). Catchment vegetation change is reconstructed from pollen data using regional hierarchical GAMs, and climate variability is represented by paleoclimate reconstructions following variable screening and selection. All datasets are temporally aligned and binned prior to analysis. (B)

Community trophic structures (CTSs) are identified in an eight-dimensional trophic space using fuzzy C-means clustering, with the optimal number of CTSs determined by average membership degree (AMD). CTSs are then assigned through time and visualized in terms of their composition and temporal dynamics. (C) Multivariate analyses use redundancy analysis (RDA)–based variation partitioning to quantify the unique ("pure") and shared contributions of climate (Clim) and vegetation change (VC) to community variation. Models estimate total explained variance ([Full]), individual effects ([Clim], [VC]), pure effects ([PureClim], [PureVC]), and shared variance ([S]). Temporal dynamics in driver contributions are further explored using a moving-window framework.

Fig. S2.

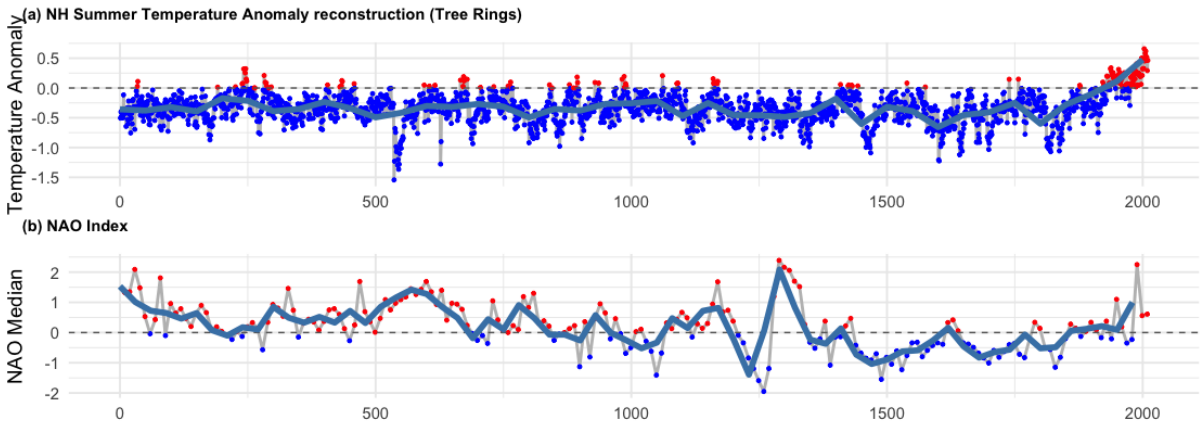

Figure S2. Long-term climatic variability over the past two millennia from hemispheric to regional scales. (a) Northern Hemisphere summer temperature anomalies reconstructed from tree-ring records (Büntgen et al., 2020), showing annual values (blue points) and a smoothed trend (blue line). Red points indicate years with positive anomalies. (b) Reconstructed North Atlantic Oscillation (NAO) index for the Central Iberian Peninsula based on multi-proxy sedimentary records (Hernández et al., 2020). Annual median values are shown (grey line), with a smoothed trend (blue line). Red points indicate years with positive NAO index values.

Fig. S3.

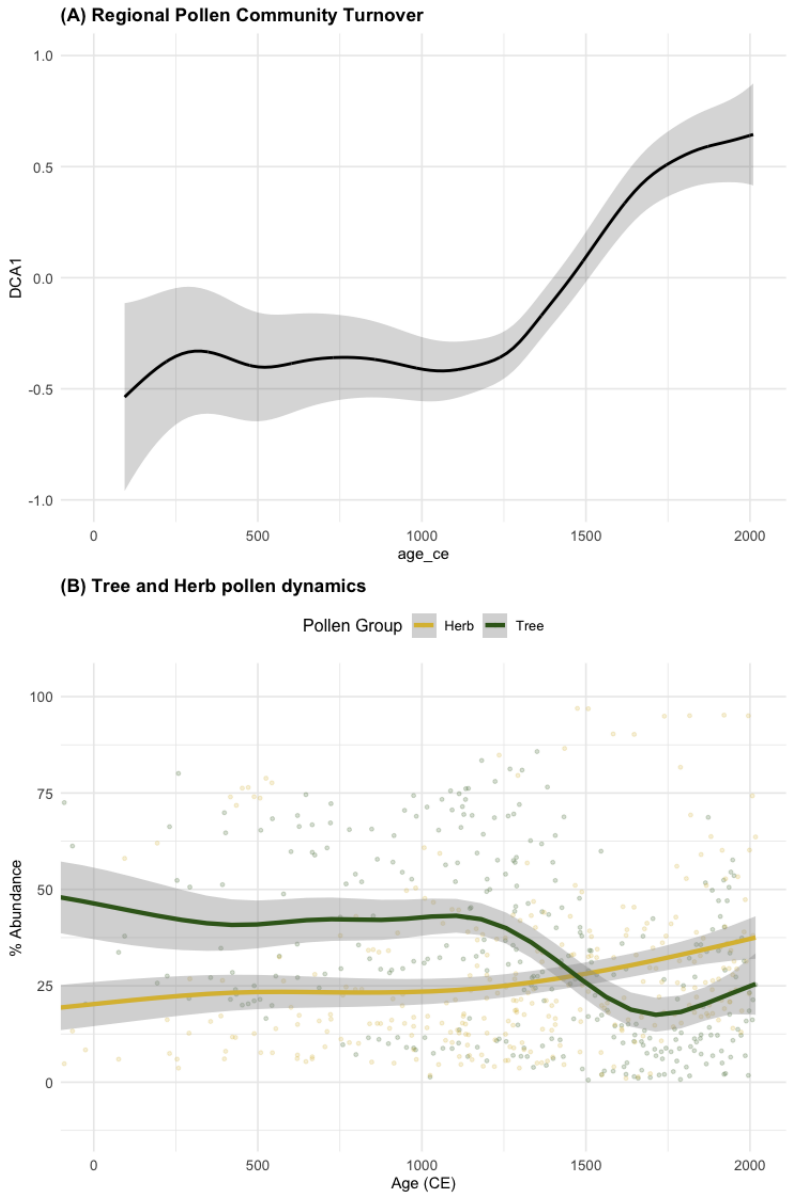

Figure S3. Regional trends in pollen community dynamics. (A) Generalized additive model (GAM) showing temporal variation in pollen community composition (DCA1 scores) across all lakes. Shaded ribbon indicates 95% confidence interval of the fitted smooth. (b) Temporal trajectories of Tree and Herb pollen groups based on relative abundance (%). Lines represent GAM-fitted smooths with 95% confidence intervals.

Fig. S4

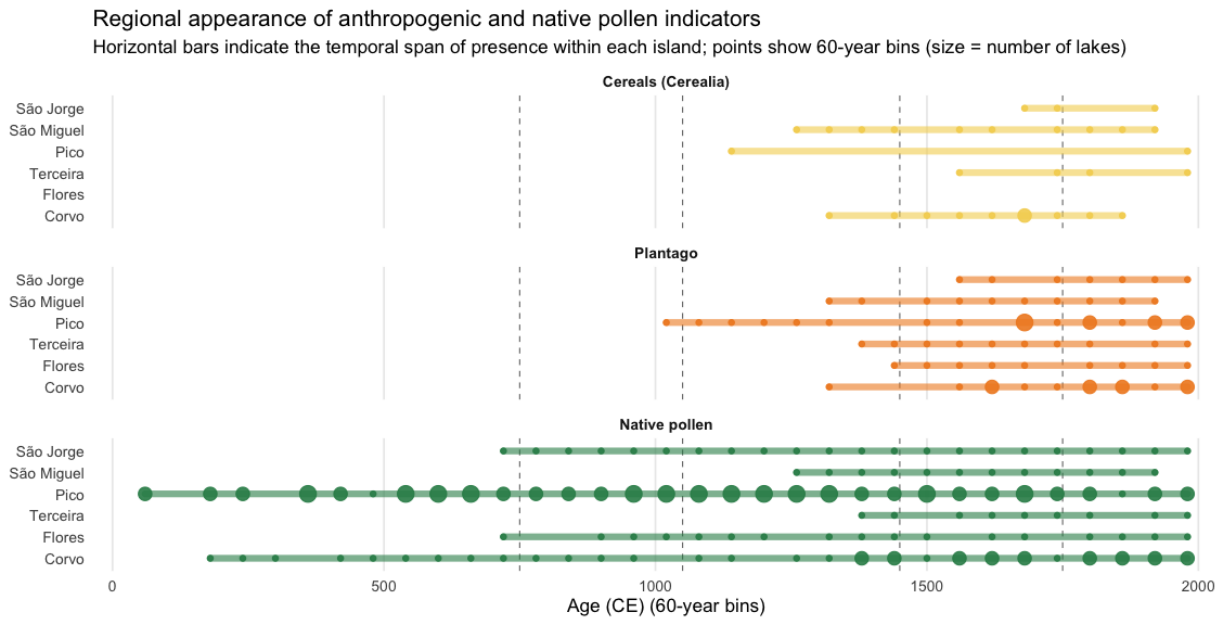

Figure S4. Regional appearance of anthropogenic and native pollen indicators across the Azores. Horizontal bars indicate the temporal span of presence of each pollen indicator within individual islands, while points represent 60-year bins (point size proportional to the number of lakes contributing data). Panels show the distribution of cereal-type pollen (Cerealia), Plantago, and native pollen taxa. The start date of the islands coincides with the oldest available age in the set of lake records for each island. Vertical dashed lines indicate major historical phase boundaries used in the main analyses. This figure provides contextual detail on the timing and spatial heterogeneity of land-use indicators that complement the regional vegetation proxy employed in the quantitative models.

Fig. S5

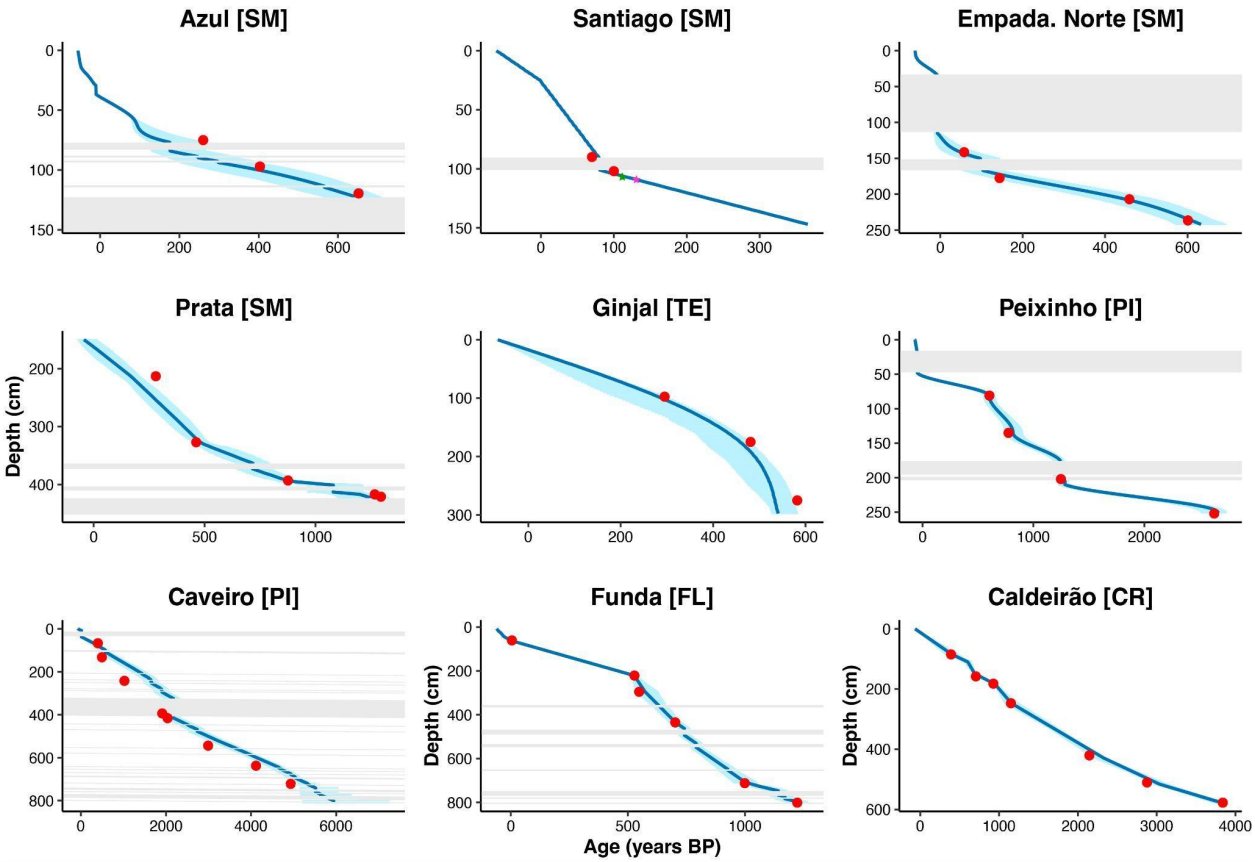

Figure S5. Age–depth models for the nine studied lakes. Age–depth models were constructed using combinations of radiocarbon (^{14}C) dates, ^{210}Pb and ^{137}Cs profiles (see Supplementary methods - Dating section for further information). Each panel shows modelled age (years BP) versus depth (cm) for a given lake, with calibrated radiocarbon dates indicated by red dots and shaded blue regions representing modelled 95% confidence intervals. Grey bands mark stratigraphic tie points and/or tephra layers where applicable.

Fig. S6

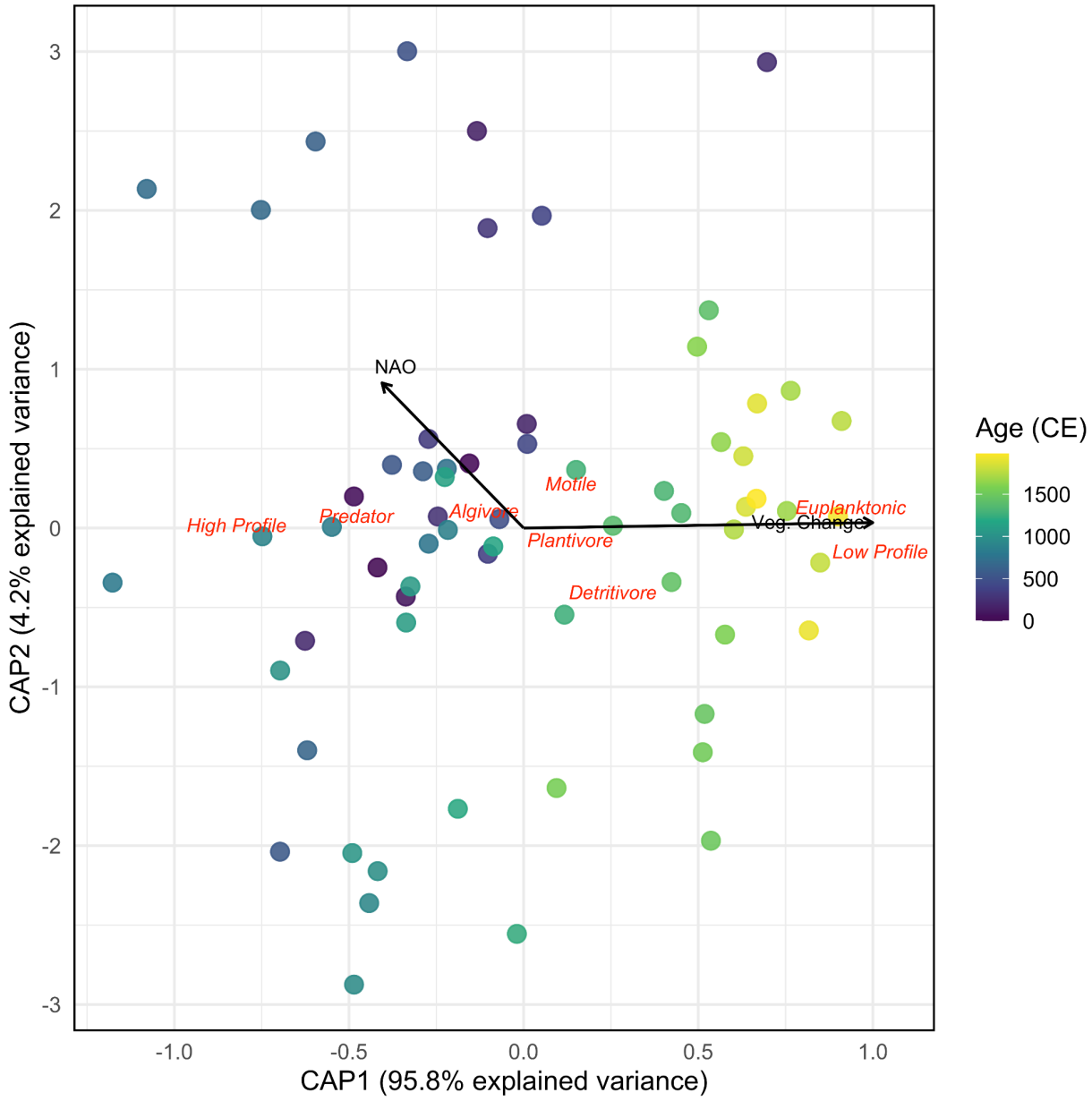

Figure S6. Constrained ordination of lake trophic guild composition in relation to climate and vegetation change. Canonical analysis of principal coordinates (CAP) based on Hellinger-transformed trophic guild abundances across all lakes and time bins. Arrows represent the direction and strength of the two selected environmental predictors—North Atlantic Oscillation (NAO) and vegetation change—retained after multicollinearity filtering and forward selection. Trophic guild centroids (red) indicate the positions of trophic groups in ordination space, including primary producers (high-profile, low-profile, motile, euplanktonic diatoms) and consumer guilds (algivores, detritivores, plantivores, predators). Points represent community composition for each 30-year time bin, colored by age (CE). Percentage inside brackets indicate constrained variance by each axes, CAP1 (89.6%) and CAP2 (10.4%).

Fig. S7

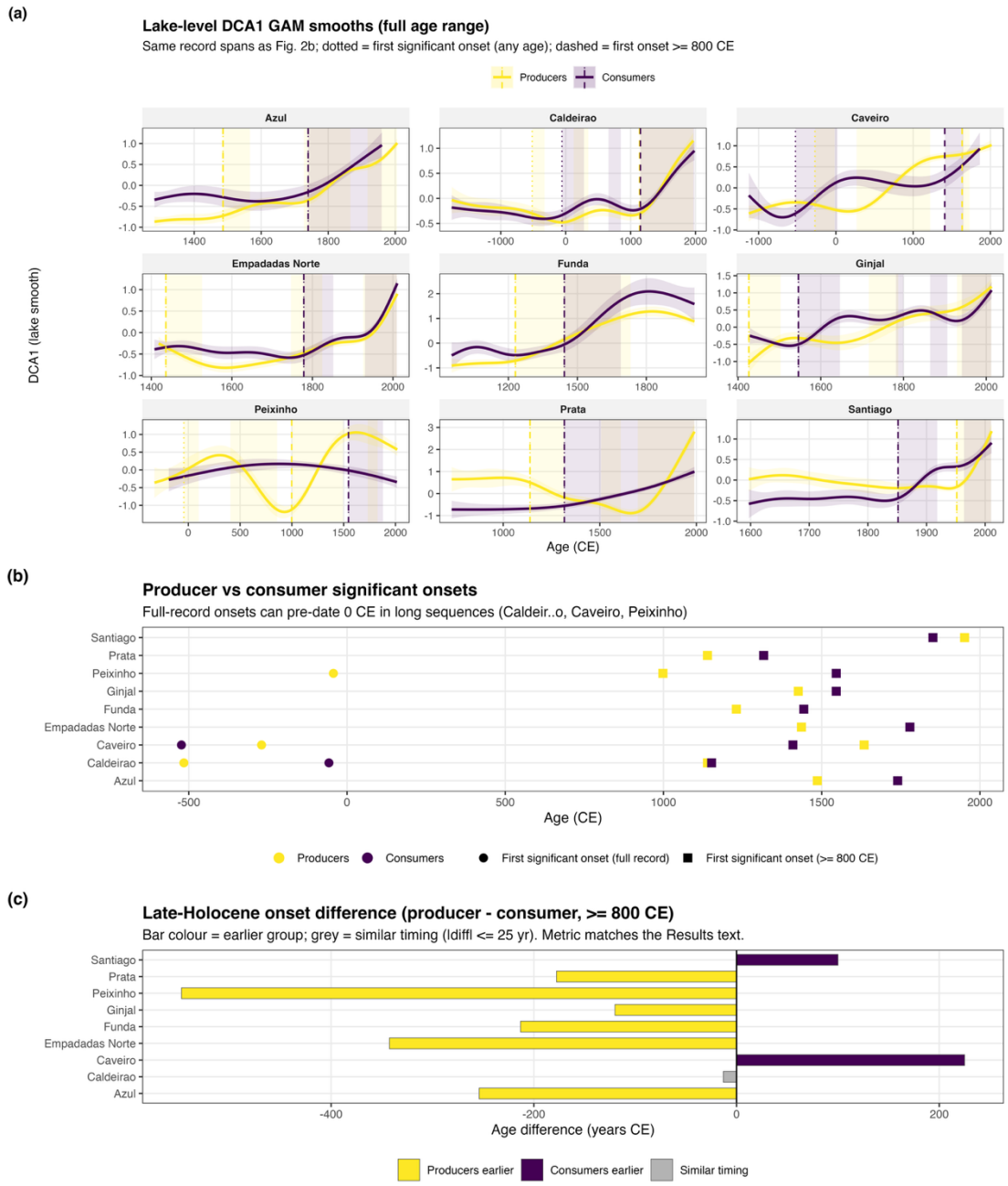

Fig. S7. Lake-level timing of late-Holocene compositional change for producers (diatoms) and consumers (chironomids). Per-lake DCA1 GAMs use the same records as Fig. 2b; significant change is assessed only for ages ≥800 CE (simultaneous 90% CI of the first derivative excludes zero), contemporaneous with regional vegetation restructuring. Earlier change intervals in long records are excluded by design. (a) First significant onset ages. (b) Onset difference (producer − consumer); negative = producers earlier. Producer turnover preceded consumer turnover in 6/9 lakes; Caldeirão near-synchrony; Caveiro and Santiago consumer-first.

Fig. S8

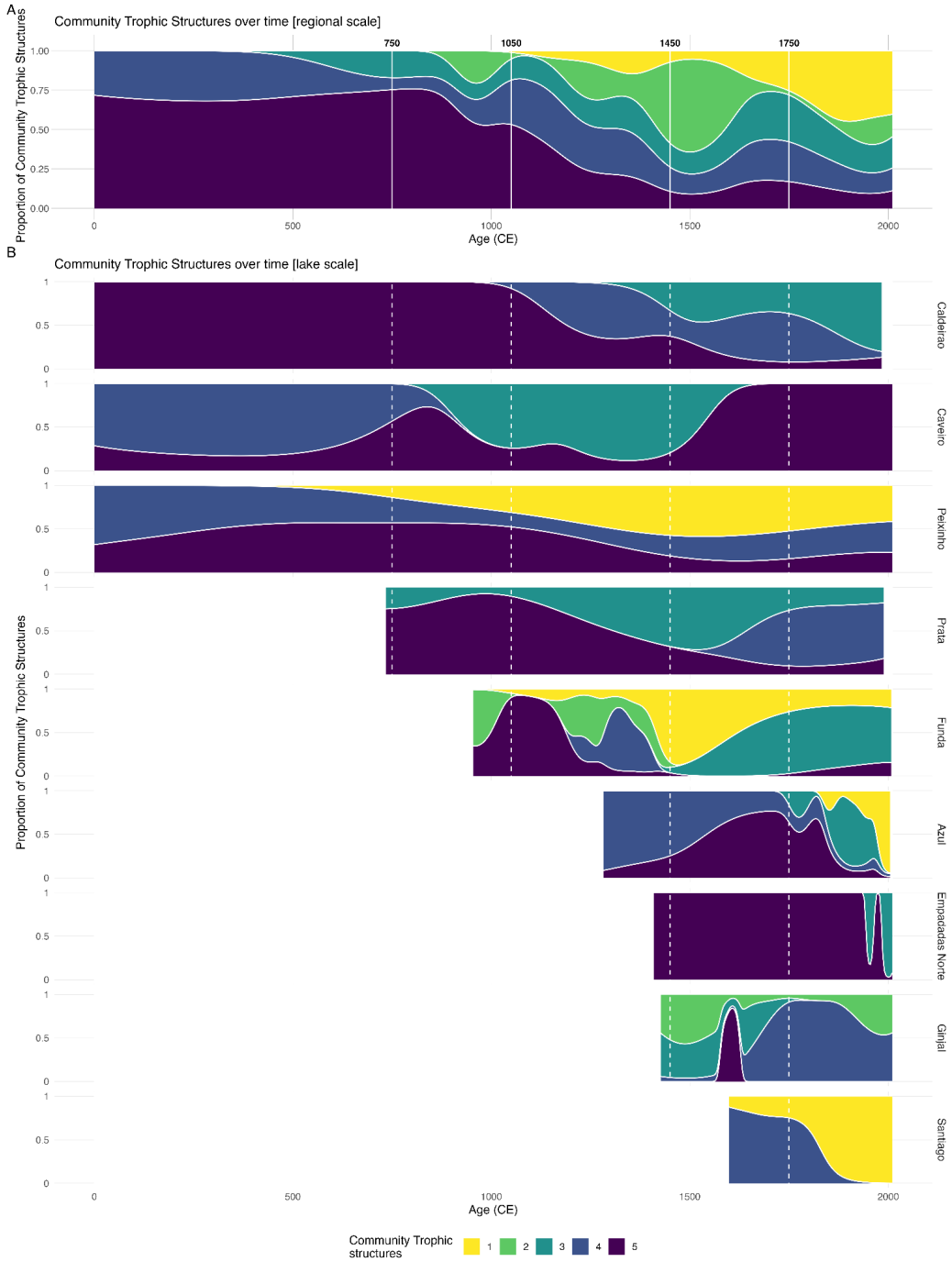

Figure S8. Temporal changes in community trophic structures at regional and lake scales. (A) Regional scale: Proportion of community trophic structures over time (0–2000 CE) aggregated at the regional level using a density function. Known shifts in lake ecosystems due to anthropogenic disturbance across the islands are indicated (700, 1050, 1450 and 1750 CE). The relative abundances of trophic guilds across different trophic structures (CTS1–CTS5). Notably, CTS1 (yellow) is dominated by euplanktonic diatoms, while CTS5 (dark purple) is characterised by greater relative abundances of predators and algivores. The intermediate community trophic structures (CTS2–CTS4) display varying contributions from high-profile, low-profile and motile diatoms, reflecting shifts in the composition and richness of different guilds along the trophic gradient (b) Lake scale: Temporal dynamics of community trophic structures for individual lakes (labeled on the right). The stacked areas show the relative proportions of community trophic structures over time within each lake, highlighting heterogeneity in the timing and direction of

shifts across lakes. This figure reveals both synchronised and asynchronous shifts in community trophic structures, with clear variability in responses at the regional versus lake scale.

Fig. S9

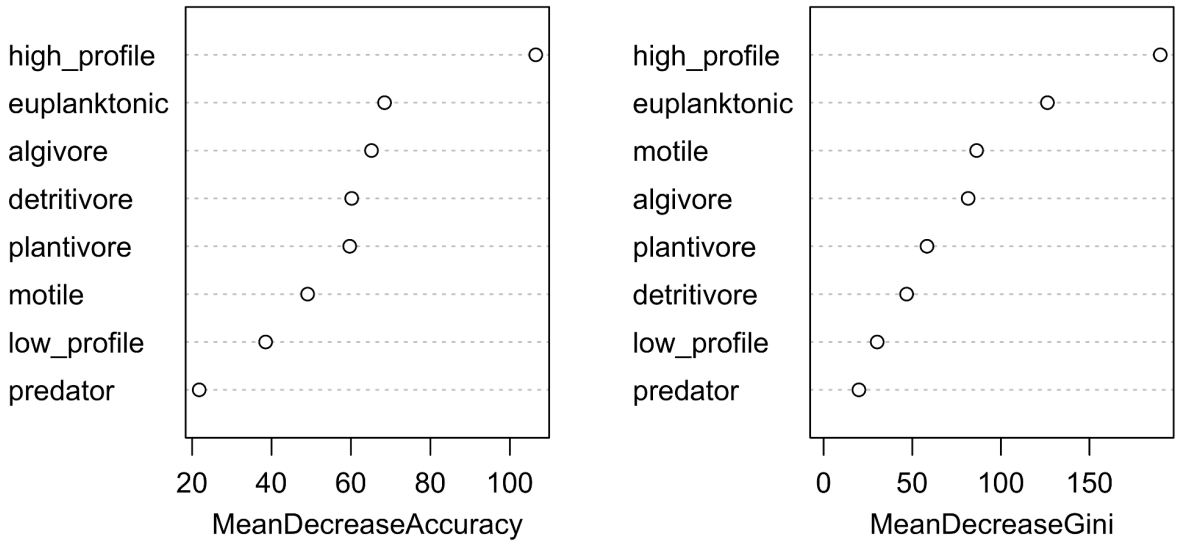

Figure S9. Random forest variable importance plot for predicting community trophic structures. Variable importance was quantified using two metrics: Mean Decrease in Accuracy (left), reflecting the reduction in predictive performance when each variable is permuted, and Mean Decrease in Gini (right), which measures each variable's contribution to node purity in the classification process. Variables associated with primary production (e.g., algivores, high-profile and euplanktonic diatoms) exhibited the greatest influence in both metrics, indicating their key role in differentiating trophic structural states.

Fig. S10

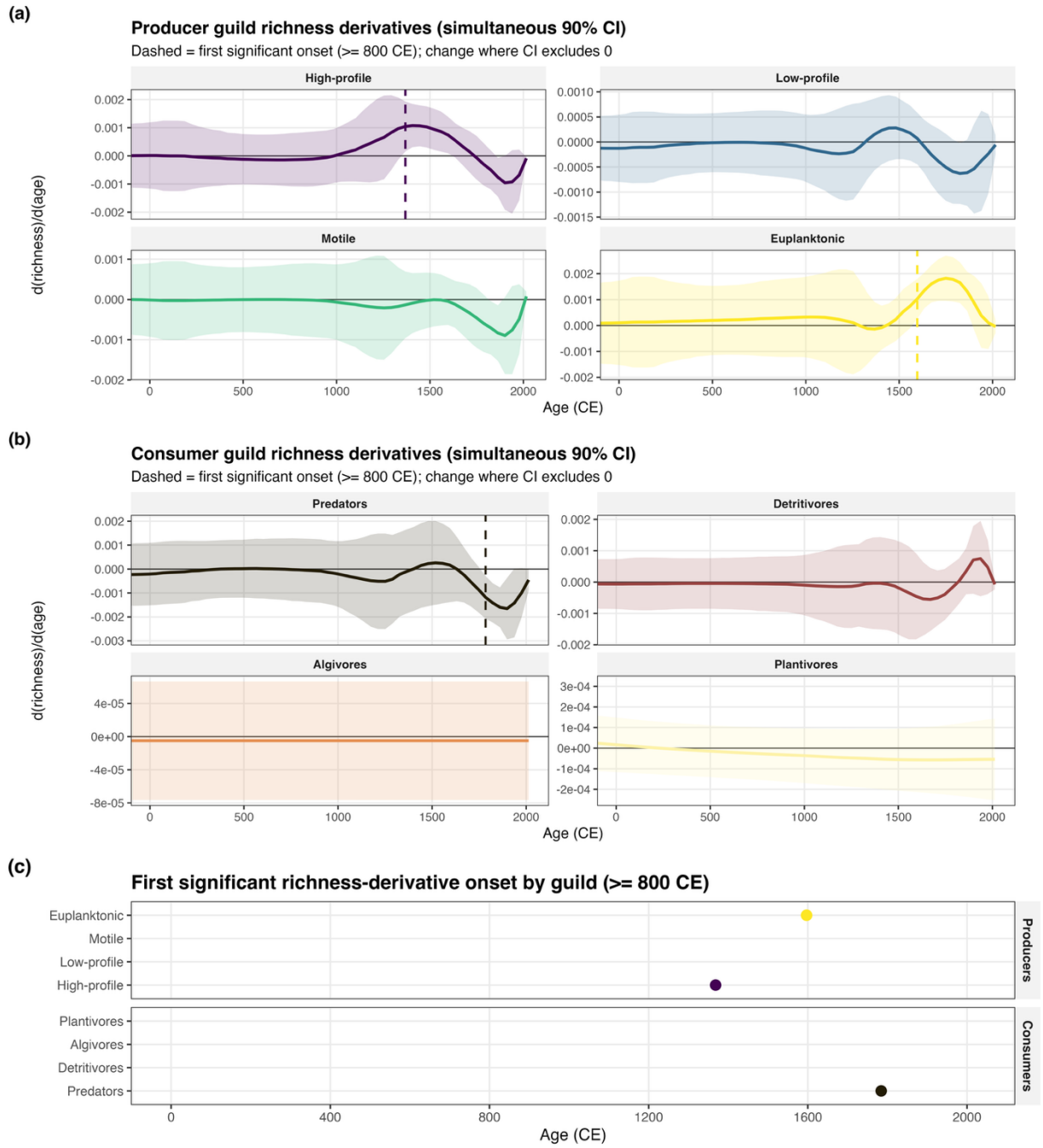
(a)
Producer guild richness derivatives (simultaneous 90% CI)
Dashed = first significant onset (>= 800 CE); change where CI excludes 0
High-profile
Low-profile
Motile
Euplanktonic
d(richness)/d(age)
Age (CE)
(b)
Consumer guild richness derivatives (simultaneous 90% CI)
Dashed = first significant onset (>= 800 CE); change where CI excludes 0
Predators
Detritivores
Algivores
Plantivores
d(richness)/d(age)
Age (CE)
(c)
First significant richness-derivative onset by guild (>= 800 CE)
Euplanktonic
Motile
Low-profile
High-profile
Plantivores
Algivores
Detritivores
Predators
Producers
Consumers
Age (CE)

Fig. S10. Timing of significant change in regional standardised guild-richness HGAM smooths (same models as Fig. 4). Significant change was defined where the simultaneous 90% confidence interval for the first derivative of s(age_ce) excludes zero. Dashed lines mark the first significant onset ≥800 CE. (a) Producer guild derivatives (high-profile, low-profile, motile, euplanktonic). (b) Consumer guild derivatives (predators, detritivores, algivores, plantivores). (c) First significant onset ages by guild.Fig. S11

Fig. S10

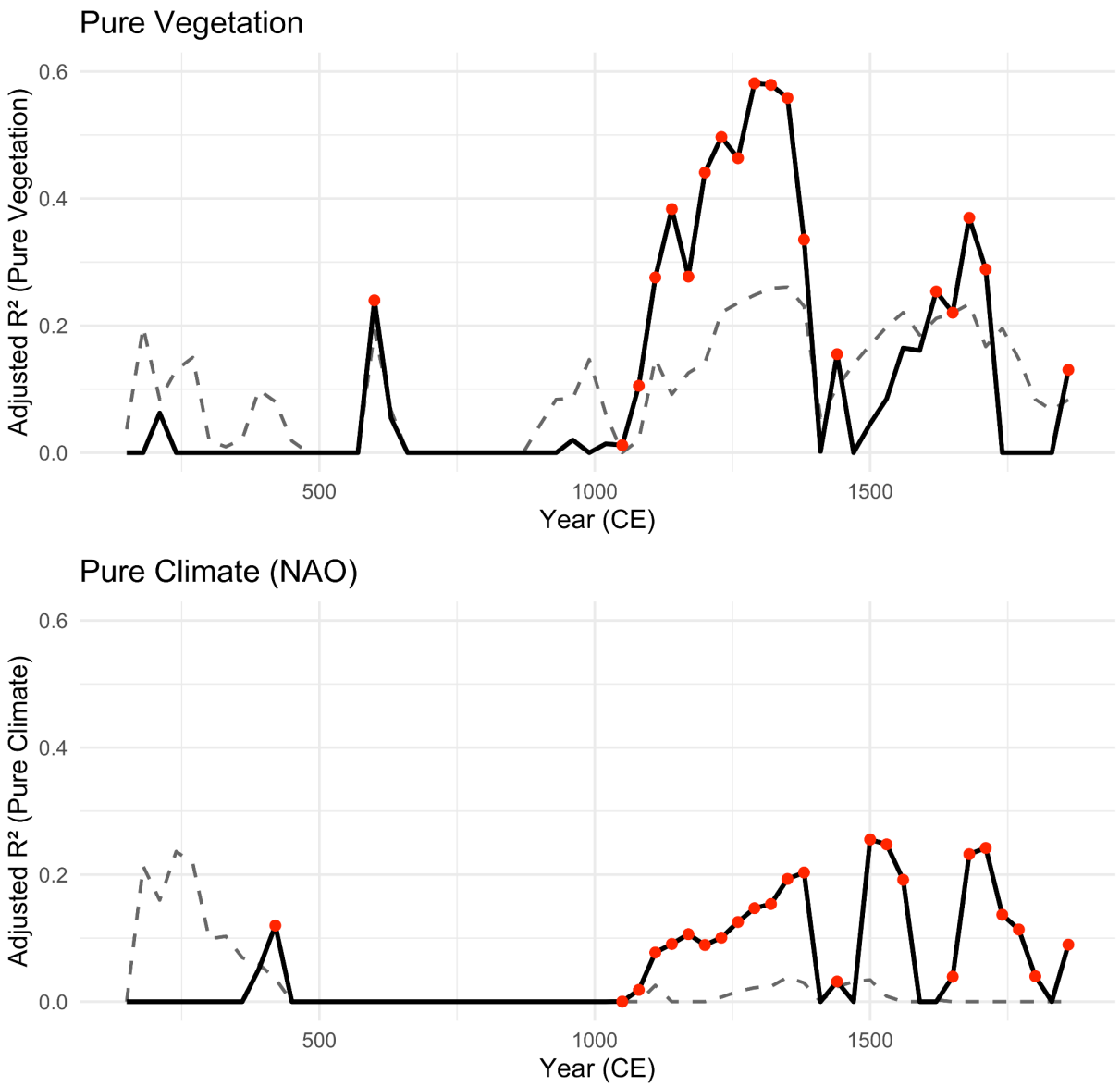

Figure S11. Observed versus null expectations for moving-window vegetation and climate effects. Observed adjusted R^2 values (solid black lines) for the pure vegetation (top) and pure climate (NAO; bottom) fractions from the moving-window variance partitioning are compared with the median expectation from a circular-shift null model (dashed grey lines). Red points indicate windows where observed values exceed the 50th percentile of the null distribution. The null model preserves lake-specific record length and within-lake variance while randomizing temporal alignment, thereby testing whether inferred signals arise solely from uneven core lengths or record position. The frequent exceedance of null expectations—particularly for vegetation during periods of major ecological reorganisation—demonstrates that the detected signals reflect genuine temporal coherence across lakes rather than artefacts of differing record lengths or coverage.

Tables

Table S1. Evidence for anthropogenic impacts across Azorean islands and historical phases. Presence indicates sustained or recurrent evidence within a phase; approximate onset dates are shown where first detected. The presence of fire is considered an indicator of human presence. Livestock presence inferred from the detection of Coprophilous fungal spores and 5β-stigmastanol. Deforestation is inferred from declines of arboreal pollen or drastic changes in relative proportions of non-arboreal and grass pollen. Agricultural indicators include cereals (*Cerealia*-type pollen) and *Plantago lanceolata*-type pollen. Fish introduction refers to historical or recent stocking events. Phases correspond to those shown in Fig. 1.

Island	Phase 1 <750	Phase 2 750–1050	Phase 3 1050–1450	Phase 4 1450–1750	Phase 5 >1750	Key references
Corvo	Fire	Fire; Livestock (~800)	Fire; Livestock; Deforestation (~1280); Plantago (~1350)	Fire; Livestock; Deforestation; Plantago; Cereals (~1550)	Fire; Livestock; Deforestation; Plantago; Cereals; Fish introduction	(Connor et al., 2012; Costa et al., 2021a; Raposeiro et al., 2021)
Pico	Fire	Fire; Livestock (~700)	Fire; Livestock; Plantago (~1050); Deforestation (~1150); Cereals (~1200)	Fire; Livestock; Deforestation; Plantago; Cereals	Fire; Livestock; Deforestation; Plantago; Cereals; Fish introduction	(Connor et al., 2012; Costa et al., 2021a; Raposeiro et al., 2021)
Terceira	—	—	Fire	Fire; Plantago (~1400)	Fire; Plantago; Cereals (~1550); Fish introduction	(Raposeiro et al., 2021); this study.
São Miguel	—	—	Fire	Fire; Livestock (~1280); Deforestation; Plantago (~1300); Cereals (~1290)	Fire; Livestock; Deforestation; Plantago; Cereals; Fish introduction	(Costa et al., 2021a; Raposeiro et al., 2021; Rull et al., 2017)
Flores	Fire	Fire	Fire	Fire; Livestock (~1350); Deforestation (~1420)	Fire; Livestock; Deforestation; Fish introduction	(Connor et al., 2012; Costa et al., 2021a; Raposeiro et al., 2021; Ritter et al., 2022)
São Jorge	—	—	Livestock (~1380); Deforestation (~1320)	Livestock; Deforestation; Plantago (~1600); Cereals (~1720)	Livestock; Deforestation; Plantago; Cereals; Fish introduction	(Costa et al., 2021a); this study.

Table S2: Location and main hydromorphological characteristics of the studied lakes. Lat - Latitude; Long - Longitude; Alt - Altitude; LA - Lake surface area; Zmax - Maximum depth; Catc area - Catchment area; Agri area - Agriculture area; Fore area - Forested area; Other area - other land uses (Porteiro 2000). * Lake Prata is currently a peatland, representing an advanced stage of lake terrestrialization.

Island	Lake	Lat (UTM)	Long (UTM)	Alt (m)	LA (km^2)	Zmax (m)	Catc area (km^2)	Agri area (%)	Fore area (%)	Other area (%)
São Miguel	Azul	4 192 418	608 244	260	3.59	25.4	15.4	42.3	52.4	7.6
São Miguel	Empadadas Norte	4 187 226	610 176	740	0.02	3.3	0.07	0	96.1	3.9
São Miguel	Santiago	4 189 551	607 989	360	0.25	28.8	0.8	0	100	0
São Miguel	Prata*	4 185 094	611 204	520	0.005	0.0	0.024	1.0	99.0	0
Terceira	Ginjal	4 282 978	486 248	390	0.006	1.0	0.073	100	0	0
Pico	Peixinho	4 254 694	397 515	870	0.013	7.8	0.344	99.3	0	0.7
Pico	Caveiro	4 254 780	395 554	903	0.004	3.1	0.032	0	0	100
Flores	Funda	4 363 277	653 538	360	0.35	31.9		15.2	84.7	0.1
Corvo	Caldeirão	4 397 542	661 871	410	0.23	2.2	2.95	70.4	26.3	3.3

Table S3: Main physicochemical parameters of the studied Azorean lakes. Cond - Conductivity; **TP** - Total phosphorus; **TN** - Total Nitrogen; **Si** - Silica; **Cl*a*** - Chlorophyll *a*; **Trophic State.** Data are derived from the Azores Regional Lake Monitoring Programme, conducted by the regional environmental authorities, with regular physicochemical surveys carried out between 2006 and 2020**,** data based on the regional monitoring program from 2006-2020

Island	Lake	pH	Cond ($\mu s\ cm^{-1}$)	TP ($\mu g\ P\ l^{-1}$)	TN ($mg\ N\ l^{-1}$)	Si ($mg\ SiO_2\ l^{-1}$)	Cl*a* ($\mu g\ l^{-1}$)	Trophic State
São Miguel	Azul	7.8±0.1	98±1.3	17.7±1.5	0.6±01	2.0±1.1	6.0±1.1	Mesotrophic
São Miguel	Empadadas Norte	6.9±01	35±0.8	21.6±1.3	0.6±0.1	2.3±0.3	6.1±1.3	Mesotrophic
São Miguel	Santiago	8.4±0.1	127±6.7	30.3±3.4	0.6±0.1	3.3±0.3	18.2±2.8	Eutrophic
São Miguel	Prata	n/a	n/a	n/a	n/a	n/a	n/a	n/a
Terceira	Ginjal	n/a	n/a	n/a	n/a	n/a	n/a	n/a
Pico	Peixinho	6.9±0.2	32±5.4	33.7±2.1	0.63±0.1	3.15±0.2	49.3±3.4	Eutrophic
Pico	Caveiro	7.0	38	10	0.4	n/a	4.83	Mesotrophic
Flores	Funda	8.7±0.1	100.4±10.1	28.8±3.1	0.28±0.2	7.9±0.3	53.4±4.6	Eutrophic
Corvo	Caldeirão	6.0±0.1	78.2±3.1	94±2.2	0.9±0.3	2.2±0.2	9.6±3.8	Mesotrophic

Table S4. Radiocarbon dating results of sedimentary sequences from the Azores archipelago. Radiocarbon data include laboratory codes (UCIMAS – University of California, ULA – Université Laval and Beta – Beta Analytic), sample core labels, composite depths (cm), material type, pre-treatment methods, fraction modern ($F^{14}C$) and associated error (±), $\Delta^{14}C$ values and error (±), measured (uncalibrated) radiocarbon ages and error (±), and calibrated ages expressed as median probability (cal yr BP) with 2σ ranges. Samples are from lake sediments on São Miguel, Terceira, Pico, Flores and Corvo islands (Sáez et al., 2025). "Plant macrorest" refer to identifiable fragments of land plants (e.g. leaves, wood or stems) preserved in the sediments and used for radiocarbon dating to avoid aquatic reservoir effects.

Laboratory code	Sample core label	Composite depth cm	Material	Pre Treatments	$F^{14}C$	±	$D^{14}C$	±	Measured ^{14}C age	±	Median probability (cal a BP)	2σ (years)
Lake Azul (São Miguel Island)												
Beta-326,594	AZ11–02-55	55	Plant macrorest	none					154.4 ± 0.4 pMC	1990 CE		
Beta-316,595	AZ11–02-460	75	Plant macrorest	HCl-NaOH-HCl					260	30	305	−27/25
Beta-331,408	AZ11–02-610	90	Pollen con.	HCl-NaOH-HCl					410	30	480	−50/37
Beta-331,409	AZ11–02-860	121	Plant macrorest	HCl-NaOH-HCl					690	30	654	−22/23
Lake Empadadas Norte (São Miguel Island)												
Beta-316,589	EMN04/02–54	141.5	Plant macrorest	none					50	30	58	0.26/26
Beta-333,756	EMN04/02–90	177.5	Plant macrorest	none					150	30	144	−24/88

Beta-316,590	EMN04/02–119.5	207	Plant macrorest	none			390	30	459	−33/48
Beta-316,591	EMN11/04–03–23	236.5	Plant macrorest	none			630	30	601	−48/55
Lake Prata (São Miguel Island)										
UCIAMS_243063	M5_12–14	213	raw sample	none	−24.4	1.7	200	15	280	−13/13
UCIAMS_243065	M7_26–28	327	raw sample	none	−44.9	1.6	370	15	462	−32/32
UCIAMS_243067	M8–42-44	393	raw sample	none	−108.8	1.5	925	15	876	−33/33
UCIAMS_243068	M9_16–18	417	raw sample	none	−150.1	1.5	1305	15	1267	−21/21
UCIAMS_243069	M9_20–22	421	raw sample	none	−158.0	1.3	1380	15	1295	−12/12
Lake Santiago (São Miguel Island)										
Beta-321,974	SA11_01B-4	4	Plant macrorest	HCl-NaOH-HCl			106.4 +/− 0.3 pMC	1996 CE		
Beta-321,975	SA11_01B-19	19	Plant macrorest	HCl-NaOH-HCl			114.5 +/− 0.4 pMC	1995 CE		
Beta-331,413	SA11_01B-79	79	Plant macrorest	HCl-NaOH-HCl			430	30	496	−57/30
Beta-331,414	SA11_02B_50	50	Plant macrorest	HCl-NaOH-HCl			114.8 ± 0.4 pMC	30	1994 CE	

Beta-331,415	SA11_02B_103	103	Plant macrorest	HCl-NaOH-HCl				330	30	390	−70/81	
Beta-321,655	SA11_02B-124	124	Plant macrorest	HCl-NaOH-HCl				570	30	600	−13/43	
Beta-321,977	SA11_03B_41(s)	41	Plant macrorest	HCl-NaOH-HCl				100	30	1870 CE/80 BP		
Beta-321,978	SA11_03B_64(s)	64	Plant macrorest	HCl-NaOH-HCl				70	30	1893 CE/57 BP		
Beta-321,973	SA11_01B-1	1	Plant macrorest	HCl-NaOH-HCl				105.8 +/− 0.3 pMC	1996 CE			
Lake Ginjal (Terceira Island)												
ULA-8211	GW01–02-47.5	97.5	raw sample	HCl				245	15	295	-0.7142857	
ULA-8210	GW01–04-25	175	raw sample	none				400	20	481	−36/14	
ULA-8212	GW01–05-37.5	275	raw sample	HCl				690	20	605	−16/28	
Lake Caveiro (Pico Island)												
ULA-5793	CVL-1B-1-65-68	67	Pollen con.	none	0.9645	0.0017	−35.5	1.7	290	15	400	−14/29
ULA-5713	CVL-1B-1-132-133	132.5	Pollen con.	none	0.9489	0.0022	−51.1	2.2	420	20	495	−34/19
ULA-5724	CVL-1B-2-79-80	260	Pollen con.	HCl	0.8768	0.002	−123.2	2	1055	20	946	−23/29

ULA-5715	CVL-1B-3-63-64	423	Pollen con. none	0.789	0.0018	−211.0	1.8	1905	20	1807	−67/66
ULA-5717	CVL-1B-3-43-44	401	Pollen con. HCl	0.7803	0.0018	−219.7	1.8	1995	20	1933	−61/59
ULA-5714	CVL-1B-4-8-9	551	Pollen con. none	0.6996	0.0017	−300.4	1.7	2870	20	2991	−63/79
ULA-6290	CVL-1B-4-82-83	644.5	Pollen con. HCl	0.6268	0.0012	−373.2	1.2	3750	20	4116	−39/39
ULA-5722	CVL-1B-5-13-14	736	Pollen con. HCl	0.5797	0.0015	−420.3	1.5	4380	25	4931	−69/50
ULA-6289	CVL-1B-5-53-54	782	Pollen con. HCl	0.5652	0.0012	−434.8	1.2	4585	20	5311	−26/13
ULA-5723	CVL-1B-6-7-8	911	Pollen con. HCl	0.3991	0.0011	−600.9	1.1	7380	25	8193	−30/129
Lake Peixinho (Pico Island)											
ULA-5708	PEX-1B-1-36	36	Pollen con. none	1.1946	0.0031	194.6	3.1	Modern		1985 CE	
ULA-6292	PEX-1B-50	51	Pollen con. HCl	0.9454	0.0018	−54.6	1.8	450	20	507	−15/18
ULA-5705	PEX-1 A-1-81	81	Pollen con. none	0.9264	0.0021	−73.6	2.1	615	20	603	−22/46
ULA-5788	PEX-1 A-1-135	135	Pollen con. none	0.895	0.0016	−105.0	1.6	890	15	775	-2.1578947
ULA-5707	PEX-1Csup-53	202	Pollen con. none	0.8491	0.0021	−150.9	2.1	1315	20	1248	−3/46

ULA-5719	PEX-1Csup-104	252	Pollen con.	HCl	0.7288	0.0017	−271.2	1.7	2540	20	2631	−67/90
Lake Funda (Flores Island)												
ULA-7746	FN02–01-52.8	60.8	Pollen con.	HCl-NaOH-HCl	1.0097	0.0025	9.7	2.5	Modern		1955 CE	−3/3
ULA-7657	FN02–02-34	221.2	Pollen con.	HCl-NaOH-HCl	0.9385	0.0017	−61.5	1.7	510	15	528	−14/13
ULA-7745	FN02–02-108	295.2	Pollen con.	HCl-NaOH-HCl	0.9338	0.0022	−66.2	2.2	550	20	548	−22/08
ULA-7744	FN02–03-67	435	Pollen con.	HCl-NaOH-HCl	0.9067	0.0022	−93.3	2.2	785	20	702	−26/24
ULA-7739	FN02–04-135	712	Pollen con.	HCl-NaOH-HCl	0.8722	0.002	−127.8	2	1100	20	999	−42/13
ULA-7737	FN02–05-73	801	Pollen con.	HCl-NaOH-HCl	0.8508	0.002	−149.2	2	1300	20	1223	−46/02
Lake Caldeirão (Corvo Island)												
ULA-7749	CL08–01-55	58	Pollen con.	HCl-NaOH-HCl	0.9432	0.0022	−56.8	2.2	470	20	514	−16/14
ULA-7653	CL08–02-59	242	Pollen con.	HCl-NaOH-HCl	0.7824	0.0015	−217.6	1.5	1970	20	1900	−36/45
ULA-7652	CL08–03-77	454	Pollen con.	HCl-NaOH-HCl	0.6204	0.0013	−379.6	1.3	3835	20	4230	−80/68

Table S5: Summary of the studied proxies and their sampling resolution (cm) per lake

Island	Lake	Diatoms	Chironomids	Pollen	Bulk organic matter	Reference
São Miguel	Azul	2	1	2	1	(Raposeiro et al., 2017, 2021; Rull et al., 2017; Vázquez-Loureiro et al., 2023)
São Miguel	Empadadas Norte	1-4	1-2	na	1	(Hernández et al., 2017)
São Miguel	Santiago	1-2	1	na	1	(Vázquez-Loureiro et al., 2023)
São Miguel	Prata	4-8	4-8	na	4-8	(Raposeiro et al., 2024)
Terceira	Ginjal	2.5-5	2.5-5	10	5	(Raposeiro et al., 2021)
Pico	Peixinho	4	4	4-8	4	(Raposeiro et al., 2021)
Pico	Caveiro	5-10	5-10			(Benavente Marín, 2024)
Flores	Funda	10	10	5-10	5	(Ritter et al., 2022)
Corvo	Caldeirão	5-10	5-10	10-20	5-10	(Raposeiro et al., 2021)

Table S6. Sensitivity of phase-based variance partitioning to historical phase boundaries. For each historical phase, we report the median absolute deviation in adjusted R^2 (Δ Adj. R^2) of pure climate (NAO), pure vegetation, and shared variance components across 625 alternative phase configurations. Phase boundaries were systematically perturbed by ±30–60 years while preserving phase order and minimum sample-size requirements. Low median deviations across all phases indicate high robustness of variance partitioning results to reasonable boundary shifts.

Phase	Variance component	Median absolute Δ Adj. R^2
Phase 1	Pure NAO	0.00
Phase 1	Pure vegetation	0.00
Phase 1	Shared	0.00
Phase 2	Pure NAO	0.00
Phase 2	Pure vegetation	0.00
Phase 2	Shared	0.00
Phase 3	Pure NAO	0.01
Phase 3	Pure vegetation	0.05
Phase 3	Shared	0.00
Phase 4	Pure NAO	0.05
Phase 4	Pure vegetation	0.07
Phase 4	Shared	0.00
Phase 5	Pure NAO	0.03
Phase 5	Pure vegetation	0.07
Phase 5	Shared	0.08

Table S7. Leave-one-out sensitivity of phase-based variance partitioning. For each lake removed in turn, values summarize the mean and median adjusted R^2 of the pure climate (NAO; A), pure vegetation (B), and shared components across the five historical phases. Δ values indicate deviation from the baseline analysis, including all lakes. Dominance metrics report the proportion of phases in which vegetation explained more variance than climate.

Lake excluded	Mean pure Clim	Mean pure VC	Mean shared	Median pure Clim	Median pure VC	Mean (VC − Clim)	Δ mean pure Clim	Δ mean pure VC	Δ mean shared	Phases	VC dominant (prop.)
Funda	0.025	0.249	0.054	0	0.154	0.224	−0.011	0.057	0.042	5	1
Prata	0.048	0.161	0.014	0.006	0.128	0.113	0.013	−0.031	0.002	5	1
Ginjal	0.046	0.164	0.005	0	0.127	0.118	0.01	−0.029	−0.007	5	1
Azul	0.02	0.167	~0	0	0.171	0.146	−0.015	−0.026	−0.012	5	1
Caldeirão	0.045	0.205	0.017	0.004	0.141	0.16	0.01	0.013	0.005	5	1
Santiago	0.038	0.18	0.004	~0	0.122	0.142	0.003	−0.013	−0.008	5	1
Empadadas N.	0.034	0.202	0.002	0	0.125	0.168	−0.001	0.01	−0.010	5	1
Peixinho	0.026	0.191	0.022	0.017	0.151	0.165	−0.010	−0.002	0.01	5	1
Caveiro	0.021	0.193	0.007	0	0.173	0.173	−0.015	0.001	−0.005	5	1

Table S8. Leave-one-out (LOO) sensitivity of moving-window variance partitioning. For each lake removed in turn, the table reports mean and median adjusted R^2 values for the pure climate (A; NAO) and pure vegetation (B) fractions across all 300-year moving windows, the mean difference between vegetation and climate effects (B − A), and the proportion of windows in which vegetation or climate explained the larger share of variance. Across all LOO iterations, vegetation consistently dominates over climate in the majority of windows, and effect sizes and temporal patterns remain stable, indicating that the observed dominance of vegetation is not driven by any single lake record.

leave_out	mean_pure_A	mean_pure_B	median_pure_A	median_pure_B	mean_diff_BA	prop_windows_B_dominant	prop_windows_A_dominant
Azul	0.038	0.108	0.000	0.000	0.070	0.879	0.121
Caldeirao	0.083	0.131	0.002	0.004	0.048	0.759	0.241
Caveiro	0.056	0.120	0.000	0.017	0.064	0.793	0.207
Empadadas Norte	0.051	0.124	0.000	0.004	0.073	0.862	0.138
Funda	0.053	0.144	0.000	0.020	0.092	0.828	0.172
Ginjal	0.042	0.111	0.000	0.007	0.069	0.879	0.121
Peixinho	0.048	0.108	0.000	0.000	0.060	0.845	0.155
Prata	0.076	0.102	0.018	0.008	0.026	0.741	0.259
Santiago	0.055	0.117	0.000	0.001	0.062	0.862	0.138

References

Appleby, P. G., & Oldfield, F. (1978). The calculation of lead-210 dates assuming a constant rate of supply of unsupported 210Pb to the sediment. *Catena*, (5), 1–8.

Benavente Marín, M. (2024). The biogeochemical imprint of the Azores Archipelago lacustrine sedimentary infill. A linkage between the climatic effects of the north Atlantic atmospheric circulation and the tectono-volcanic landscape of the triple junction during the late Holocene [Ph.D. Thesis, Universitat de Barcelona]. In *TDX (Tesis Doctorals en Xarxa)*. https://www.tdx.cat/handle/10803/693403

Blaauw, M., Christen, J. A., Vazquez, J. E., & Goring, S. (2020). clam: Classical Age-Depth Modelling of Cores from Deposits. *R Package Version 2.3.7*. https://cran.r-project.org/package=clam

Brooks, S. J., Langdon, P. G., & Heiri, O. (2007). *The Identificiation and Use of Palaeartic Chironomidae Larvae in Palaeoecology*. Quarternary Research Association.

Buchaca, T., Skov, T., Amsinck, S. L., Gonçalves, V., Azevedo, J. M. N., Andersen, T. J., & Jeppesen, E. (2011). Rapid Ecological Shift Following Piscivorous Fish Introduction to Increasingly Eutrophic and Warmer Lake Furnas (Azores Archipelago, Portugal): A Paleoecological Approach. *Ecosystems*, *14*(3), 458–477. https://doi.org/10.1007/s10021-011-9423-0

Connor, S. E., Lewis, T., van Leeuwen, J. F. N., van der Knaap, W. O. (Pim), Schaefer, H., Porch, N., Gomes, A. I., Piva, S. B., Gadd, P., Kuneš, P., Haberle, S. G., Adeleye, M. A., Mariani, M., & Elias, R. B. (2024). Original plant diversity and ecosystems of a small, remote oceanic island (Corvo, Azores): Implications for biodiversity conservation. *Biological Conservation*, *291*, 110512. https://doi.org/10.1016/j.biocon.2024.110512

Connor, S. E., van Leeuwen, J. F. N., Rittenour, T. M., van der Knaap, W. O., Ammann, B., & Björck, S. (2012). The ecological impact of oceanic island colonization – a palaeoecological perspective from the Azores. *Journal of Biogeography*, *39*(6), 1007–1023. https://doi.org/10.1111/j.1365-2699.2011.02671.x

Costa, A. C., Balibrea, A., Raposeiro, P. M., Santos, S., Souto, M., & Gonçalves, V. (2021a). Non-indigenous and Invasive Freshwater Species on the Atlantic Islands of the Azores Archipelago. *Frontiers in Ecology and Evolution*, *9*. https://doi.org/10.3389/fevo.2021.631214

Costa, A. C., Balibrea, A., Raposeiro, P. M., Santos, S., Souto, M., & Gonçalves, V. V. (2021b). Non-indigenous and Invasive Freshwater Species on the Atlantic Islands of the Azores Archipelago. *Frontiers in Ecology and Evolution*, *9*(631214), 211. https://doi.org/10.3389/fevo.2021.631214

Cugny, C., Mazier, F., & Galop, D. (2010). Modern and fossil non-pollen palynomorphs from the Basque mountains (western Pyrenees, France): The use of coprophilous fungi to reconstruct pastoral activity. *Vegetation History and Archaeobotany*, *19*, 391–408.

Demske, D., Tarasov, P. E., Nakagawa, T., & Members, S. P. (2013). Atlas of pollen, spores and further non-pollen palynomorphs recorded in the glacial-interglacial Ia Quaternary sediments of lake Suigetsu, central Japan. *Quaternary International*, *290–291*, 164–238.

Flynn, W. W. (1968). The determination of low levels of polonium-210 in environmental materials. *Analytica Chimica Acta*, *43*, 221–227.

Frutuoso, G. (1978). *Livro Sexto das Saudades da Terra*.

Frutuoso, G. (1981). *Livro Quarto das Saudades da Terra*. Instituto Cultural de Ponta Delgada.

Gonçalves, V., Marques, H., & Fonseca, A. (2010). Lista das Diatomáceas (Bacillariophyta). In P. A. V. Borges, J. Bried, A. Costa, R. Cunha, R. Gabriel, V. Gonçalves, A. F. Martins, I. Melo,

M. Parente, P. Raposeiro, P. Rodrigues, R. S. Santos, L. Silva, P. Vieira, & V. Vieira (Eds.), *Listagem dos Organismos Terrestres e Marinhos dos A{c}cores* (pp. 81–97). Princípia.

Hernández, A., Sáez, A., Bao, R., Raposeiro, P. M., Trigo, R. M., Doolittle, S., Masqué, P., Rull, V., Gonçalves, V., Vázquez-Loureiro, D., Rubio-Inglés, M. J., Sánchez-López, G., & Giralt, S. (2017). The influences of the AMO and NAO on the sedimentary infill in an Azores Archipelago lake since ca. 1350CE. *Global and Planetary Change*, *154*, 61–74. https://doi.org/10.1016/j.gloplacha.2017.05.007

Kottelat, M., & Freyhof, J. (2007). *Handbook of European freshwater fishes*. Publications Kottelat, Cornol and Freyhof.

Krammer, K., & Lange-Bertalot, H. (1986). *Bacillariophyceae* (H. Ettl, J. Gerloff, H. Heynig, & D. Mollenhauer, Eds.). Fischer-Verlag.

Krammer, K., & Lange-Bertalot, H. (1988). *Bacillariophyceae 2/2 Bacillariaceae, Epithemiaceae, Surirellaceae.* (H. Ettl, Ed.). G. Fisher Verlag.

Krammer, K., & Lange-Bertalot, H. (1991a). *Bacillariophyceae. 2/3: Centrales, Fragilariaceae, Eunotiaceae* (H. Ettl, Ed.). G. Fisher Verlag.

Krammer, K., & Lange-Bertalot, H. (1991b). *Bacillariophyceae. 2/4: Achnanthaceae* (H. Ettl, Ed.). G. Fisher Verlag.

Krammer, K., & Lange-Bertalot, H. (2000). *Bacillariophyceae. 2/5: English and French translation of the keys* (H. Ettl, Ed.). G. Fisher Verlag.

Lhoumeau, S., & Borges, P. A. V. (2023). Assessing the Impact of Insect Decline in Islands: Exploring the Diversity and Community Patterns of Indigenous and Non-Indigenous Arthropods in the Azores Native Forest over 10 Years. *Diversity*, *15*(6). https://doi.org/10.3390/d15060753

Moller Pillot, H. K. (2009). *Chironomidae Larvae: Chironomini: Biology and Ecology of the Chironomini: Vol. 2*. KNNV Publishing.

Moller Pillot, H. K. (2014). *Chironomidae Larvae—Biology and Ecology of the Aquatic Orthocladiinae: Vol 3*. KNNV Publishing.

Moreira, J. M. (1987). *Alguns aspectos de intervenção humana na evolução da paisagem da ilha de S. Miguel (Açores): Natureza e*. Serviço Nacional de Parques, Reservas e Conservação da Natureza.

Oyarzabal, G., Cardoso, P., Rigal, F., Boieiro, M., Santos, A. M. C., Amorim, I. R., Malumbres-Olarte, J., Costa, R., Lhoumeau, S., Pozsgai, G., Gabriel, R., & Borges, P. A. V. (2025). Species traits may predict extinction risk of Azorean endemic arthropods. *Insect Conservation and Diversity*, *n/a*(n/a). https://doi.org/10.1111/icad.12822

Raposeiro, P. M., Hernández, A., Pla-Rabes, S., Gonçalves, V., Bao, R., Sáez, A., Shanahan, T., Benavente, M., de Boer, E. J., Richter, N., Gordon, V., Marques, H., Sousa, P. M., Souto, M., Matias, M. G., Aguiar, N., Pereira, C., Ritter, C., Rubio, M. J., … Giralt, S. (2021). Climate change facilitated the early colonization of the Azores Archipelago during medieval times. *Proceedings of the National Academy of Sciences*, *118*(41), e2108236118. https://doi.org/10.1073/pnas.2108236118

Raposeiro, P. M., Ritter, C., Abbott, M., Hernandez, A., Pimentel, A., Lasher, E., Płóciennik, M., Berlajolli, V., Kotrys, B., Pombal, X. P., Souto, M., Giralt, S., & Gonçalves, V. (2024). Late Holocene climate dynamics in the Azores archipelago. *Quaternary Science Reviews*, *331*. Scopus. https://doi.org/10.1016/j.quascirev.2024.108617

Raposeiro, P. M., Rubio, M. J., González, A., Hernández, A., Sánchez-López, G., Vázquez-Loureiro, D., Rull, V., Bao, R., Costa, A. C., Gonçalves, V., Sáez, A., & Giralt, S. (2017).

Impact of the historical introduction of exotic fishes on the chironomid community of Lake Azul (Azores Islands). *Palaeogeography, Palaeoclimatology, Palaeoecology*, *466*, 77–88. https://doi.org/10.1016/j.palaeo.2016.11.015

Reille, M. (1999). *Pollen et Spores d'Europe et d'Afrique du Nord* (Seconde édition, Vols. 1–3). Laboratoire de Botanique Historique et Palynologie.

Reimer, P. J., Austin, W. E. N., Bard, E., Bayliss, A., Blackwell, P. G., Ramsey, C. B., Butzin, M., Cheng, H., Edwards, R. L., Friedrich, M., Grootes, P. M., Guilderson, T. P., Hajdas, I., Heaton, T. J., Hogg, A. G., Hughen, K. A., Kromer, B., Manning, S. W., Muscheler, R., … Talamo, S. (2020). The IntCal13 Northern Hemisphere radiocarbon age calibration curve (0-55 cal kBP. *Radiocarbon*, *62*, 725–757.

Renberg, I. (1990). A procedure for preparing large sets of diatom slides from sediment cores. *Journal of Paleolimnology*, *4*, 87–90.

Richter, N., Russell, J. M., Amaral-Zettler, L., DeGroff, W., Raposeiro, P. M., Gonçalves, V., de Boer, E. J., Pla-Rabes, S., Hernández, A., Benavente, M., Ritter, C., Sáez, A., Bao, R., Trigo, R. M., Prego, R., & Giralt, S. (2022). Long-term hydroclimate variability in the sub-tropical North Atlantic and anthropogenic impacts on lake ecosystems: A case study from Flores Island, the Azores. *Quaternary Science Reviews*, *285*. Scopus. https://doi.org/10.1016/j.quascirev.2022.107525

Rieradevall, M., & Brooks, S. J. (2001). An identification guide to subfossil Tanypodinae larvae (Insecta: Diptera: Chrironomidae) based on cephalic setation. *Journal of Paleolimnology*, *25*(1), 81–99. https://doi.org/10.1023/A:1008185517959

Ritter, C., Gonçalves, V., Pla-Rabes, S., de Boer, E. J., Bao, R., Sáez, A., Hernández, A., Sixto, M., Richter, N., Benavente, M., Prego, R., Giralt, S., & Raposeiro, P. M. (2022). The vanishing

and the establishment of a new ecosystem on an oceanic island – Anthropogenic impacts with no return ticket. *Science of the Total Environment*, *830*. Scopus. https://doi.org/10.1016/j.scitotenv.2022.154828

Robbins, J. A. (1978). Geochemical and geophysical applications of radioactive lead. In J. O. Nriagu (Ed.), *The biogeochemistry of lead in the environment* (pp. 285–393). Elsevier.

Ruiz-Fernández, A. C., & Hillaire-Marcel, C. (2009). 210Pb-derived ages for the reconstruction of terrestrial contaminant history into the Mexican Pacific coast: Potential and limitations. *Marine Pollution Bulletin*, *59*, 134–145.

Rull, V., Lara, A., Rubio-Inglés, M. J., Giralt, S., Gonçalves, V., Raposeiro, P., Hernández, A., Sánchez-López, G., Vázquez-Loureiro, D., Bao, R., Masqué, P., & Sáez, A. (2017). Vegetation and landscape dynamics under natural and anthropogenic forcing on the Azores Islands: A 700-year pollen record from the São Miguel Island. *Quaternary Science Reviews*, *159*, 155–168. https://doi.org/10.1016/j.quascirev.2017.01.021

Rull, V., Stansell, N. D., Montoya, E., Bezada, M., & Abbott, M. B. (2010). Palynological signal of the Younger Dryas in the tropical Venezuelan andes. *Quaternary Science Reviews*, *29*, 3045–3056.

Sáez, A., Hernández, A., Pimentel, A., Andrade, M., Bao, R., Raposeiro, P. M., Gonçalves, V., Benavente, M., Pla-Rabes, S., Ramalho, R., & Giralt, S. (2025). Westerlies migrations and volcanic records over the past 4000 years from the Azores lacustrine sequences. Exploring correlations and impacts on Western Europe. *Global and Planetary Change*, *246*, 104698. https://doi.org/10.1016/j.gloplacha.2025.104698

Sanchez-Cabeza, J. A., Masqué, P., & Ani-Ragolta, I. (1998). Lead-210 and Po-210 analysis in sediments and soils by microwave acid digestion. *Journal of Radioanalytical and Nuclear Chemistry*, *227*, 19–22.

Sanchez-Cabeza, J. A., & Ruiz-Fernández, A. C. (2012). 210Pb sediment radiochronology: An integrated formulation and classification of dating models. *Geochimica et Cosmochimica Acta*, *82*, 183–200.

Sanchez-Cabeza, J. A., Ruiz-Fernández, A. C., Ontiveros-Cuadras, J. F., Bernal, L. H. P., & Olid, C. (2014). Monte Carlo uncertainty calculation of 210Pb chronologies and accumulation rates of sediments and peat bogs. *Quaternary Geochronology*, *23*, 80–93.

Skov, T., Buchaca, T., Amsinck, S. L., Landkildehus, F., Odgaard, B. V., Azevedo, J., Gonçalves, V., Raposeiro, P. M., Andersen, T. J., & Jeppesen, E. (2010). Using invertebrate remains and pigments in the sediment to infer changes in trophic structure after fish introduction in Lake Fogo: A crater lake in the Azores. *Hydrobiologia*, *654*(1), 13–25. https://doi.org/10.1007/s10750-010-0325-5

Strandberg, N. A., Steinbauer, M. J., Walentowitz, A., Gosling, W. D., Fall, P. L., Prebble, M., Stevenson, J., Wilmshurst, J. M., Sear, D. A., Langdon, P. G., Edwards, M. E., & Nogué, S. (2024). Floristic homogenization of South Pacific islands commenced with human arrival. *Nature Ecology & Evolution*, *8*(3), 511–518. https://doi.org/10.1038/s41559-023-02306-3

Triantis, K. A., Borges, P. A. V., Ladle, R. J., Hortal, J., Cardoso, P., Gaspar, C., Dinis, F., Mendonça, E., Silveira, L. M. A., Gabriel, R., Melo, C., Santos, A. M. C., Amorim, I. R., Ribeiro, S. P., Serrano, A. R. M., Quartau, J. A., & Whittaker, R. J. (2010). Extinction debt on oceanic Islands. *Ecography*, *33*(2), 285–294. https://doi.org/10.1111/j.1600-0587.2010.06203.x

Vallenduuk, H. J., & Moller Pillot, H. K. M. (2007). *Chironomidae Larvae. In: Tanypodinae: General Ecology and Tanypodinae*. KNNV Publishing.

Valois, & Silva, F. (1886). Descrição das águas minerais das Furnas na ilha de São Miguel, Archivo dos Açores. In *Typografia do archivo dos Açores* (pp. 437–446). Arquivos dos Açores.

van Geel, B., & Aptroot, A. (2006). Fossil ascomycetes in Quaternary deposits. *Nova Hedwigia*, *82*(3–4), 313–329. https://doi.org/10.1127/0029-5035/2006/0082-0313

van Geel, B., Buurman, J., Brinkkemper, O., Schelvis, J., Aptroot, A., van Reenen, G., & Hakbijl, T. (2003). Environmental reconstruction of a Roman Period settlement site in Uitgeest (The Netherlands), with special reference to coprophilous fungi. *Journal of Archaeological Science*, *30*(7), 873–883. https://doi.org/https://doi.org/10.1016/S0305-4403(02)00265-0

Vázquez-Loureiro, D., Sáez, A., Gonçalves, V., Buchaca, T., Hernández, A., Raposeiro, P. M., Boer, E. J. de, Masqué, P., Giralt, S., & Bao, R. (2023). Recent global warming induces the coupling of dissimilar long-term sedimentary signatures in two adjacent volcanic lakes (Azores Archipelago, Portugal). *Quaternary Science Reviews*, *303*, 107968. https://doi.org/10.1016/j.quascirev.2023.107968

Vicente, A. (1956). Introdução de peixes de água doce nas lagoas de S.Miguel. *Açoreana : Boletim Da Sociedade Afonso de Chaves*, *5*(3), 297–305.

Humans simplified trophic structures in island lake ecosystems

Authors

Miguel G. Matias[1,2*], Vítor Gonçalves[3,4], Sergi Pla-Rabes[5,6,7], Armand Hernández[8], Manuel Mendoza[1], Miguel B. Araújo[1,2,9], Jacqueline van Leeuwen[10,11], Sandra Nogué[5,7], Nora Richter[12], Martin Souto[3,4], Ricardo Trigo[13], Roberto Bao[7], Alberto Sáez[14], Santiago Giralt[15] and Pedro M. Raposeiro[3,4]

Affiliations

[1] Departamento de Biogeografía y Cambio Global, Museo Nacional de Ciencias Naturales, CSIC, Madrid, Spain

[2] Rui Nabeiro Biodiversity Chair, MED– Mediterranean Institute for Agriculture, Environment and Development & CHANGE Global Change and Sustainability Institute, Institute for Advanced Studies and Research, University of Évora, Évora, Portugal

[3] CIBIO, Centro de Investigação em Biodiversidade e Recursos Genéticos, InBIO Laboratório Associado, Pólo dos Açores, Rua da Mãe de Deus, 9500-321 Ponta Delgada, Portugal

[4] Faculdade de Ciências e Tecnologia, Universidade dos Açores, Rua da Mãe de Deus, 9500-321 Ponta Delgada, Portugal

[5] Universitat Autònoma de Barcelona, Edifici C, 08193 Cerdanyola del Vallès, Spain

[6] Department of Geography, Environmental Management and Energy Studies, University of Johannesburg, Corner Ditton and University Avenue, Auckland Park, Johannesburg, South Africa

[7] CREAF, Cerdanyola del Vallès (Bellaterra), Spain

[8] Universidade da Coruña, GRICA-BIOpast Group, Centro Interdisciplinar de Química e Bioloxía (CICA), Rúa das Carballeiras, 15071 A Coruña, Spain

[9] German Centre for Integrative Biodiversity Research (iDiv), Halle-Jena-Leipzig, Puschstrasse 4, Leipzig 04103, Germany

[10] Institute of Plant Sciences, University of Bern, Altenbergrain 21, Bern 3013, Switzerland

[11] Oeschger Centre for Climate Change Research, University of Bern, Hochschulstrasse 4, Bern 3012, Switzerland
[12] Department of Surface Waters - Research and Management, Swiss Federal Institute of Aquatic Science and Technology (EAWAG), Dübendorf, Switzerland
[13] Instituto Dom Luiz, Faculdade de Ciências, Universidade de Lisboa, 1749-016 Lisboa, Portugal
[14] UB-Geomodels Research Institute. Departament de Dinàmica de la Terra i de l'Oceà, Facultat de Ciències de la Terra, Universitat de Barcelona, Martí i Franquès s/n, 08028 Barcelona, Spain
[15] Geosciences Barcelona (GEO3BCN), CSIC, Lluís Solé i Sabarís s/n, 08028 Barcelona, Spain

* Corresponding Author: Miguel G. Matias: miguel.matias@mncn.csic.es

Abstract

Lakes on oceanic islands are exceptionally vulnerable ecosystems and serve as natural archives of long-term environmental change, yet long-term reconstructions spanning multiple trophic levels remain rare. We reconstruct 2,000 years of ecological change across nine Azorean lakes by analysing sediment records of community composition and trophic-guild richness for aquatic producers and consumers, interpreted alongside catchment vegetation and hydroclimatic variability. We identified an archipelago-wide trajectory of trophic restructuring and simplification, consistent with a shift toward plankton-dominated structures. Widespread catchment vegetation change was followed by major reorganisation of aquatic compositional turnover, with producers typically responding earlier than consumers. This multi-trophic, multi-lake perspective reveals that human land use initiated a long-term trajectory of ecosystem restructuring, with the initial reorganisation phase occurring between approximately 1050 and 1450 CE. Land-use effects persisted thereafter, while climatic variability increasingly interacted with already modified catchments after approximately 1600 CE. These findings indicate that ecological baselines are not fixed states but dynamic outcomes of long-term interactions among humans, climate, and ecosystem resilience.

Introduction

Freshwater ecosystems are increasingly impacted by anthropogenic pressures and climate change, driving biodiversity loss and ecosystem disruption (Merz et al., 2023; Pla-Rabes et al., 2024; Woolway et al., 2021). Much of the current understanding of long-term changes in aquatic ecosystems has emerged from the study of lake sediments, natural archives of environmental changes (Catalan et al., 2013), preserving decades to millennia of biodiversity and biogeochemical data (Bradley, 2015). Despite invaluable contributions to the study of past responses to climate variability (Pla-Rabes et al., 2024; Smol, 2010) and human-driven vegetation change (Dubois et al., 2018; Jenny et al., 2019; Nogué et al., 2021; Raposeiro et al., 2021), and their interactions (Berglund, 2003; Lotter & Birks, 2003), progress in this field has often been hindered by two challenges. First, paleoecological studies often focus on individual taxa or functional groups, hindering insights into system-level trophic dynamics that underpin resilience and long-term trajectories (González-Trujillo, Mendoza, et al., 2025; Kidwell, 2015). Second, although multi-lake studies are becoming more common, paleoecological research has frequently relied on single-lake records, making it hard to distinguish local from regional drivers. Emerging standardised paleoecological datasets now enable integrated, multi-site and multi-trophic reconstructions of lake ecosystems at a regional scale, from primary producers to consumers, spanning decadal to millennial timescales, revealing landscape-wide patterns and responses.

To address the lack of system-level reconstructions of trophic dynamics, we apply a trophic-community modelling approach that infers lake ecosystem structure from trophic-guild distribution and richness (Mendoza & Araújo, 2019, 2022). Unlike traditional biodiversity assessments based on individual species (Araújo et al., 2019), this framework describes communities by their functional trophic composition (i.e., the proportions of producers and consumers), providing an ecologically meaningful link between food-web structure and the pathways through which energy and matter are transferred within ecosystems (Carpenter et al., 1987; Mehner et al., 2018), thereby capturing how environmental change propagates across multiple trophic levels to reshape freshwater biodiversity and ecosystem functioning (Oester et al., 2025). Here, we present the first application of this trophic-community modelling framework to freshwater systems, using multi-trophic lake data from across the Azorean archipelago spanning the last two millennia (Fig. 1a, Sáez et al., 2025). This approach has been successfully applied to identify global regularities and climate-driven reorganisations across diverse systems, including terrestrial mammals (Mendoza & Araújo, 2019, 2022), non-marine birds (González-del-

Pliego et al., 2023), marine vertebrates and fish (González-Trujillo, Assis, et al., 2025). Island lakes are highly sensitive to human impacts due to their isolation, high endemism, simplified food webs, and the abrupt onset of human colonization, which often triggers rapid ecological reorganisation following first settlement (Nogué et al., 2021; Whittaker & Fernández-Palacios, 2007), yet predicting their responses remains challenging. We integrated high-resolution paleoecological, geochemical and climatic data to (1) detect recurring trophic-community patterns (i.e., discrete and repeatedly occurring trophic structures defined by producer and consumer guild composition and relative abundances) across space and time and (2) evaluate the influences of climate versus land-use intensification.

Over the last two millennia, the Azores have experienced pronounced climate variability and multiple phases of human activity (Fig. 1b; Appendix S1, Table S1), ranging from pre-colonization baselines to successive waves of land-use intensification involving fire, livestock grazing, deforestation, crop introduction, and fish stocking (Elias et al., 2022; Raposeiro et al., 2017, 2021, 2022; Rull, 2023). The multiproxy paleoecological record across the archipelago provides a robust chronological framework for identifying pre-human ecological baselines and assessing how successive disturbances have shaped present-day lake ecosystems (Fig. 1b). Climate variability during this period was dominated by changes in the North Atlantic Oscillation (NAO), which represents the dominant mode of atmospheric variability influencing precipitation and hydroclimate in the Azores (Hernández et al., 2016) and provides a temporally continuous, regionally coherent signal suitable for multi-lake, millennial-scale analyses (Hernández et al., 2020; Raposeiro et al., 2024). NAO variability directly modulates winter precipitation, storm frequency, and runoff intensity, thereby influencing catchment erosion, nutrient delivery, and lake hydrology, among other processes (Hernández et al., 2020; Raposeiro et al., 2024). Consistent with NAO-linked hydroclimatic dynamics, regional hydroclimatic conditions in the Azores exhibited relatively stable early conditions (0–750 CE), increased variability during the Medieval Climate Anomaly, cooler and wetter conditions during the Little Ice Age, and a transition to industrial-era forcing (Hernández et al., 2020; Raposeiro et al., 2021; Fig. 1).

Nine sediment cores were analysed for diatoms (assigned to producer guilds) and chironomids (assigned to consumer guilds) (Appendix S1). A fuzzy-clustering algorithm then discriminated between distinct community trophic structures or trophic communities (Mendoza & Araújo, 2019, 2022). Community data were then combined with an independent reconstruction of the NAO (Appendix S1, Fig. S2), used as the primary regional-scale climatic forcing variable, and fossil

pollen–based vegetation records as a proxy for catchment-scale land-use change (Appendix S1, Figs S3 and S4).

Materials and Methods

Study area: Azores archipelago

The Azores archipelago comprises nine volcanic islands in the mid-North Atlantic Ocean (Fig. 2), spanning latitudes 36°45′N to 39°43′N and longitudes 24°45′W to 31°17′W, approximately 1,300 km from mainland Portugal and 1,600 km from North America. This archipelago is particularly rich in freshwater ecosystems due to volcanic geomorphology and climatic conditions. The archipelago spans a total land surface area of 2,325 km^2 and hosts 88 lakes across six of the nine Azorean islands. The studied lakes (Fig. 2b; Appendix S1, Table S2) can be broadly categorised based on their geological origins into three groups: (i) those in the interior of volcano cones, calderas and maars, (ii) those in barred valleys between volcano cones, and (iii) those situated in tectonic depressions (Sáez et al., 2025). Typically, scoria cone lakes are quite small and shallow (Lakes Empadadas Norte, Prata, Ginjal, Caveiro, Peixinho), while those inside collapsed calderas tend to have a larger surface area (e.g., Lakes Azul and Caldeirão, which are deep and shallow, respectively), and maars usually exhibit greater depth (Lakes Santiago and Funda). The studied lakes cover a wide spectrum of surface area (Appendix S1, Table S2), ranging from 0.004 km^2 (Lake Prata) to 3.59 km^2 (Lake Azul). Since 1994 CE, these systems have been monitored as part of a regional limnological programme, revealing a wide range of trophic conditions from oligotrophic to eutrophic states (Matias et al., 2017) (see also Appendix S1, Table S3). Sediment cores were recovered from the main depositional basin, generally the deepest part of each lake, to minimize the likelihood of erosion or depositional hiatuses (Glew et al., 2001; Lotter & Birks, 2003). This standardised coring strategy ensured methodological consistency and maximized the comparability of long-term ecological records across the archipelago (Sáez et al., 2025). Human activity appears to have affected parts of the archipelago before documented Portuguese settlement (Fig. 1; Raposeiro et al., 2021), while widespread colonization during the 15th century initiated a more widespread phase of deforestation, agriculture, urbanization and species introductions within lake catchments (Pla-Rabes et al., 2024; Ritter et al., 2022). Further historical context is provided in the Appendix S1.

Age models

Previously published age–depth models were applied to all lake sediment sequences (Appendix S1, Table S4). Plant macrofossils and pollen concentrates selected for radiocarbon dating were pretreated via acid digestion and dated by AMS at Beta Analytic (USA), the Keck-CCAMS Group (University of California, Irvine, USA), and the Laboratoire de Radiochronologie (Université Laval, Canada). Conventional radiocarbon ages were then calibrated to cal yr BP (1950 CE reference) using the IntCal20 Northern Hemisphere curve (see Appendix S1 for full details). Lead-210 activities were measured at 1 cm intervals in the uppermost sediments through alpha spectrometry determination of ^{210}Po by alpha-particle spectrometry, at the Autonomous University of Barcelona (Spain) and at the Laboratorio de Geoquímica Isotópica y Geocronología (Instituto de Ciencias del Mar y Limnología, UNAM, Mazatlán, México). Age–depth models were generated using the *clam* package in R (v.2.3.9) (Blaauw et al., 2020). Further methodological details are provided in Appendix S1; radiocarbon dating details in Table S4 and age–depth models in Fig. S5.

Lake community data

To reconstruct long-term dynamics in aquatic communities, we analysed subfossil remains of diatoms and chironomids from sediment cores collected across all study lakes. Diatom communities were quantified following standardised protocols. Slides were prepared using Naphrax© and examined at 1000× magnification under microscopes equipped with differential interference contrast optics. A minimum of 400-500 valves were identified per sample, using harmonized taxonomic references compiled for the Azores archipelago (see Table S3 for data sources; Appendix S1 for additional methods details and full list of taxonomical references; Pla-Rabes et al., 2024). Chironomid larval head capsules were extracted from 2 cm³ subsamples taken at 1–5 cm intervals. After deflocculation in 10% KOH at 70 °C, residues were sieved into 90 and 212 µm fractions and sorted under a Zeiss Stemi stereomicroscope at 40× magnification. Capsules were mounted in Euparal and identified at 100–400× magnification under a Zeiss Axio Imager A1. Taxonomic assignments were based on mentum morphology following standard protocols, and harmonized with existing chironomid datasets from the Azores (see Appendix S1, Table S5 for data sources and taxonomical references).

Climatic reconstructions

Climate forcing was represented by the North Atlantic Oscillation (NAO). This large-scale mode of climate variability was selected because it is the primary driver controlling precipitation, storminess, and hydroclimate in the Azores (Hernández et al., 2016). We evaluated the NAO

reconstruction derived from Iberian lacustrine proxies (Hernández et al., 2020) and a Northern Hemisphere summer temperature (NHST) reconstruction based on tree-ring and multi-proxy data (Büntgen et al., 2021). These reconstructions were evaluated individually using the same multivariate screening procedure, including the variance inflation factor (VIF) and redundancy analysis (RDA; Borcard et al., 2018). Only the NAO reconstruction yielded a statistically significant RDA model explaining variation in trophic community structure. The NHST reconstruction did not explain significant additional variance and was therefore excluded from the final analyses. The NAO index thus reflects both its already established climatic relevance for the Azores and a robust representation of climate variability relevant to ecosystem dynamics across the archipelago (Hernández et al., 2016, 2020).

Quantifying changes in lake community composition over time

Our dataset includes relative abundance data for 658 taxa—588 diatom taxa and 70 chironomid taxa—from nine lake sediment records across the Azores archipelago (see Appendix S2 for lake-level stratigraphic diagrams), spanning 0 to 2010 CE. To assess changes in aquatic community composition over time, we performed a detrended correspondence analysis (DCA; Hill & Gauch, 1980) calculated using decorana function (Borcard et al., 2018), following a Hellinger transformation (square root of relative abundances) to standardise variance across species. The first DCA axis is scaled in standard deviation units of community turnover, with a shift of 4 units corresponding approximately to a complete compositional change (Pla-Rabes et al., 2024). We interpreted trends in axis scores through time as indicators of compositional turnover, a method well suited for irregularly sampled palaeoecological time series. Uncertainty around the estimated smooths is shown as 95% confidence intervals computed from the fitted HGAM using add_confint function (level = 0.95; gratia R package Simpson, 2024).

Catchment-scale vegetation dynamics

To quantify regional-scale vegetation change across the archipelago, we applied DCA to taxonomically harmonised terrestrial pollen and spore (ferns) assemblage data from nine Azorean pollen records (see details in Appendix S1). This approach relies on pollen metrics that are consistently available across all lake records, allowing vegetation change to be modelled as a coherent regional smooth signal through time. While anthropogenic indicator taxa such as the presence of *Plantago* and cereal-type pollen provide robust evidence of local agro-pastoral activity, their spatially and temporally heterogeneous occurrence makes them unsuitable for inclusion in a unified regional statistical framework. These indicators are therefore used

qualitatively to contextualize major land-use phases identified by the regional vegetation trajectory, following established Azorean studies (Connor et al., 2012; Raposeiro et al., 2021; Rull et al., 2017). The first DCA axis, summarizing the dominant gradient in taxonomic composition, was extracted for each sample and modelled using a Hierarchical Generalized Additive Model (HGAM; Pla-Rabes et al., 2024; Simpson, 2024) with sample age as the predictor. This approach provided a continuous vegetation change index integrating floristic information across sites while accounting for between-lake variation through site-level smooth terms. The resulting DCA-based HGAM captures the regional trajectory of terrestrial vegetation dynamics over the past two millennia and serves as a proxy for regional land-use transformation and catchment disturbance (Appendix S1, Fig. S3A). To interpret the ecological processes underlying this multivariate signal, we conducted complementary HGAMs on the relative abundance of arboreal and herbaceous pollen groups (Appendix S1, Fig. S3B). After normalizing sample values to control for differences in count effort and pollen influx, we modelled the temporal trends in these two major vegetation categories across lakes. The divergent trajectories of tree and herb pollen abundance provide functional insight into the DCA-defined vegetation changes, allowing us to infer the timing and direction of forest clearance, agricultural expansion and landscape transformation across the Azores.

Assigning trophic guilds

We implemented a comprehensive workflow to identify trophic guilds by integrating species-level taxonomy, trophic interactions and dietary classifications. Taxonomic names were standardised by querying publicly available taxonomic databases (ITIS, GBIF and NCBI) using the classification function in the taxize R package (Chamberlain & Szöcs, 2013). Trophic guild assignments were prioritised at the species level and, when unavailable, inferred from genus- or family-level information. For consumers, feeding interactions were retrieved from the Global Biotic Interactions (GloBI) database using the rglobi R package (Poelen et al., 2014), retaining trophic interaction types such as eats and preysOn. Retrieved interactions were filtered and classified into detailed food-source categories (e.g., nematodes, rotifers, diatoms, crustaceans, flatworms, protists, bacteria and detritus) based on the taxonomy of prey items. These categories were subsequently aggregated into six broader resource groups—Animals, Plants, Algae, Detritus/Organic Matter, Fungi and Bacteria—to facilitate higher-level trophic analyses. Trophic guilds were then identified by clustering species based on their dietary composition. Dietary compositions were quantified as the proportional contribution of major food-source categories within each taxon. Based on these dietary profiles, taxa were assigned to one of four trophic

guilds according to their predominant food source: algivores, detritivores, plantivores and predators. This integrated approach enables detailed reconstruction of paleoecological food webs, linking taxonomic classifications to functional roles within ecosystems and providing a scalable framework for understanding trophic dynamics across varying levels of ecological organisation.

For primary producers, ecological guilds were assigned using the Diat.Barcode database, accessed via the diathor R package (Gelis et al., 2024), which provides environmental trait information and ecological guild classifications for diatom taxa. Guild assignments were primarily obtained through species-level, genus-level or family-level classifications for approximately 33%, 58% and ~1% classifications, respectively. The remaining approximately 8% were assigned by expert judgement based on their morphology and established ecological affinities, ensuring complete guild classification across the dataset. This ensured comprehensive coverage and consistent classification across all taxa. Four major ecological guilds, high profile, low profile, motile and euplanktonic, were assigned following the framework of Passy (2007), leveraging ecological traits stored in the database. These guilds capture differences in resource acquisition, exposure to consumers, and sensitivity to physical disturbance, reflecting species' position relative to the sediment–water interface. High-profile diatoms include erect, stalked or filamentous forms that extend into the water column, are typically favoured under stable, nutrient-rich conditions, and are relatively exposed to grazing and physical disturbance. Low-profile diatoms consist of small, adnate or prostrate forms closely attached to substrates, which confer resistance to physical disturbance and consumer pressure and favor persistence under nutrient-poor or high-disturbance conditions. Motile diatoms can actively move across substrates, allowing them to exploit spatially heterogeneous resources and respond to changing environmental conditions. Euplanktonic diatoms are adapted to pelagic habitats and characterize systems dominated by water-column primary production, such as lakes and reservoirs. These guilds help elucidate diatom community responses to environmental gradients and are valuable for ecological assessments (Passy, 2007; Rimet & Bouchez, 2012). This hierarchical framework allowed us to classify diatoms into functional groups, even when detailed species-level information was unavailable, by utilising genus- and family-level classifications. The resulting dataset provides a robust and consistent basis for exploring the ecological roles of diatom communities and their contributions to ecosystem processes, ensuring flexibility and adaptability across diverse taxonomic datasets.

Identifying lake community trophic structures

We characterised community trophic structure using relative abundances from eight functional guilds (see Guilds section), comprising four producer guilds and four consumer guilds. Relative abundances were calculated separately for producers and consumers, such that each trophic level was standardised independently. This approach avoids introducing artificial covariance between producer and consumer guilds that would arise if all guilds were expressed as proportions of a single total community, while allowing comparisons of functional composition within each trophic level. For each trophic level, the relative abundance of taxon i within a sample was calculated as:

$$A_i = \frac{N_i}{\sum_{j=1}^{S} N_j}$$

where A_i is the relative abundance of taxon i, N_i is its observed abundance, and S is the total number of taxa within the corresponding trophic level (i.e., producers or consumers). Taxa were then assigned to functional guilds based on ecological traits, and the relative abundance of each guild was calculated as:

$$A_g = \sum_{i \epsilon g} A_i$$

where A_g is the relative abundance of functional guild g, obtained by summing the relative abundances of all taxa assigned to that guild within the corresponding trophic level. This standardised approach allows consistent comparisons of functional composition within producer and consumer communities independently. The resulting data matrix comprised approximately 900 individual communities (rows) and eight functional guilds (columns).

To identify patterns in trophic structure, we grouped lake sediment samples into community trophic structure units. The number of distinct trophic structure types was assessed using the average membership degree index (AMDi), calculated across a series of fuzzy C-means clustering runs in which the number of user-defined clusters increased from 2 to 15, as described in detail by Mendoza and Araújo (2022). AMDi quantifies cluster definition by averaging the highest membership degree of each sample (i.e., its degree of belonging to the nearest cluster), minus 1/c, where *c* is the number of clusters. AMDi values range from 0 (randomly distributed samples) to 1 (perfectly defined and compact clusters). To ensure robustness, we ran 999 replicates for each

cluster number and retained the maximum AMDi value. The optimal number of clusters, interpreted as distinct community trophic structures (CTSs), was defined as the peak of the AMDi curve. Initial analysis identified six CTS candidates, but further inspection showed that CTS5 and CTS6 were ecologically indistinguishable, both dominated by high-profile diatoms and algivores in similar proportions. The original CTS5 and CTS6 were combined and retained as the final CTS5, resulting in five CTS categories numbered CTS1–CTS5.

Identifying ecological drivers of shifts in community trophic structures

To assess the contribution of individual trophic guilds, we applied a random forest (RF) classification (Breiman et al., 2017). The dataset was constructed by integrating the relative abundances of the eight guilds as predictors with the previously assigned trophic structures serving as the categorical response variable. A RF model was trained with 1,000 decision trees, and the response variable was treated as a factor to enable classification. Model performance was evaluated using out-of-bag predictions, providing an internal validation equivalent to cross-validation. Classification accuracy was assessed by calculating the proportion of correctly assigned cases and Cohen's kappa statistic, which measures agreement beyond chance. To identify the most influential guilds driving trophic structure classifications, we computed variable importance scores using the varImpPlot function. In addition, an independent decision tree (Breiman et al., 2017) was constructed using the rpart R package to identify key thresholds in the relative abundances of functional guilds that distinguish community trophic structures. This approach provides an interpretable framework for understanding the functional composition of trophic structures and their shifts over time, offering insights into the ecological mechanisms shaping long-term community dynamics.

Identifying drivers of change in lake communities

We compiled a set of climatic and vegetation change reconstructions to evaluate the influence of external drivers on long-term changes in lake trophic structure. To ensure comparability between biological and environmental data, and to account for the mean chronological uncertainty of the sediment age–depth models (~30 years; Appendix S1, Fig. S5), we aggregated all time series into regular 30-year intervals. This binning approach reduces short-term variability that cannot be robustly resolved given dating uncertainty, while preserving meaningful ecological signals and aligning the effective temporal resolution of biological and environmental reconstructions. For each 30-year bin, we used trophic guild relative abundances of eight functional groups, ranging from primary producers (high-profile, low-profile, motile and euplanktonic diatoms) to consumer

guilds (algivores, detritivores, plantivores and predators), which were subsequently averaged across lakes to derive regional estimates per bin. The same binning procedure was initially applied to all pre-selected environmental variables (NAO, NHST and Regional Vegetation Change) to create a harmonized, time-aligned dataset suitable for multivariate analysis. A two-step variable selection procedure was implemented. First, we assessed multicollinearity among all candidate environmental variables using variance inflation factors (VIFs), excluding those with VIF > 10. Second, we performed forward selection using the ordistep function within a redundancy analysis (RDA) framework, with the Hellinger-transformed trophic guild matrix as the response and the full set of non-collinear environmental variables as predictors. This procedure identified two key explanatory variables that consistently explained significant variation in trophic structure across lakes (see ordination in Appendix S1, Fig. S6): the North Atlantic Oscillation index (Hernández et al., 2017) and a pollen-based reconstruction of vegetation change. These two variables were retained for subsequent variation partitioning analyses.

To explore how the relative influence of climate and vegetation changed over time, we conducted variance partitioning (Peres-Neto et al., 2006) using adjusted R^2 decomposition via the varpart function. We implemented two complementary approaches. First, we used a predefined phase-based framework that divided the past two millennia into five historical periods aligned with known pulses of environmental and anthropogenic change (<750, 750–1050, 1050–1450, 1450–1750 and >1750 CE) (Raposeiro et al., 2021, 2022). Second, we applied a rolling window analysis, which involves examining the data within overlapping 300-year time slices that move forward in 30-year steps. Each moving window typically contained 8–12 temporal bins (30-year intervals); windows with fewer than five bins were excluded a priori. In both approaches, HGAM-predicted trophic guild relative abundances were used as the response matrix, and NAO and vegetation change were used as explanatory variables. Pure effects were estimated using partial redundancy analysis (RDA) by conditioning on the alternate predictor, while shared effects were calculated by subtracting the sum of pure fractions from the total explained variance (see Appendix S1, Fig. S1 for workflow and variance partitioning details). To assess whether the number of temporal bins per window was sufficient to support statistical inference, we complemented the effect-size analysis with permutation-based significance testing. For each 300-year moving window (30-year step), we calculated the difference between the pure vegetation and pure climate fractions and tested the full RDA model as well as each unique variance fraction using partial RDA with up to 9,999 permutations. Non-significant pure fractions ($p \geq 0.05$) were

visually downweighted in the moving-window figures, whereas windows in which the dominant fraction was significant were displayed at full opacity. Negative adjusted R^2 values were truncated to zero to aid interpretation. This framework enabled us to identify both persistent and transient intervals of environmental influence and to assess the timing, direction and consistency of ecological transitions across fixed and continuous temporal resolutions. To evaluate the robustness of the main findings, we conducted a series of sensitivity analyses, including leave-one-out lake exclusions, perturbations of historical phase boundaries, moving-window tests, and null models accounting for record length and temporal alignment. Details of these analyses are provided in the Sensitivity Analysis section of Appendix S1.

Results

Changes in lake community composition and ecosystem organisation

Community turnover (i.e., changes in species composition over time) reveals strong temporal dynamics among aquatic producers and consumers across Azorean lakes over the past two millennia (Fig. 2a). Interpreted alongside regional hydroclimatic variability (NAO) and catchment vegetation change—reflecting progressive forest clearance and agro-pastoral expansion—regional DCA trajectories show limited directional change before ~1200 CE, when GAM uncertainty is wide. Thereafter, compositional turnover increased for vegetation, producers (diatoms) and consumers (chironomids). Rapid catchment vegetation change from ~1490 CE onward was followed by later responses in both aquatic groups, with producer turnover stronger in magnitude than consumer turnover (Fig. 2). This regional sequence is consistent with catchment-initiated forcing followed by aquatic reorganisation, with primary producers—taxa with short generation times and high sensitivity to light, nutrients and temperature (Rühland et al., 2015)—showing the strongest compositional response. At the lake level, producer–consumer coupling varied in timing and strength (Fig. 2b; Fig. S7). Significant producer turnover preceded consumer turnover in six of nine lakes, with near-synchrony in Caldeirão. Local contingencies nevertheless shaped the timing and rate of change: producer–consumer lags ranged from near-synchrony to multi-century offsets (e.g. Peixinho, Empadadas Norte). This predominantly producer-first pattern was not systematically related to lake depth, area or elevation, suggesting a climatically and anthropogenically driven restructuring of Azorean lake ecosystems.

The analysis of lake community trophic structures reveals consistent patterns across the Azores, reflecting distinct ecological configurations along environmental gradients. Ordination shows

strong associations between producer and consumer guilds and the different community trophic structure types (Fig. 3a). Euplanktonic producers occupy a distinct position in the ordination space, reflecting the dominance of pelagic production (Fig. 3a).In contrast, benthic producers, including high-profile (erect or stalked taxa extending into the water column), low-profile (small, adnate forms resistant to disturbance), and motile diatoms that actively move across substrates, cluster at the opposite end of the gradient, where they align with consumer groups such as predators, plantivores and detritus feeders. A decision tree (Fig. 3b), together with trophic guild abundances across structure types (Fig. 3c), identifies a clear gradient from phytoplankton-dominated systems to benthic- and consumer-rich assemblages with higher proportions of high-profile diatoms and diverse consumer guilds.

When examining the temporal dynamics of community trophic structures (CTS; Fig. 3d), Azorean lake ecosystems exhibited prolonged periods of relative stability interspersed with episodes of community reorganisation, particularly after ~750 CE, coinciding with known phases of anthropogenic disturbance (Raposeiro et al., 2021). This interval includes two broad early phases: a relatively stable period from ~0–750 CE, characterised by low pollen turnover and persistent CTS consistent with near-pristine conditions, followed by an initial phase of trophic reorganisation between ~750 and 1050 CE, during which CTS changed despite comparatively limited regional vegetation turnover. The subsequent period (~1050–1450 CE) was characterised by substantial changes in both CTS and surrounding vegetation, reflected by increased pollen compositional turnover, the regional expansion of anthropogenic indicator taxa (e.g., Plantago lanceolata and cereal-type pollen), and declining arboreal cover (Appendix S1, Figs S3 and S4). This interval therefore represents the initial phase of simultaneous terrestrial and aquatic reorganisation. After ~1800 CE, several lakes transitioned toward more plankton-dominated community trophic structures. At the regional scale, changes in CTS broadly followed the major trajectory of vegetation change reconstructed from Hierarchical Generalised Additive Models (HGAM; Pla-Rabes et al., 2024; Simpson, 2024) fitted to pollen DCA scores (Appendix S1, Fig. S3), although the timing of aquatic and terrestrial responses was not always synchronous. While individual lake trajectories varied (Appendix S1, Fig. S8), coherent regional patterns nevertheless emerged. Some lakes exhibited relatively synchronous changes in vegetation and aquatic community structure, whereas others showed temporal offsets spanning several sampling intervals. Similarly, some systems displayed relatively gradual transitions in CTS (e.g., Peixinho, Caveiro and Caldeirão), whereas others underwent more rapid reorganisations over the temporal resolution of the sediment record (e.g., Funda, Azul and Ginjal).

A small subset of trophic guilds strongly predicts community trophic structures in Azorean lakes. Algivores, high-profile diatoms and euplanktonic taxa consistently rank among the top predictors across both metrics (i.e., mean decrease in accuracy and Gini index; Appendix S1, Fig. S9). Model predictions closely matched observed classes with Cohen's Kappa ($\kappa = 0.96$), indicating near-perfect agreement. This strong performance underscores the potential of trophic guild structure as a predictor of lake community states and supports its use in subsequent analyses, including regime shift detection. High contributions from producer guilds suggest that changes in dominant producer types were key signals of long-term ecological restructuring, reflecting their central role in triggering or amplifying system-wide responses to external drivers (Pla-Rabes et al., 2024). In lakes shifting from benthic to planktonic dominance, such changes likely altered habitat structure, nutrient cycling and energy flows (Jeppesen et al., 2005; Scheffer et al., 2001). By contrast, consumer groups such as predators contribute less consistently, likely due to their broader ecological niches, greater mobility and longer generation times, which buffer them against environmental change and lead to delayed or attenuated responses (Woodward et al., 2010). Additionally, bottom-up dynamics mean that producers tend to respond more immediately to changes in energy (e.g., temperature, light) and matter (e.g., nutrients, clastic particle input), whereas consumers are buffered by food-web interactions (Jeppesen et al., 2005). These patterns might be explained by producers mediating the transmission of environmental signals to higher trophic levels through processes such as species compensation, coexistence, and recycling (Ratajczak et al., 2018; Rooney et al., 2006). Thus, while all trophic groups play ecological roles, these findings suggest that specific producer (i.e., high-profile, euplanktonic) and consumer (i.e., algivore) guilds may act as indicators of ecosystem restructuring in this system in response to external drivers.

Changes in species richness

Lake community trophic structures differed significantly in species richness (Fig. 3e; ANOVA, $p < 2.2^{-16}$). Benthic diatom-dominated lakes (CTS 5) supported the highest diversity, whereas euplanktonic-dominated lakes (CTS 1) showed the lowest. Post hoc comparisons confirmed that transitions toward planktonic dominance were associated with ecological simplification, often in deeper lakes (Appendix S1, Table S2). This trend towards planktonic dominance underscores the link between trophic reorganisation and biodiversity loss. It also supports earlier findings that benthic-dominated ecosystems sustain more diverse communities due to greater heterogeneity in light, substrate, resources and water motion, compared to the more homogeneous and potentially

light- and nutrients-limited pelagic conditions (Pla-Rabés & Catalan, 2018). The greater representation of multiple CTSs during recent centuries therefore indicates increasing differentiation among lake trajectories rather than increasing trophic complexity within individual lakes. Several of the CTSs that became more prominent during the later record were characterised by greater euplanktonic dominance and substantially lower species richness than the benthic-dominated CTS 5 (Fig. 3d,e). The more even recent distribution of CTS categories thus reflects the replacement and divergence of historical community configurations across lakes, while their guild composition and richness indicate simplification along several individual lake trajectories. These emerging configurations were dominated by planktonic, often bloom-forming taxa associated with eutrophic or degraded conditions (Pla-Rabes et al., 2024; Raposeiro et al., 2017) and represented comparatively depauperate structures (sensu Mendoza & Araújo, 2022) to the more diverse benthic-dominated structures rather than an enrichment of trophic organisation. Accordingly, the increasing number of CTS categories through time should be interpreted as diversification among lake trajectories under directional ecological change, not as an increase in trophic complexity.

Long-term regional trends in species richness reveal asynchronous trajectories among trophic guilds over the past two millennia (Fig. 4). Among primary producers, mean richness peaked in the early medieval period (~1100 CE) and thereafter became more guild-specific. High-profile diatoms increased earlier (~1370 CE), whereas euplanktonic diatoms showed a considerable increase after ~1600 CE (Fig. 4a; Fig. S10). The late rise of euplanktonic richness is consistent with a shift towards greater pelagic dominance under cumulative nutrient enrichment and reduced light availability (Catalan & Fee, 1994). Consumer guilds declined more gradually (Fig. 4b). Plantivores and detritivores maintained comparatively high richness through much of the earlier record but declined thereafter—detritivores after a mid-second-millennium peak—whereas predator richness significantly declined from approximately 1784 CE onwards (Fig. S10). Algivores remained relatively stable at low richness and did not increase after 1500 CE. These patterns are consistent with progressive weakening of consumer guilds, especially predators, and reduced support for higher trophic levels. In Lake Azul, rising lake levels (Sáez et al., 2025), combined with the introduction of exotic fish, led to major reductions in chironomid diversity, particularly among predaceous and detritivorous taxa (Raposeiro et al., 2017), highlighting the susceptibility of island lake consumers to top-down pressures. Beyond the generally weaker or later consumer richness response, asynchronous producer–consumer trajectories indicate growing decoupling of trophic responses and community restructuring. Comparable long-term shifts have

been documented across oceanic and alpine island lakes, where vegetation clearance, introduced species and human-induced hydrological and biogeochemical changes have led to lasting alterations in lake trophic structure and biodiversity (Cuenca-Cambronero et al., 2022; Nogué et al., 2021).

Interplay between climate variability and land-use intensification

Across both variance-partitioning approaches (historical phases and a 300-year moving window), we observed consistent temporal patterns in the contributions of vegetation change and climate variability to lake trophic structure, identifying three major ecological transitions around ~1000, 1450, and 1750 CE (Fig. 5a, b). These transitions coincide with shifts in catchment vegetation turnover, volcanic disturbances, and successive phases of human land use, including settlement, grazing, and species introductions (Raposeiro et al., 2017, 2021; Ritter et al., 2022; Sáez et al., 2025). Vegetation change, measured as pollen turnover capturing deforestation and agro-pastoral expansion, was the dominant explanatory factor from approximately 1050 to 1750 CE (phases 3 and 4; Fig. 5a). Within this broad interval, the period from approximately 1050 to 1450 CE corresponded to the initial phase of ecological reorganisation, whereas vegetation effects remained important thereafter as climatic influence became increasingly coupled with catchment disturbance i.e. widespread land-use intensification and deforestation (Raposeiro et al., 2021). This pattern was reinforced by two peaks in vegetation-explained variance in the moving window analysis (Fig. 5b), and by consistently positive vegetation–climate effect size contrasts over the same period (Fig. 5c), indicating that vegetation effects generally exceeded climatic effects during this interval. In contrast, the influence of climate, mainly represented by the NAO (Cropper & Hanna, 2014; Hernández et al., 2016) was more intermittent rather than dominant, with detectable contributions during ecological transitional intervals and again during the Little Ice Age (LIA; ~1300–1850 CE) (Raposeiro et al., 2021; Sáez et al., 2025). In the Azores, the LIA was characterised by colder and more humid conditions associated with a predominantly negative NAO (Raposeiro et al., 2024). These conditions are reflected in climate simulations and aquatic diatom records from deep lakes such as Lakes Funda and Azul, indicating enhanced runoff and hydrological variability (Raposeiro et al., 2021).

Moving-window analyses show that climate effects were more evident during early LIA phases (~1300–1450 CE), coinciding with transient reversals in vegetation–climate effect size contrasts (Fig. 5c), but did not persist as a dominant driver. Instead, climate exerted episodic influence superimposed on longer-term vegetation-driven restructuring. A sharp rise in shared variance

fractions after ~1600 CE in both historical-phase and moving-window analyses, peaking after 1750 CE (Fig. 5a, b),indicates that climatic variability increasingly acted in concert with vegetation change in catchments already transformed by sustained human activity. This pattern does not indicate that climate replaced land use as the principal driver, but rather that the effects of hydroclimatic variability became increasingly intertwined with persistent land-use legacies. This increased coupling is consistent with independent sedimentological and geochemical records from Azorean lakes (Sáez et al., 2025), which document shifts in sedimentation regimes during these ecological transition phases, when both climate variability and vegetation change influenced lake communities. During the period of increased shared variance after ~1600 CE, particularly between ~1600 and 1750 CE, a transition from organic-rich sediments toward mineral-rich (clastic) inputs derived from catchment erosion led to increased sediment accumulation rates, while enhanced precipitation produced lake-level fluctuations (Sáez et al., 2025). Before major deforestation, intact native vegetation likely buffered climate impacts by regulating hydrological and biogeochemical processes (Zawiska et al., 2020). As catchments became increasingly disturbed, vegetation may have ceased to act as an effective buffer against erosion and nutrient mobilization (de la Casa et al., 2025), a mechanism consistent with recent evidence that catchment land-cover change cascades through freshwater food webs and ecosystem functioning across multiple trophic levels (Oester et al., 2025). The multivariate temporal patterns were supported by sensitivity analyses, including leave-one-out lake exclusions, perturbations of historical phase boundaries, moving-window analyses, and null models accounting for record length and temporal alignment (Appendix S1).

Discussion

Together, these analyses reveal a long-term trajectory initiated by human-driven vegetation change, with the principal phase of terrestrial and aquatic reorganisation occurring between approximately 1050 and 1450 CE. Land-use effects persisted beyond this interval, while climate variability became increasingly coupled with catchment disturbance after approximately 1600 CE, as already modified landscapes became more responsive to hydroclimatic forcing. Rather than replacing human influence, climate therefore appears to have increasingly modulated ecosystems whose catchments had already been transformed. This intensifying environmental coupling during the centuries following human settlement and into the industrial era may reflect a reduction in terrestrial buffering capacity caused by vegetation loss and catchment disturbance. Such dynamics are consistent with broader patterns of human-driven ecosystem simplification on oceanic islands (Nogué et al., 2021), which heighten sensitivity to climatic forcing. Our trophic-level analysis

589 further shows that restructuring in Azorean lakes was functionally decoupled across trophic
590 levels, with asynchronous producer and consumer responses reflecting differences in sensitivity to
591 nutrient inputs, hydrology, and habitat structure. Producer communities generally reorganised
592 earlier and more strongly than consumers, consistent with their short generation times and rapid
593 responses to changes in nutrients, light and hydrology (Wentzky et al., 2020; Zeng et al., 2024).
594 Consumer responses were more delayed and spatially variable, potentially reflecting their
595 dependence on habitat structure, food availability and indirect pathways of environmental change
596 (Siqueira et al., 2024). These contrasting trajectories indicate that whole-ecosystem reorganisation
597 cannot be reliably inferred from a single biological proxy, for example, an apparently gradual
598 change at one trophic level may coincide with abrupt or persistent change at another.
599 By identifying ecological thresholds and interaction points between vegetation change and
600 climate variability, our framework provides a mechanistic basis for understanding how these
601 insular lake ecosystems may adapt,or become increasingly vulnerable, to continued anthropogenic
602 pressure and future climate change.
603
604 The absence of strong independent climate signals before ~850 CE may reflect several, not
605 mutually exclusive, factors: (1) climate variability alone may not have been sufficient to drive
606 major ecological change, as regional reconstructions indicate relatively stable long-term
607 precipitation conditions in the Azores during the late Holocene, punctuated by shorter-term
608 variability associated with changes in North Atlantic atmospheric circulation, particularly the
609 NAO (Andrade et al., 2025; Hernández et al., 2016; Vicente-Serrano et al., 2025); (2) NAO–
610 ecosystem relationships are likely non-stationary, with shifting spatial and ecological effects
611 (Halifa-Marín et al., 2025) and ecological impacts that may shift over time (Raposeiro et al.,
612 2024), while catchment vegetation likely buffered lakes from climate variability before human
613 modification (~700 CE); and (3) volcanic activity may have masked climate signals in sediments,
614 such as the deposition of tephra from the P17 eruption in Lake Azul (Vázquez-Loureiro et al.,
615 2023).
616
617 Community trophic structures in Azorean lake ecosystems show a progressive trajectory of
618 trophic simplification, defined by long-term declines in species richness and repeated transitions
619 toward plankton-dominated, species-poor trophic structures. Together, these patterns indicate a
620 sustained reduction in trophic complexity across the archipelago. Human land use initiated and
621 sustained this trajectory, while climatic variability increasingly modulated ecosystem responses

after catchments had already been transformed, even if total primary production and energy throughput may have increased in some systems.

By integrating producers and consumers, our multi-trophic approach not only identified when reorganisations occurred and their associated drivers, but also distinguished transient from persistent shifts, exposing a millennium-long trajectory of human-driven trophic simplification, a dimension of ecological change that would remain partly hidden in single-proxy reconstructions. Our analysis highlights that trophic decoupling and reduced functional diversity can easily be overlooked in single-proxy studies. This underscores the value of integrating multi-trophic records with trait-based classifications (Antczak-Orlewska et al., 2021; Nevalainen et al., 2015; Raposeiro et al., 2017) and of operationalizing these approaches in routine assessments to better detect, understand, and ultimately prevent further ecosystem simplification. Building on the approach presented here, future studies should extend comparable multi-trophic reconstructions across a wider diversity of lake ecosystems to evaluate the generality of long-term trajectories of trophic simplification, trophic decoupling, and shifting ecological baselines across contrasting environmental and biogeographic contexts. Such comparisons would provide a stronger basis for distinguishing universal ecological responses to global change from those shaped by regional biogeographic and environmental contexts, thereby improving the transferability of dynamic baseline concepts for conservation and ecosystem management.

Our archipelago-wide reconstruction also provides a framework for defining dynamic baselines that incorporate both natural variability and responses to perturbation at lake and regional scales. These assessments can help distinguish lakes that retain recovery potential from those constrained by persistent catchment and ecological legacies, thereby informing where interventions such as catchment vegetation restoration, nutrient-load reduction, hydrological management or control of introduced species are most likely to be effective. On islands, where colonization has been rapid and transformative, these legacies are especially pronounced (Nogué et al., 2021; Raposeiro et al., 2021). Understanding which lakes can recover, which remain vulnerable, and what interventions may still prevent further ecological simplification is essential for more adaptive strategies in a changing world.

References

Andrade, M., Hernández, A., Pimentel, A., Cruz, J. V., Ramos, A. M., Ludwig, P., Schindlbeck-Belo, J. C., & Ramalho, R. S. (2025). Controls on Water-Magma Interactions at Hydraulically-Charged Volcanic Islands. *Geophysical Research Letters*, *52*(18), e2025GL115727. https://doi.org/10.1029/2025GL115727

Antczak-Orlewska, O., Płóciennik, M., Sobczyk, R., Okupny, D., Stachowicz-Rybka, R., Rzodkiewicz, M., Siciński, J., Mroczkowska, A., Krąpiec, M., Słowiński, M., & Kittel, P. (2021). Chironomidae Morphological Types and Functional Feeding Groups as a Habitat Complexity Vestige. *Frontiers in Ecology and Evolution*, *8*. https://doi.org/10.3389/fevo.2020.583831

Araújo, M. B., Anderson, R. P., Barbosa, A. M., Beale, C. M., Dormann, C. F., Early, R., Garcia, R. A., Guisan, A., Maiorano, L., Naimi, B., O'Hara, R. B., Zimmermann, N. E., & Rahbek, C. (2019). Standards for distribution models in biodiversity assessments. *Science Advances*, *5*(1), eaat4858. https://doi.org/10.1126/sciadv.aat4858

Berglund, B. E. (2003). Human impact and climate changes—Synchronous events and a causal link? *Quaternary International, Environmental Variability in East and West Eurasia*, *105*(1), 7–12. https://doi.org/10.1016/S1040-6182(02)00144-1

Blaauw, M., Christen, J. A., Vazquez, J. E., & Goring, S. (2020). clam: Classical Age-Depth Modelling of Cores from Deposits. *R Package Version 2.3.7*. https://cran.r-project.org/package=clam

Borcard, D., Gillet, F., & Legendre, P. (2018). *Numerical Ecology with R*. Springer International Publishing. https://doi.org/10.1007/978-3-319-71404-2

Bradley, R. S. (2015). Chapter 1—Paleoclimatic Reconstruction. In R. S. Bradley (Ed.), *Paleoclimatology (Third Edition)* (pp. 1–11). Academic Press. https://doi.org/10.1016/B978-0-12-386913-5.00001-6

678 Breiman, L., Friedman, J., Olshen, R. A., & Stone, C. J. (2017). *Classification and Regression*
679 *Trees*. Chapman and Hall/CRC. https://doi.org/10.1201/9781315139470
680 Büntgen, U., Allen, K., Anchukaitis, K. J., Arseneault, D., Boucher, É., Bräuning, A., Chatterjee,
681 S., Cherubini, P., Churakova (Sidorova), O. V., Corona, C., Gennaretti, F., Grießinger, J.,
682 Guillet, S., Guiot, J., Gunnarson, B., Helama, S., Hochreuther, P., Hughes, M. K.,
683 Huybers, P., … Esper, J. (2021). The influence of decision-making in tree ring-based
684 climate reconstructions. *Nature Communications*, *12*(1), 3411.
685 https://doi.org/10.1038/s41467-021-23627-6
686 Carpenter, S. R., Kitchell, J. F., Hodgson, J. R., Cochran, P. A., Elser, J. J., Elser, M. M., Lodge,
687 D. M., Kretchmer, D., He, X., & von Ende, C. N. (1987). Regulation of Lake Primary
688 Productivity by Food Web Structure. *Ecology*, *68*(6), 1863–1876.
689 https://doi.org/10.2307/1939878
690 Catalan, J., & Fee, F. (1994). Interanual variability in limnic ecosystems:origin, patterns and
691 predictability. In R. Margalef (Ed.), *Limnology Now: A Paradigm of Planetary Problems*.
692 Elsewier Science.
693 Catalan, J., Pla-Rabés, S., Wolfe, A. P., Smol, J. P., Rühland, K. M., Anderson, N. J., Kopáček, J.,
694 Stuchlík, E., Schmidt, R., Koinig, K. A., Camarero, L., Flower, R. J., Heiri, O., Kamenik,
695 C., Korhola, A., Leavitt, P. R., Psenner, R., & Renberg, I. (2013). Global change revealed
696 by palaeolimnological records from remote lakes: A review. *Journal of Paleolimnology*,
697 *49*(3), 513–535. https://doi.org/10.1007/s10933-013-9681-2
698 Chamberlain, S. A., & Szöcs, E. (2013). taxize: Taxonomic search and retrieval in R.
699 *F1000Research*, *2*, 191.
700 Connor, S. E., van Leeuwen, J. F. N., Rittenour, T. M., van der Knaap, W. O., Ammann, B., &
701 Björck, S. (2012). The ecological impact of oceanic island colonization - a
702 palaeoecological perspective from the Azores: Palaeoecology of human colonization of

the Azores. *Journal of Biogeography*, *39*(6), 1007–1023. https://doi.org/10.1111/j.1365-2699.2011.02671.x

Cropper, T. E., & Hanna, E. (2014). An analysis of the climate of Macaronesia, 1865–2012. *International Journal of Climatology*, *34*(3), 604–622. https://doi.org/10.1002/joc.3710

Cuenca-Cambronero, M., Courtney-Mustaphi, C. J., Greenway, R., Heiri, O., Hudson, C. M., King, L., Lemmen, K. D., Moosmann, M., Muschick, M., Ngoepe, N., Seehausen, O., & Matthews, B. (2022). An integrative paleolimnological approach for studying evolutionary processes. *Trends in Ecology & Evolution*, *37*(6), 488–496. https://doi.org/10.1016/j.tree.2022.01.007

de la Casa, J., Nogué, S., De Cáceres, M., Pla-Rabés, S., Sardans, J., Benavente, M., Giralt, S., Hernandez, A., Raposeiro, P. M., & Peñuelas, J. (2025). Unveiling two millennia of ecosystem changes in the Azores through elementome trajectory analysis. *Ecological Indicators*, *176*, 113630. https://doi.org/10.1016/j.ecolind.2025.113630

Dubois, N., Saulnier-Talbot, É., Mills, K., Gell, P., Battarbee, R., Bennion, H., Chawchai, S., Dong, X., Francus, P., Flower, R., Gomes, D. F., Gregory-Eaves, I., Humane, S., Kattel, G., Jenny, J., Langdon, P., Massaferro, J., McGowan, S., Mikomägi, A., … Valero-Garcés, B. (2018). First human impacts and responses of aquatic systems: A review of palaeolimnological records from around the world. *The Anthropocene Review*, *5*(1), 28–68. https://doi.org/10.1177/2053019617740365

Elias, R. B., Connor, S. E., Góis-Marques, C. A., Schaefer, H., Silva, L., Sequeira, M. M., Moura, M., Borges, P. A. V., & Gabriel, R. (2022). Is there solid evidence of widespread landscape disturbance in the Azores before the arrival of the Portuguese? *Proceedings of the National Academy of Sciences*, *119*(4), e2119218119. https://doi.org/10.1073/pnas.2119218119

Gelis, M. M. N., Sathicq, M. B., & Cochero, J. (2024). *diathor: Calculate Ecological Information and Diatom Based Indices*. https://cran.r-project.org/web/packages/diathor/index.html

Glew, J. R., Smol, J. P., & Last, W. M. (2001). Sediment Core Collection and Extrusion. In W. M. Last & J. P. Smol (Eds.), *Tracking Environmental Change Using Lake Sediments: Basin Analysis, Coring, and Chronological Techniques* (pp. 73–105). Springer Netherlands. https://doi.org/10.1007/0-306-47669-X_5

González-del-Pliego, P., Mendoza, M., Santana, J., Ribeiro, J., Reino, L., & Araújo, M. B. (2023). Vacant niches help predict invasion risk by birds. *Journal of Biogeography*, *50*(11), 1827–1837. https://doi.org/10.1111/jbi.14693

González-Trujillo, J. D., Assis, J., Serrão, E., Costello, M. J., Fragkopoulou, E., Mendoza, M., & Araújo, M. B. (2025). Trophic convergence of marine vertebrate communities worldwide. *Proceedings of the National Academy of Sciences*, *122*(17), e2403754122. https://doi.org/10.1073/pnas.2403754122

González-Trujillo, J. D., Mendoza, M., & Araújo, M. B. (2025). Projecting community trophic structures for the last 120 000 years. *Ecography*, *2025*(3), e06899. https://doi.org/10.1111/ecog.06899

Halifa-Marín, A., Pravia-Sarabia, E., Torres-Vázquez, M. A., Trigo, R., Vicente-Serrano, S. M., Jerez, S., Turco, M., Jiménez-Guerrero, P., & Montávez, J. P. (2025). Unparalleled EA-like leading mode of variability in the early 20th century highlights the need for understanding non-stationarity in the North Atlantic climate system. *Atmospheric Research*, *314*, 107796. https://doi.org/10.1016/j.atmosres.2024.107796

Hernández, A., Kutiel, H., Trigo, R. M., Valente, M. A., Sigró, J., Cropper, T., & Santo, F. E. (2016). New Azores archipelago daily precipitation dataset and its links with large-scale modes of climate variability. *International Journal of Climatology*, *36*(14), 4439–4454. https://doi.org/10.1002/joc.4642

Hernández, A., Sáez, A., Bao, R., Raposeiro, P. M., Trigo, R. M., Doolittle, S., Masqué, P., Rull, V., Gonçalves, V., Vázquez-Loureiro, D., Rubio-Inglés, M. J., Sánchez-López, G., & Giralt, S. (2017). The influences of the AMO and NAO on the sedimentary infill in an Azores Archipelago lake since ca. 1350CE. *Global and Planetary Change*, *154*, 61–74. https://doi.org/10.1016/j.gloplacha.2017.05.007

Hernández, A., Sánchez-López, G., Pla-Rabes, S., Comas-Bru, L., Parnell, A., Cahill, N., Geyer, A., Trigo, R. M., & Giralt, S. (2020). A 2,000-year Bayesian NAO reconstruction from the Iberian Peninsula. *Scientific Reports*, *10*(1), 14961. https://doi.org/10.1038/s41598-020-71372-5

Hill, M. O., & Gauch, H. G. (1980). Detrended correspondence analysis: An improved ordination technique. *Vegetatio*, *42*(1), 47–58. https://doi.org/10.1007/BF00048870

Jenny, J.-P., Koirala, S., Gregory-Eaves, I., Francus, P., Niemann, C., Ahrens, B., Brovkin, V., Baud, A., Ojala, A. E. K., Normandeau, A., Zolitschka, B., & Carvalhais, N. (2019). Human and climate global-scale imprint on sediment transfer during the Holocene. *Proceedings of the National Academy of Sciences*, *116*(46), 22972–22976. https://doi.org/10.1073/pnas.1908179116

Jeppesen, E., Søndergaard, M., Jensen, J. P., Havens, K. E., Anneville, O., Carvalho, L., Coveney, M. F., Deneke, R., Dokulil, M. T., Foy, B., Gerdeaux, D., Hampton, S. E., Hilt, S., Kangur, K., Köhler, J., Lammens, E. H. h. r., Lauridsen, T. L., Manca, M., Miracle, M. R., … Winder, M. (2005). Lake responses to reduced nutrient loading – an analysis of contemporary long-term data from 35 case studies. *Freshwater Biology*, *50*(10), 1747–1771. https://doi.org/10.1111/j.1365-2427.2005.01415.x

Kidwell, S. M. (2015). Biology in the Anthropocene: Challenges and insights from young fossil records. *Proceedings of the National Academy of Sciences*, *112*(16), 4922–4929. https://doi.org/10.1073/pnas.1403660112

Lotter, A. F., & Birks, H. J. B. (2003). The Holocene palaeolimnology of Sägistalsee and its environmental history – a synthesis. *Journal of Paleolimnology*, *30*(3), 333–342. https://doi.org/10.1023/A:1026091511403

Matias, M. G., Pereira, C. L., Raposeiro, P. M., Gonçalves, V., Cruz, A. M., Costa, A. C., & Araújo, M. B. (2017). Divergent trophic responses to biogeographic and environmental gradients. *Oikos*, *126*(1), 101–110. https://doi.org/10.1111/oik.02604

Mehner, T., Lischke, B., Scharnweber, K., Attermeyer, K., Brothers, S., Gaedke, U., Hilt, S., & Brucet, S. (2018). Empirical correspondence between trophic transfer efficiency in freshwater food webs and the slope of their size spectra. *Ecology*, *99*(6), 1463–1472. https://doi.org/10.1002/ecy.2347

Mendoza, M., & Araújo, M. B. (2019). Climate shapes mammal community trophic structures and humans simplify them. *Nat Commun*, *10*(1), 1–9.

Mendoza, M., & Araújo, M. B. (2022). Biogeography of bird and mammal trophic structures. *Ecography*, *2022*(7). https://doi.org/10.1111/ecog.06289

Merz, E., Saberski, E., Gilarranz, L. J., Isles, P. D. F., Sugihara, G., Berger, C., & Pomati, F. (2023). Disruption of ecological networks in lakes by climate change and nutrient fluctuations. *Nature Climate Change*, *13*(4), 389–396. https://doi.org/10.1038/s41558-023-01615-6

Nevalainen, L., Luoto, T. P., Manca, M., & Weisse, T. (2015). A paleolimnological perspective on aquatic biodiversity in Austrian mountain lakes. *Aquatic Sciences*, *77*(1), 59–69. https://doi.org/10.1007/s00027-014-0363-6

Nogué, S., Santos, A. M. C., Birks, H. J. B., Björck, S., Castilla-Beltrán, A., Connor, S., de Boer, E. J., de Nascimento, L., Felde, V. A., Fernández-Palacios, J. M., Froyd, C. A., Haberle, S. G., Hooghiemstra, H., Ljung, K., Norder, S. J., Peñuelas, J., Prebble, M., Stevenson, J.,

Whittaker, R. J., … Steinbauer, M. J. (2021). The human dimension of biodiversity changes on islands. *Science*, *372*(6541), 488–491. https://doi.org/10.1126/science.abd6706

Oester, R., Keck, F., Moretti, M. S., Altermatt, F., Bruder, A., & Ferreira, V. (2025). A Global Synthesis on Land-Cover Changes in Watersheds Shaping Freshwater Detrital Food Webs. *Global Change Biology*, *31*(8), e70380. https://doi.org/10.1111/gcb.70380

Passy, S. I. (2007). Diatom ecological guilds display distinct and predictable behavior along nutrient and disturbance gradients in running waters. *Aquatic Botany*, *86*(2), 171–178. https://doi.org/10.1016/j.aquabot.2006.09.018

Peres-Neto, P. R., Legendre, P., Dray, S., & Borcard, D. (2006). Variation partitioning of species data matrices: Estimation and comparison of fractions. *Ecology*, *87*(10), 2614–2625.

Pla-Rabés, S., & Catalan, J. (2018). Diatom species variation between lake habitats: Implications for interpretation of paleolimnological records. *Journal of Paleolimnology*, *60*(2), 169–187. https://doi.org/10.1007/s10933-018-0017-0

Pla-Rabes, S., Matias, M. G., Gonçalves, V., Vázquez Loureiro, D., Marques, H., Bao, R., Buchaca, T., Hernández, A., Giralt, S., Sáez, A., Simpson, G. L., Nogué, S., & Raposeiro, P. M. (2024). Global warming triggers abrupt regime shifts in island lake ecosystems in the Azores Archipelago. *Communications Earth & Environment*, *5*(1), 1–14. https://doi.org/10.1038/s43247-024-01744-6

Poelen, J. H., Simons, J. D., & Mungall, C. J. (2014). Global biotic interactions: An open infrastructure to share and analyze species-interaction datasets. *Ecological Informatics*, *24*, 148–159. https://doi.org/10.1016/j.ecoinf.2014.08.005

Raposeiro, P. M., Hernández, A., Pla-Rabes, S., Gonçalves, V., Bao, R., Sáez, A., Shanahan, T., Benavente, M., de Boer, E. J., Richter, N., Gordon, V., Marques, H., Sousa, P. M., Souto, M., Matias, M. G., Aguiar, N., Pereira, C., Ritter, C., Rubio, M. J., … Giralt, S. (2021). Climate change facilitated the early colonization of the Azores Archipelago during

826 medieval times. *Proceedings of the National Academy of Sciences*, *118*(41), e2108236118.
827 https://doi.org/10.1073/pnas.2108236118
828 Raposeiro, P. M., Hernández, A., Pla-Rabes, S., Gonçalves, V., Bao, R., Sáez, A., Shanahan, T.,
829 Benavente, M., de Boer, E. J., Richter, N., Gordon, V., Marques, H., Sousa, P. M., Souto,
830 M., Matias, M. G., Aguiar, N., Pereira, C., Ritter, C., Rubio, M. J., … Giralt, S. (2022).
831 Reply to Elias et al.: Multiproxy evidence of widespread landscape disturbance in multiple
832 Azorean lakes before the Portuguese arrival. *Proceedings of the National Academy of*
833 *Sciences*, *119*(4), e2120107119. https://doi.org/10.1073/pnas.2120107119
834 Raposeiro, P. M., Ritter, C., Abbott, M., Hernandez, A., Pimentel, A., Lasher, E., Płóciennik, M.,
835 Berlajolli, V., Kotrys, B., Pombal, X. P., Souto, M., Giralt, S., & Gonçalves, V. (2024).
836 Late Holocene climate dynamics in the Azores archipelago. *Quaternary Science Reviews*,
837 *331*. Scopus. https://doi.org/10.1016/j.quascirev.2024.108617
838 Raposeiro, P. M., Rubio, M. J., González, A., Hernández, A., Sánchez-López, G., Vázquez-
839 Loureiro, D., Rull, V., Bao, R., Costa, A. C., Gonçalves, V., Sáez, A., & Giralt, S. (2017).
840 Impact of the historical introduction of exotic fishes on the chironomid community of
841 Lake Azul (Azores Islands). *Palaeogeography, Palaeoclimatology, Palaeoecology*, *466*,
842 77–88. https://doi.org/10.1016/j.palaeo.2016.11.015
843 Ratajczak, Z., Carpenter, S. R., Ives, A. R., Kucharik, C. J., Ramiadantsoa, T., Stegner, M. A.,
844 Williams, J. W., Zhang, J., & Turner, M. G. (2018). Abrupt Change in Ecological
845 Systems: Inference and Diagnosis. *Trends in Ecology & Evolution*, *33*(7), 513–526.
846 https://doi.org/10.1016/j.tree.2018.04.013
847 Rimet, F., & Bouchez, A. (2012). Life-forms, cell-sizes and ecological guilds of diatoms in
848 European rivers. *Knowledge and Management of Aquatic Ecosystems*, (406), Article 406.
849 https://doi.org/10.1051/kmae/2012018

Ritter, C., Gonçalves, V., Pla-Rabes, S., de Boer, E. J., Bao, R., Sáez, A., Hernández, A., Sixto, M., Richter, N., Benavente, M., Prego, R., Giralt, S., & Raposeiro, P. M. (2022). The vanishing and the establishment of a new ecosystem on an oceanic island – Anthropogenic impacts with no return ticket. *Science of the Total Environment*, *830*. Scopus. https://doi.org/10.1016/j.scitotenv.2022.154828

Rooney, N., McCann, K., Gellner, G., & Moore, J. C. (2006). Structural asymmetry and the stability of diverse food webs. *Nature*, *442*(7100), 265–269. https://doi.org/10.1038/nature04887

Rühland, K. M., Paterson, A. M., & Smol, J. P. (2015). Lake diatom responses to warming: Reviewing the evidence. *Journal of Paleolimnology*, *54*(1), 1–35. https://doi.org/10.1007/s10933-015-9837-3

Rull, V. (2023). Settlement and anthropization of the Azores Islands. *Journal of Biogeography*, *50*(12), 2008–2011. https://doi.org/10.1111/jbi.14712

Rull, V., Lara, A., Rubio-Inglés, M. J., Giralt, S., Gonçalves, V., Raposeiro, P., Hernández, A., Sánchez-López, G., Vázquez-Loureiro, D., Bao, R., Masqué, P., & Sáez, A. (2017). Vegetation and landscape dynamics under natural and anthropogenic forcing on the Azores Islands: A 700-year pollen record from the São Miguel Island. *Quaternary Science Reviews*, *159*, 155–168. https://doi.org/10.1016/j.quascirev.2017.01.021

Sáez, A., Hernández, A., Pimentel, A., Andrade, M., Bao, R., Raposeiro, P. M., Gonçalves, V., Benavente, M., Pla-Rabes, S., Ramalho, R., & Giralt, S. (2025). Westerlies migrations and volcanic records over the past 4000 years from the Azores lacustrine sequences. Exploring correlations and impacts on Western Europe. *Global and Planetary Change*, *246*, 104698. https://doi.org/10.1016/j.gloplacha.2025.104698

Scheffer, M., Carpenter, S., Foley, J. A., Folke, C., & Walker, B. (2001). Catastrophic shifts in ecosystems. *Nature*, *413*(6856), 591–596. https://doi.org/10.1038/35098000

Simpson, G. L. (2024). gratia: An R package for exploring generalized additive models. *Journal of Open Source Software*, *9*(104), 6962. https://doi.org/10.21105/joss.06962

Siqueira, T., Hawkins, C. P., Olden, J. D., Tonkin, J., Comte, L., Saito, V. S., Anderson, T. L., Barbosa, G. P., Bonada, N., Bonecker, C. C., Cañedo-Argüelles, M., Datry, T., Flinn, M. B., Fortuño, P., Gerrish, G. A., Haase, P., Hill, M. J., Hood, J. M., Huttunen, K.-L., … Ruhi, A. (2024). Understanding temporal variability across trophic levels and spatial scales in freshwater ecosystems. *Ecology*, *105*(2), e4219. https://doi.org/10.1002/ecy.4219

Smol, J. P. (2010). The power of the past: Using sediments to track the effects of multiple stressors on lake ecosystems. *Freshwater Biology*, *55*(s1), 43–59. https://doi.org/10.1111/j.1365-2427.2009.02373.x

Vázquez-Loureiro, D., Sáez, A., Gonçalves, V., Buchaca, T., Hernández, A., Raposeiro, P. M., Boer, E. J. de, Masqué, P., Giralt, S., & Bao, R. (2023). Recent global warming induces the coupling of dissimilar long-term sedimentary signatures in two adjacent volcanic lakes (Azores Archipelago, Portugal). *Quaternary Science Reviews*, *303*, 107968. https://doi.org/10.1016/j.quascirev.2023.107968

Vicente-Serrano, S. M., Tramblay, Y., Reig, F., González-Hidalgo, J. C., Beguería, S., Brunetti, M., Kalin, K. C., Patalen, L., Kržič, A., Lionello, P., Lima, M. M., Trigo, R. M., El-Kenawy, A. M., Eddenjal, A., Türkes, M., Koutroulis, A., Manara, V., Maugeri, M., Badi, W., … Potopová, V. (2025). High temporal variability not trend dominates Mediterranean precipitation. *Nature*, *639*(8055), 658–666. https://doi.org/10.1038/s41586-024-08576-6

Wentzky, V. C., Tittel, J., Jäger, C. G., Bruggeman, J., & Rinke, K. (2020). Seasonal succession of functional traits in phytoplankton communities and their interaction with trophic state. *Journal of Ecology*, *108*(4), 1649–1663. https://doi.org/10.1111/1365-2745.13395

Whittaker, R. J., & Fernández-Palacios, J. M. (2007). *Island biogeography: Ecology, evolution, and conservation*. Oxford University Press, USA.

Woodward, G., Perkins, D. M., & Brown, L. E. (2010). Climate change and freshwater ecosystems: Impacts across multiple levels of organization. *Philosophical Transactions of the Royal Society B: Biological Sciences*, *365*(1549), 2093–2106. https://doi.org/10.1098/rstb.2010.0055

Woolway, R. I., Sharma, S., Weyhenmeyer, G. A., Debolskiy, A., Golub, M., Mercado-Bettín, D., Perroud, M., Stepanenko, V., Tan, Z., Grant, L., Ladwig, R., Mesman, J., Moore, T. N., Shatwell, T., Vanderkelen, I., Austin, J. A., DeGasperi, C. L., Dokulil, M., La Fuente, S., … Jennings, E. (2021). Phenological shifts in lake stratification under climate change. *Nature Communications*, *12*(1), 2318. https://doi.org/10.1038/s41467-021-22657-4

Zawiska, I., Dimante-Deimantovica, I., Luoto, T. P., Rzodkiewicz, M., Saarni, S., Stivrins, N., Tylmann, W., Lanka, A., Robeznieks, M., & Jilbert, T. (2020). Long-Term Consequences of Water Pumping on the Ecosystem Functioning of Lake Sekšu, Latvia. *Water*, *12*(5), 1459. https://doi.org/10.3390/w12051459

Zeng, L., Engels, S., Cao, Y., Huang, X., & Chen, X. (2024). Divergent sensitivity of primary producers and benthic invertebrates to hydrological alteration in floodplain lakes. *Anthropocene*, *47*, 100441. https://doi.org/10.1016/j.ancene.2024.100441

Figure 1

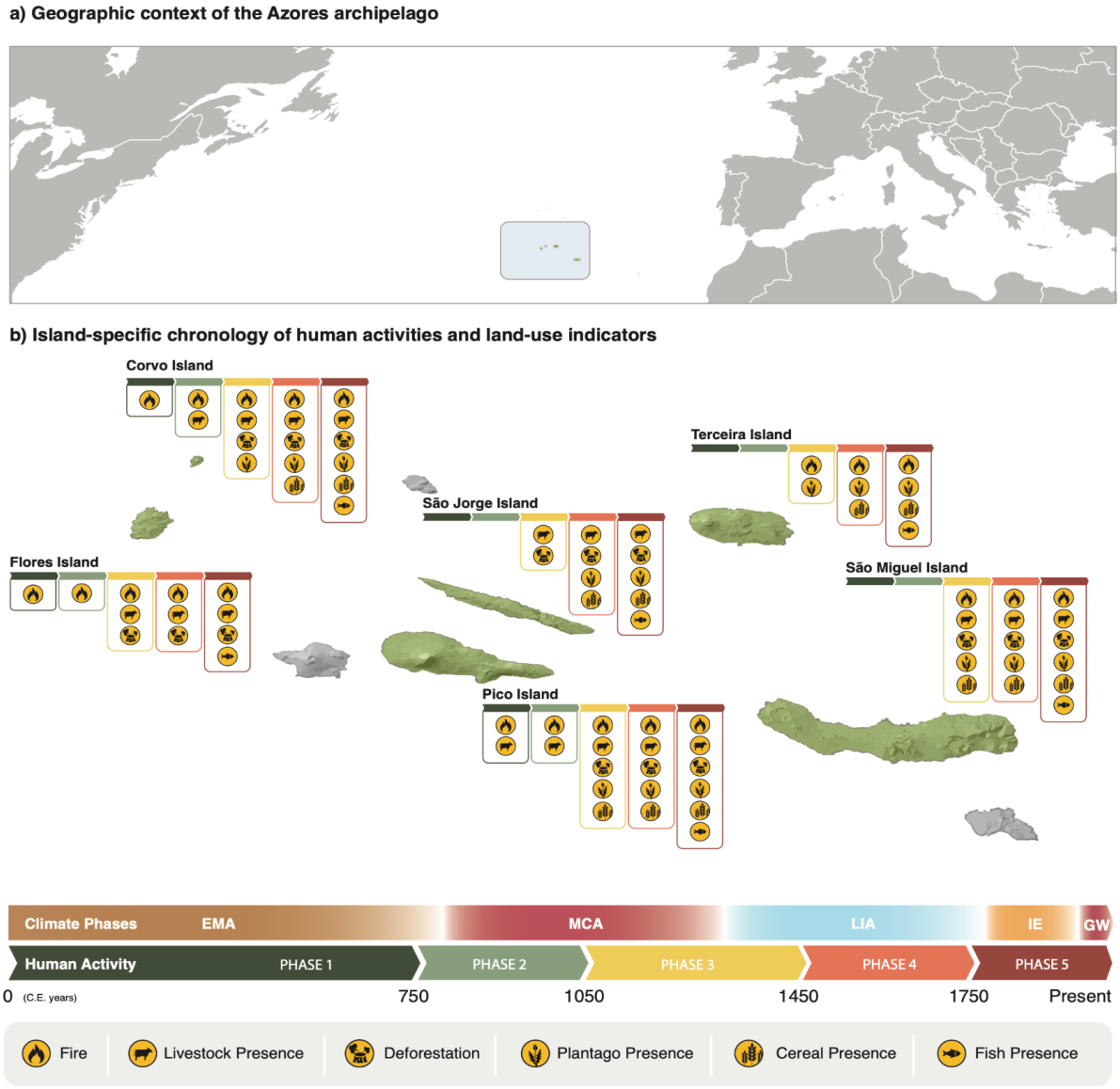

Figure 1. Climatic and anthropogenic context of lake ecosystem change in the Azores over the last 2000 years. (a) Geographic context of the Azores archipelago in the North Atlantic. (b) Island-specific chronology of major climatic phases, vegetation change, and human activity indicators inferred from multiproxy paleoecological and paleolimnological evidence. Shaded bands indicate major climatic intervals (Early Medieval Period, Medieval Climate Anomaly, Little Ice Age, Industrial Era, and recent Global Warming), while colored timelines summarize phases of human activity. Icons denote the timing of first appearances or sustained increases of disturbance proxies at individual islands, including fire activity, livestock presence, deforestation, crop cultivation (*Plantago* and cereals), and fish introductions. Phase boundaries correspond to historically and paleoecologically defined transitions in land use and human pressure across the archipelago. This synthesis follows and extends the framework of Raposeiro et al. (2021),

illustrating how climate variability modulated access to the archipelago and influenced the timing and intensity of successive waves of human occupation and ecosystem disturbance.

Figure 2

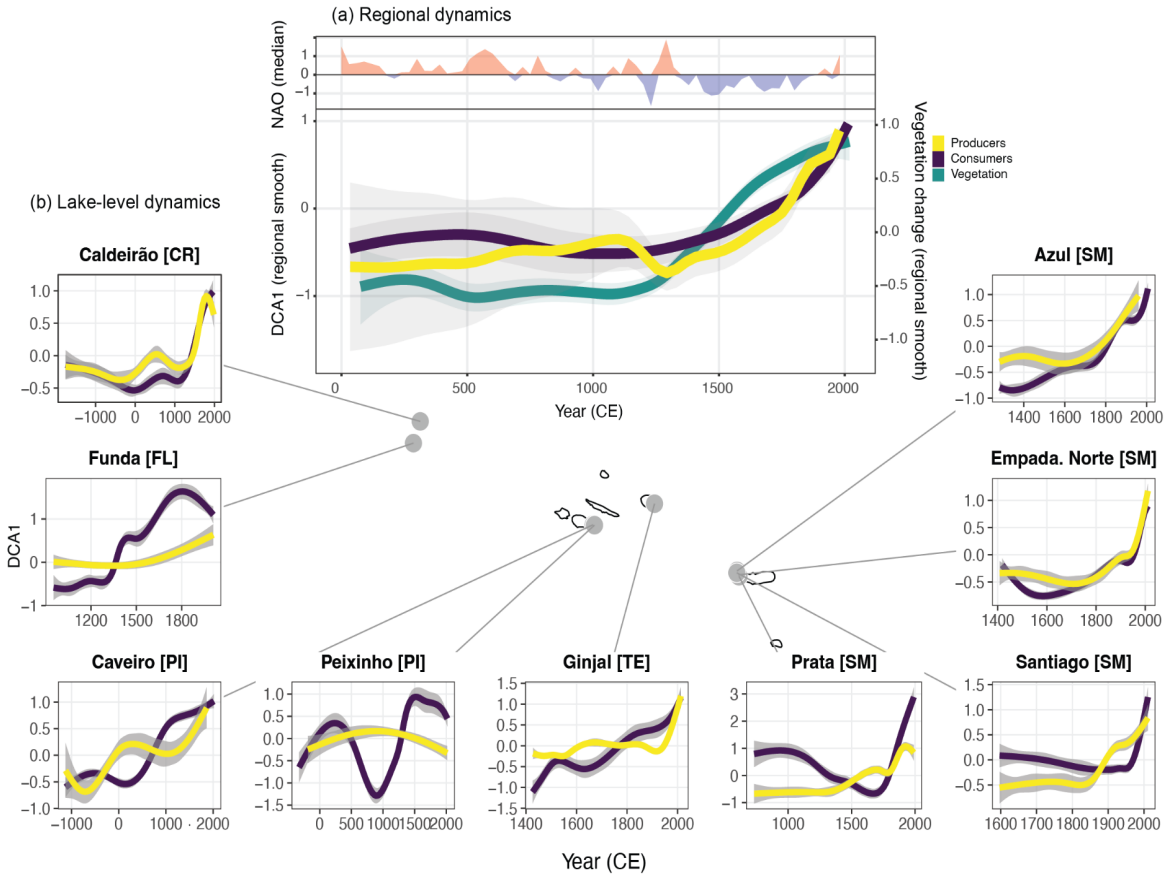

Figure 2. Integrated climatic, vegetation, and trophic dynamics across Azorean lake ecosystems. (a) Regional-scale dynamics of lake community turnover inferred from hierarchical generalized additive models (HGAMs), shown separately for primary producers, consumers, and catchment vegetation. The upper panel displays the standardised North Atlantic Oscillation (NAO) index, providing climatic context for ecosystem change. (b) Lake-specific trajectories of community turnover for individual sites across the Azores archipelago (y-axis: first axis of detrended correspondence analysis, DCA1) plotted against calendar age (CE). Colored lines represent fitted HGAM trends for primary producers (yellow) and consumers (purple), with shaded bands indicating 95% confidence intervals. Grey points and connectors indicate the geographic location of each lake within the archipelago (where CR = Corvo, FL = Flores, PI = Pico, TE = Terceira, and SM = São Miguel), allowing direct comparison between regional forcing and site-level ecological responses.

Figure 3

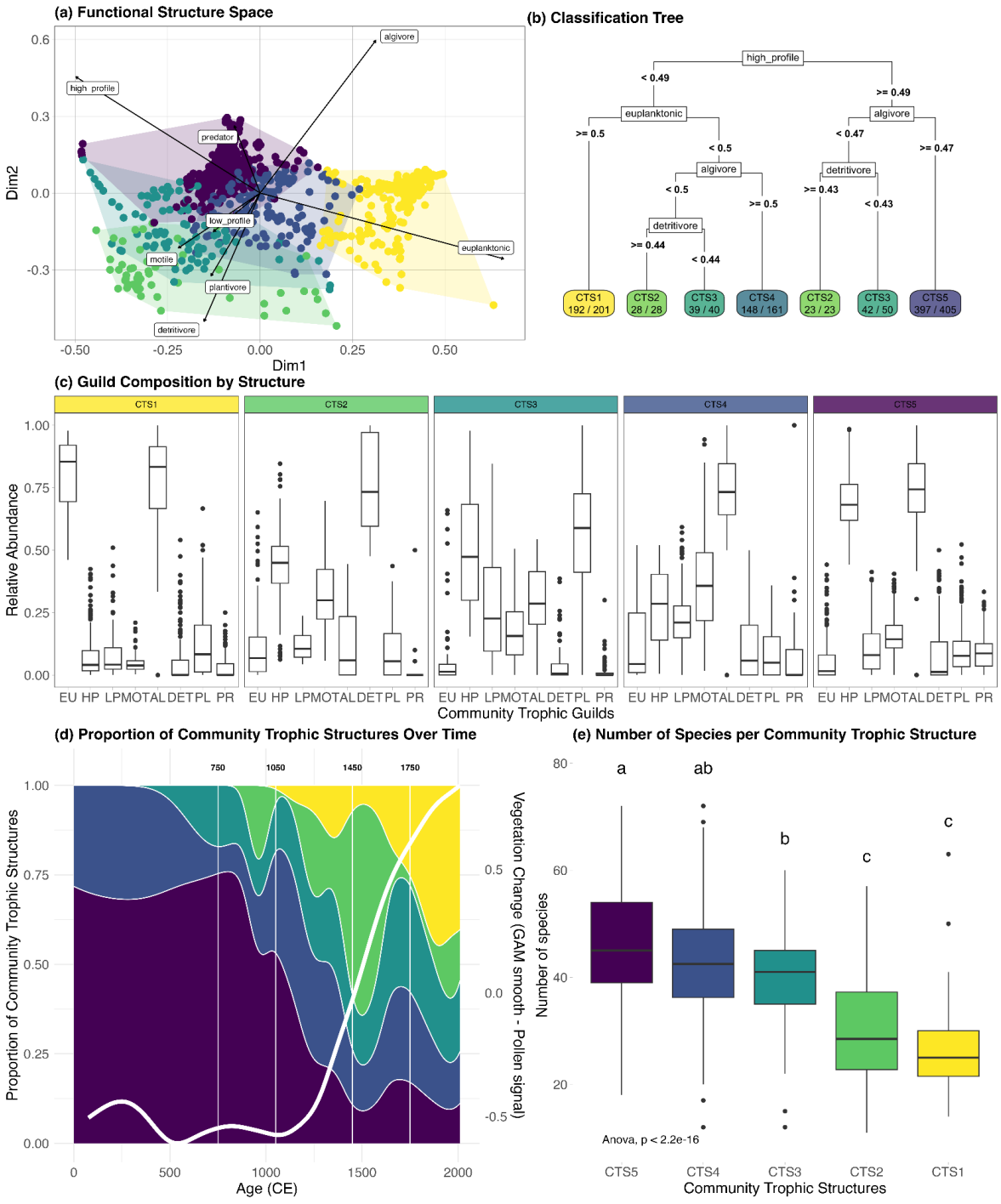

Figure 3. Community trophic structures and their long-term dynamics in Azorean lakes. (a) Ordination of lake assemblages showing correlations between trophic guilds and ordination axes (Dim1 and Dim2), with colors indicating community trophic structures (CTS1–CTS5). Vectors represent major producer guilds, euplanktonic (EU), low profile (LP), high profile (HP), and motile (MOT), and consumer guilds, algivore (AL), detritivore (DET), plantivore (PL), and predator (PR). (b, c) Classification of samples into five distinct community trophic structures (CTS1–CTS5), based on relative abundances of key trophic guilds. The decision tree (b)

highlights the abundance thresholds used for classification, while the boxplots (c) summarize the distribution of trophic guilds across the five types. CTS1 (yellow) is defined by high abundances of euplanktonic diatoms and algivores and low abundance of high-profile diatoms. CTS2 (light green) shows low algivore and high detritivore abundance. CTS3 (dark green) combines low detritivore abundance, intermediate algivore levels and high planktivore abundance. CTS4 (dark blue) features intermediate levels of high-profile diatoms and high algivore abundance. CTS5 (dark purple) is characterised by high abundance of both high-profile diatoms and algivores. (d) Temporal dynamics of community trophic structures across the Azorean archipelago over the past two millennia. Stacked density plot shows the proportion of each CTS through time, with major periods of anthropogenic disturbance (700, 1050, 1450 and 1750 CE) indicated by vertical lines (Raposeiro et al. 2021). The white line represents vegetation turnover based on a GAM of pollen DCA scores. (e) Species richness is associated with each trophic structure. Significant differences (ANOVA, $p < 2.2e{-}16$) are denoted by letters (a, b, c), with CTS5 exhibiting the highest median richness and CTS1 the lowest.

Figure 4

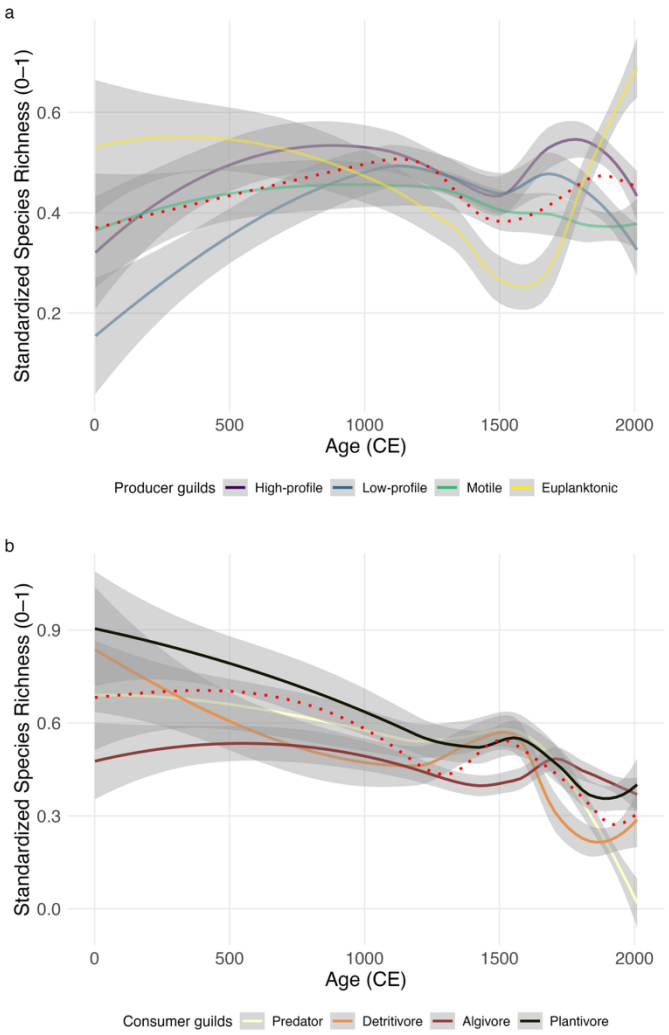

Figure 4. Temporal trends in standardised species richness for producers and consumers at the regional scale. Species richness was calculated per guild and sample, then min–max standardised to 0–1 within each lake × guild. (a) Producers: high-profile, low-profile, motile and euplanktonic. (b) Consumers: predators, detritivores, algivores and plantivores. Shaded bands are confidence intervals around the fitted smooths; the red dotted line is the overall smooth across guilds within each panel.

Figure 5

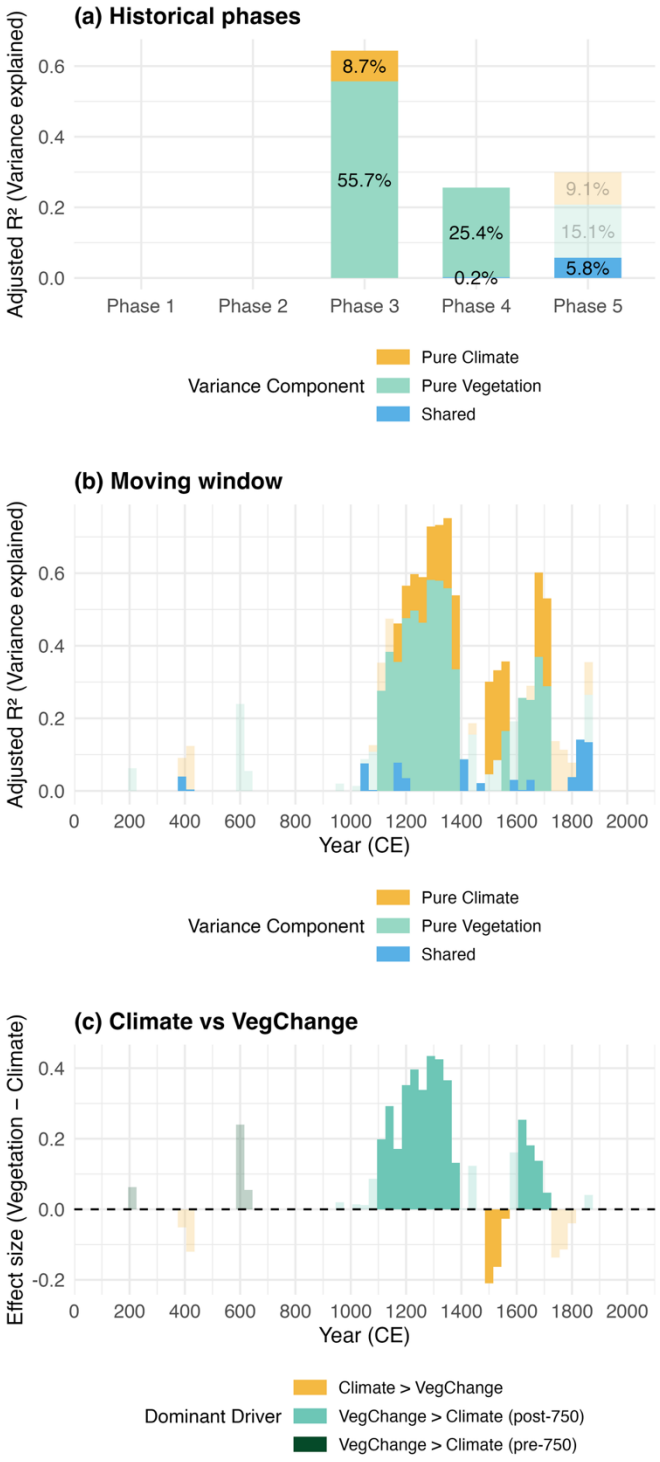

Figure 5. Temporal dynamics in the relative influence of climate and vegetation change on lake trophic structure. Adjusted R^2 values from variance partitioning models are shown for three temporal approaches: (A) historically defined phases following Raposeiro et al. (2021); (B) a 300-year moving window advanced in 30-year steps; and (C) the difference in unique effect sizes

between vegetation and climate predictors over time (pure vegetation − pure climate). In (A) and (B), pure vegetation (light green) represents variance uniquely explained by vegetation change inferred from pollen turnover, pure climate (orange) reflects variance uniquely explained by the North Atlantic Oscillation (NAO) after accounting for vegetation, and shared variance (blue) is jointly explained. In (B), vegetation effects are shown separately for pre- and post-colonization intervals to indicate ecological context. In (C), positive values indicate stronger vegetation effects relative to climate; negative values indicate the reverse. Opacity in (C) reflects whether the dominant unique fraction in each window is statistically significant ($p < 0.05$). Vertical dotted lines in (B–C) align with historical phase boundaries shown in (A).

Acknowledgments
Sampling locations are publicly accessible and not subject to restricted regulations. All procedures followed local and national guidelines.

Funding:
Spanish Ministry of Economy and Competitiveness grant CGL2010-15767 (PaleoNAO), grant CGL2013-40608-R (RapidNAO), and grant CGL2016-75281-C2 (PaleoModes) (A.S., S.G.)
MCIN/AEI/10.13039/501100011033 grants RyC-2016-19348, RTI2018-095749-A-I00, and PID2022-137749NB-I00, co-funded by the European Social Fund "ESF Investing in your future" and the European Regional Development Fund "ERDF A way of making Europe" (M.G.M.)
Spanish Ministry of Science and Innovation Ramón y Cajal Scheme grant RYC2020-029253-I (A.H.)
Spanish Ministry of Science and Innovation grant PID2024-159356NB-I00 (M.B.A.)
European Research Council Consolidator Grant ERC-CoG-2021-101045309 TIME-LINES (S.P.-R., S.N.)
Fundação para a Ciência e a Tecnologia grant DL57/2016/ICETA/EEC2018/25 and DISCOVERAZORES research project grant PTDC/CTA-AMB/28511/2017 (P.M.R.) and under the Projects UIDB/50027/2023 & UID/50027 (Rede de Investigação em Biodiversidade e Biologia Evolutiva, CIBIO _Açores)
European Union QREN/FEDER/COMPETE grants UIDB/50027/2020, UIDP/50027/2020, and LA/P/0048/2020 supporting CIBIO/InBIO (P.M.R.)

Author contributions:
Conceptualization: MGM, PMR
Methodology: MGM, PMR, VG, SP, AH, MM, MBA, RB, AS, SG
Investigation: PMR, VG, SP, AH, JL, RB, AS, SG
Formal Analysis: MGM, PMR, VG, SP
Writing—original draft: MGM, PMR
Writing—review & editing: MGM, PMR, VG, SP, AH, MM, MBA, RB, AS, SG, JL
Funding acquisition: MGM, PMR, VG, AH, RB, AS, SG

Competing interests: Authors declare that they have no competing interests

Data and materials availability: We provide a GitHub repository containing all code and data necessary to reproduce the analyses and figures in the manuscript: https://github.com/miguelmatias/trophic_simplification_azores. Following eventual acceptance, this repository will be archived and assigned a DOI via Zenodo for permanent access.